PASTE EXTRUSION OF POLYTETRAFLUOROETHYLENE FINE POWDER RESINS

by

ALFONSIUS B. ARIAWAN

Master of Applied Science (Chem. Eng.), The University of British Columbia, 1998
Bachelor of Applied Science (Chem. Eng.), The University of British Columbia, 1996

A THESIS SUBMITTED IN PARTIAL FULFILLMENT OF THE
REQUIREMENTS FOR THE DEGREE OF

DOCTOR OF PHILOSOPHY

in

the Faculty of Graduate Studies
Department of Chemical and Bio-Resource Engineering

We accept this thesis as conforming to the required standard

THE UNIVERSITY OF BRITISH COLUMBIA
October 2001

In presenting this thesis in partial fulfilment of the requirements for an advanced degree at the University of British Columbia, I agree that the Library shall make it freely available for reference and study. I further agree that permission for extensive copying of this thesis for scholarly purposes may be granted by the head of my department or by his or her representatives. It is understood that copying or publication of this thesis for financial gain shall not be allowed without my written permission.

Department of Chemical Engineering

The University of British Columbia
Vancouver, Canada

Date Dec 20, 2001

ABSTRACT

Due to its high melting point and melt viscosity, polytetrafluoroethylene (PTFE) is processed by a number of unusual techniques. These include paste extrusion. In PTFE paste extrusion, a free-flowing fine powder resin, having a typical individual particle diameter of 0.2 μm, is processed with the aid of a lubricating liquid to form an extrudate of considerable strength. The process is carried out at near ambient temperatures and is usually followed by sintering. Although PTFE paste extrusion has been commercialized, little is known of the fundamental mechanisms underlying the process.

In this work, the fundamental theoretical and experimental aspects of PTFE paste extrusion were studied. Five resins of different molecular structure were tested. Experiments were conducted using Instron capillary rheometers, equipped with barrels of different diameters and dies of various design. Analyses were performed using a differential scanning calorimeter (DSC), scanning electon microscope (SEM) and micro-Raman spectrometer. The tensile properties of paste extrudates were determined using a universal Instron mechanical testing machine. In addition, visualization experiments were performed to determine the pattern of PTFE paste flow during extrusion.

Prior to extrusion, the PTFE powder-lubricant mixture (paste) is preformed to produce a compacted cylindrical billet. The preforming behavior of PTFE pastes was studied in this work, in order to identify and determine the effects of important processing variables. It was found that the minimum preforming pressure and the duration required to ensure uniform paste compaction are dependent on the resin molecular structure. An empirical relationship was established to illustrate this. In the rheological study, the effects of various operating parameters were investigated. To quantitatively describe the flow behavior of PTFE paste, a one-dimensional mathematical model was developed, based on observations from flow visualization experiments. The model takes into account the elastic-plastic (strain hardening) and viscous nature of the material in its non-melt state. Finally, the mechanism of PTFE paste flow, which involves the formation of fibrils, was determined using SEM and verified using DSC. The properties of the extrudates were also analyzed, in terms of fibril quantity and quality (i.e. fibril orientation and continuity). A balance between fibril quantity and quality was found to be necessary to ensure acceptable product quality, as illustrated through the effects of various operating variables on the extrudate tensile strength.

TABLE OF CONTENTS

LIST OF FIGURES

LIST OF TABLES

ACKNOWLEDGEMENTS

I wish to express my sincere gratitude to my supervisor, Prof. Savvas G. Hatzikiriakos, for his guidance and support during the course of this study.

I sincerely thank Dr. Sina Ebnesajjad for his mentorship, his many useful suggestions during our discussions and most importantly, for his friendship during the course of this work, and for insisting that I visited DuPont Fluoroproducts, Wilmington, DE, USA for a training program (twice). The experiences that I have had at DuPont have been most fun, useful and rewarding, both for this work and for me, personally. I am also thankful for the excellent hospitality that Dr. Ebnesajjad has extended to me while I was in Wilmington.

Thanks also to Mr. John McAdam for the training that he has provided me at DuPont. His useful discussions on the practical aspects of paste extrusion are very much appreciated. John, thank you for suggesting me to check "the phase of the moon" regularly, to explain any "weird" experimental findings. At times, I found it consoling.

Thanks to DuPont Fluoroproducts for the financial support and the supply of the polymer samples. I am also appreciative of the many testing conducted by DuPont technicians.

My colleagues and ex-colleagues from RheoLab at UBC have helped me in various ways. I wish to thank Evgueni E. Rozenbaoum, Divya Chopra and Manish Seth for their helpful discussions and exchange of ideas.

Finally, I would like to extend a special note of thanks to my parents for their love and continuing support, and to my wife, Fujanarti, and my son, Antonius, who have been a source of strength and motivation for success.

CHAPTER 1:

FUNDAMENTALS

1.1 Introduction

Polytetrafluoroethylene (PTFE) is a material of great commercial value. Its unique properties have earned it special recognition in the plastic industry. Since its discovery by Dr. Roy Plunkett in 1938 (Plunkett, 1941), it has "revolutionized the plastic industry and led to vigorous applications not otherwise possible" (Plunkett, 1987). In this chapter, the chemistry and properties of PTFE are examined, and the various polymerization techniques involved in its production are discussed. The various fabrication methods for PTFE, that are rather unconventional for a thermoplastic polymer, are also reviewed. Particular emphasis is placed on the process of paste extrusion, which bears the most relevance to the present work.

1.2 Chemical Properties of PTFE

PTFE is a member of the fluoropolymer group, having a chemical formula of $[-(CF_2-CF_2)_n-]$. It is a perfluorinated, high molecular weight polymer, having a straight chain molecular configuration. PTFE is chemically inert, resistant to heat, and has excellent electrical insulation properties, as well as a low coefficient of friction over a wide temperature range (Gangal, 1989; Gangal, 1994; Ebnesajjad, 2000). These properties can be attributed to its molecular structure, in particular the C-F bond. The two types of bonds that made up a PTFE chain, the C-F bonds and C-C bonds, are extremely strong (Cottrell, 1958; Sheppard and Sharts, 1969), causing PTFE to have excellent mechanical strength and resistance to heat. The fluorine atoms can be envisioned to wrap around the backbone of the C-C chain, providing a protective shield to the chain from chemical attack. The size and electronic state of the fluorine atoms is exactly right, accounting for the chemical inertness and stability of PTFE (Gangal, 1994; Ebnesajjad, 2000). The protective shield also reduces surface energy, causing PTFE to have a low coefficient of friction and non-stick properties (Zisman, 1965; Gangal, 1994). PTFE, with its thermal and chemical stability, makes an excellent electrical insulator. It does not absorb water and its volume resistivity remains unchanged even after prolonged soaking. The dielectric constant of PTFE also remains constant over a very wide temperature range (Gangal, 1994).

Since PTFE is insoluble in many common solvents, its molecular weight cannot be determined by conventional techniques. In practice, the number average molecular weight (M_n) is usually estimated from the standard specific gravity (SSG) of the polymer. Higher SSG implies greater crystallinity and hence, lower molecular weight (Gangal, 1994; DuPont, 2001). Due to the linearity of PTFE molecules, the crystallinity of a virgin PTFE resin may be as high as 92-98% (Gangal, 1989). As a result, the SSG of PTFE is high for a polymer, typically ranging from 2.1 to 2.3. Following the standard procedure for measuring SSG (ASTM D4895), the number average molecular weight can be determined from

$$M_n = 5.97\text{x}10^5 \log_{10}\left(\frac{0.157}{2.306 - SSG}\right)^{-1} \tag{1.1}$$

for resins with SSG > 2.18 (Doban *et al.*, 1956; DuPont, 2001). The calculated molecular weights for PTFE with SSG < 2.18 are quite large (probably unrealistic), due to the asymptotic behavior of Eq. (1.1) in this range.

M_n has also been correlated to the second heat of melting, or the heat of recrystallization of PTFE (ΔH_{m2}), obtained using differential scanning calorimetry (DSC) (Suwa *et al.*, 1973; Gangal, 1994). It was found that

$$M_n = 3.39 \text{ x } 10^{13}.\Delta H_{m2}^{-5.16}. \tag{1.2}$$

for ΔH_{m2} ranging between 13.8 J/g to 32.7 J/g. Typically, M_n is in the 10^6 to 10^7 range (Gangal, 1994). It should be noted, however, that Eqs. (1.1) and (1.2) are valid only for homopolymer PTFE resins. Comparison of PTFE molecular weight, regardless of whether or not the resins contain other comonomers, can be made by considering the resin melt creep viscosity instead. The melt creep viscosity, as detailed in US Patent 3,819,594 (Holmes *et al.*, 1974), is higher for a higher molecular weight PTFE resin (DuPont, 2001).

The melting point of virgin PTFE is 342°C (Sperati, 1989), which is high for a thermoplastic polymer. DSC analysis indicates that the melting point of PTFE is irreversible (Gangal, 1994). A previously melted (sintered) PTFE will show a lower melting point of 327°C, which is the value that is often reported in the literature (i.e. second melting point).

This implies that cooling does not re-crystallize the chains back to the original virgin configuration, making the resin less crystalline. During melting, a volume increase of 30% is typical (Sperati, 1989). The melt is stable, since even at 380°C, the melt viscosity is relatively high at approximately 10 GPa.s. Due to this high melting temperature and melt viscosity, it is not possible to fabricate PTFE resin using conventional polymer melt processes (Gangal, 1994; Ebnesajjad, 2000).

Besides the melting point, PTFE has other transition temperatures, two of which are particularly important. These are shown in the partial phase diagram of PTFE in Fig. 1.1 (Sperati, 1989). Under ambient pressure conditions, the first transition occurs at 19°C. This is an especially important transition point due to its proximity to the ambient temperature. Fig. 1.2 shows a schematic diagram of a PTFE molecule, depicting the helical arrangement of the fluorine atoms around the carbon backbone (Blanchet, 1997). At around 19°C, a PTFE molecule undergoes a slight untwisting from a 180° twist per 13 CF_2 groups to a 180° twist per 15 CF_2 groups. The chain segments change from a perfect three-dimensional order to a less ordered one, and this results in a volume increase of about 1.3%. The second transition occurs at 30°C. Above this temperature, the number of CF_2 groups per 180° twist remains the same at 15. However, the extent of disorder of the rotational orientation of molecules about their long axis is increased. The total volume change as temperature is increased from below 19°C to above 30°C can be as high as 1.8% (Clark, 1962; Blanchet, 1997). This change in volume affects the density of the PTFE resin.

1.3 Commercial Production of PTFE: Polymerization Techniques

In the production of PTFE, tetrafluoroethylene monomer (TFE) is polymerized in a highly exothermic reaction. It is essential that the molecular weight of the resulting polymer is extremely high. Low molecular weight polymer will not have the strength needed in end use applications and will be of little commercial value.

Polymerization of TFE is carried out in an aqueous medium involving either one of two procedures. The first procedure is known as suspension polymerization. In this method, little or no dispersing agent is used along with an initiator in a medium, which is subjected to vigorous agitation. This initially causes a stable dispersion of PTFE for a brief period of

time. The PTFE particles later precipitate due to the lack of dispersing agent and the presence of agitation. The resulting dried polymer is 'stringy, irregular, and variable in shape' and is known as granular resin. The particle sizes of granular resin and its powder flow property can be varied, depending on the end product requirements, by size reduction (cutting), or by mixing different grades (Gangal, 1994).

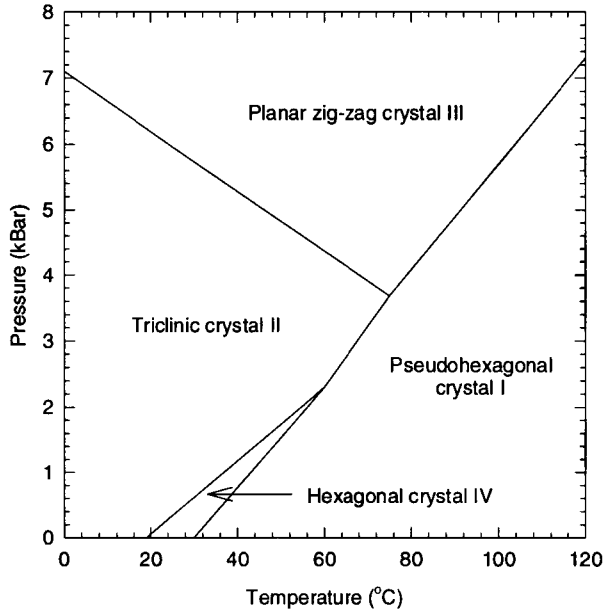

Fig. 1.1 Partial phase diagram of polytetrafluoroethylene (Sperati, 1989).

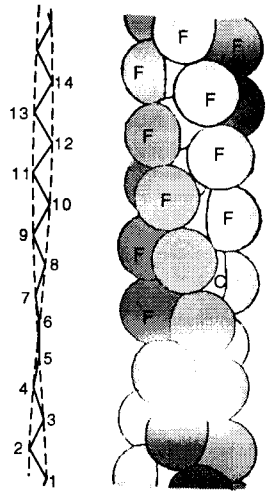

Fig. 1.2 Schematic diagram of a PTFE molecule, showing the helical arrangement of the fluorine atoms around the carbon backbone (Blanchet, 1997).

The second technique of polymerization is called aqueous emulsion polymerization. The procedure involves sufficient dispersing agent along with an emulsifying agent and an initiator. Gentle stirring is usually employed to ensure dispersion stability. It is important that the dispersion is not only stable, so that the PTFE particles do not coagulate prematurely, but that it is also unstable enough to allow subsequent coagulation to form a fine powder. The amount of emulsifying agent influences the rate of polymerization and particle shape. The resulting dispersion may be stabilized using a noninonic or anionic surfactant, and concentrated to 60-65 wt.% solid by electodecantation, evaporation, or thermal concentration. It may also be subjected to a mechanical separation instead. In the latter case, a fine powder resin is obtained. The resin is susceptible to mechanical damage and hence, during separation, shearing is carefully avoided (Gangal, 1994).

Although the two procedures result in the same high molecular weight PTFE polymer, the products are distinctly different. The granular product can be molded in various forms. However, the resin obtained from aqueous dispersion polymerization cannot be molded, but has to be fabricated by dispersion coating, in the case of the concentrated dispersion, or by paste extrusion, in the case of fine powder resin (Blanchet, 1997; Ebnesajjad, 2000).

1.4 Processing and Applications of PTFE

It is not possible to process PTFE resin by melt techniques, due to its high melt viscosity. Techniques involving cold pressing and sintering have to be employed instead. These techniques resemble those used in metallurgy, but are unconventional as far as thermoplastics processing is concerned.

Granular PTFE resin can be fabricated into an end product by pressing the resin in a mold at room temperature to produce a preform of the desired shape. Preforming serves to reduce voids between the resin particles (Ebnesajjad, 2000), which would otherwise render the final product mechanically weak. The preform is then sintered at a temperature above the melt temperature of PTFE to allow coalescence of particles into a dense homogeneous structure. During sintering, the rate of temperature rise is important to allow the temperature distribution to be as uniform as possible. After sintering, the product is cooled at a specific cooling rate, which is also important in influencing the mechanical properties of the product. Fast cooling will lead to lower crystallinity and, consequently, higher tensile strength and

elongation at break, and better flex life for the product (Blanchet, 1997; Ebnesajjad, 2000). On the other hand, a slow cooling rate will result in a product with greater creep resistance, lower permeability to gases and solvents, and lower residual stress and distortion. Sintering and cooling may be done under pressure or freely. Pressure cooling may reduce the tendency of the product to distort, although it is more costly (Blanchet, 1997).

In the production of continuous moldings such as pipes and rods, the method described above is not appropriate. Instead, a reciprocating ram extruder is used (Ebnesajjad, 2000). Screw extrusion, which is normally employed in the processing of most other thermoplastics, is virtually impossible in the case of PTFE due to the high melt viscosity of the resin and the tendency of the unmelted powder to be compacted by the screw. In ram extrusion, the resin is sequentially charged into the reciprocating extruder to be preformed. The product is then pressed down a heated tube, where melting and coalescence occur. Granular PTFE resin is commonly used to produce tubes, seals and piston rings, bearings, gaskets, and other basic shapes (DuPont, 1996; Blanchet, 1997; Ebnesajjad, 2000).

Aqueous dispersions of PTFE are commonly applied as coatings, or formed into films or fibers. With particle diameters ranging from 0.1 to 0.3 μm and concentrations between 30% to 60%, the dispersion may be applied on surfaces by spraying, or by flow or dip coating methods (Gangal, 1994; Blanchet, 1997). Drying is then carried out at a temperature below 100°C, before baking at temperatures between 216°C to 316°C to allow the removal of the wetting agent. Subsequently, the coating is sintered at a temperature higher than 360°C. Generally, surfaces are coated with PTFE to provide protection against chemical attack, or to provide a non-stick property to the surfaces (Blanchet, 1997). PTFE film may also be produced, by casting the dispersion on a smooth surface. Subsequent drying, baking and sintering of the film is followed by the stripping of the film from the surface. To form PTFE fiber, an aqueous dispersion is forced through a spinneret and into a coagulating bath. The fiber is then heated, sintered and hot drawn to develop strength (Ebnesajjad, 2000). Aqueous dispersion finds a number of applications in fabric coating, in the production of porous fabric structures, such as Gore-Tex, and in other antistick applications (Blanchet, 1997).

The processing of PTFE fine powder resin is of particular interest in this work. Fine powder resin is susceptible to mechanical damage above the transition temperature of 19°C.

Figure 1.3 shows the crystalline structure of a PTFE powder (Blanchet, 1997). Below 19°C, shearing will cause crystal units to slide pass each other. Above 19°C, however, molecules are packed more loosely and shearing will cause the unwinding of molecules, creating fibrils (Mazur, 1995; Ebnesajjad, 2000). It is important that fine powder resin does not undergo pre-mature fibrillation. The presence of fibrils before processing will result in excessive extrusion pressure and mechanically defective products (Mazur, 1995; Ebnesajjad, 2000). Because of this, the storage and transportation of fine powder resin are carried out at temperatures below 19°C (DuPont, 1991).

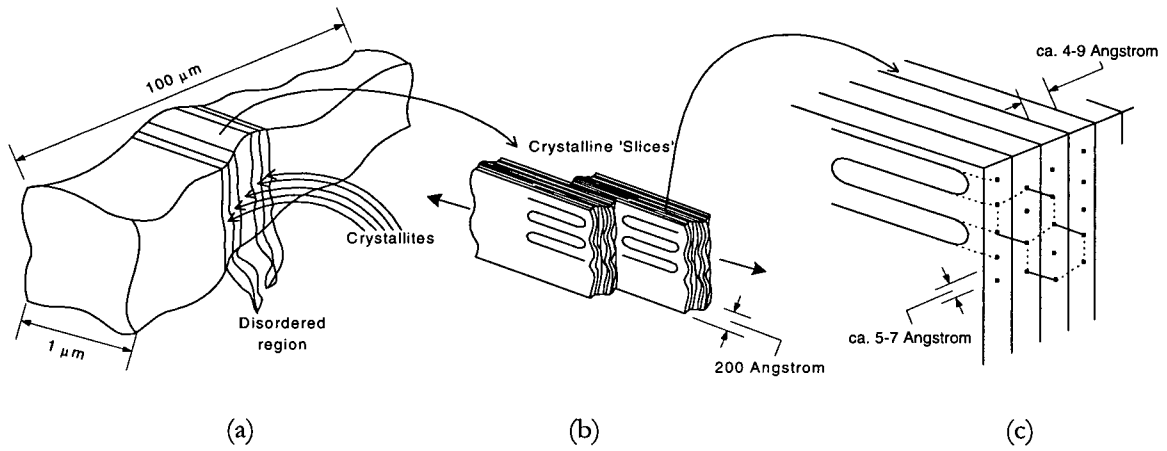

Fig. 1.3 Crystalline structure of PTFE: (a) band, (b) crystalline slices, which may slip during deformation via shear in the disordered regions which separate them, (c) hexagonal array of PTFE molecules within crystalline slice (Blanchet, 1997).

Fine powder resin is processed through paste extrusion. The resin is initially mixed with a lubricating liquid of low boiling point, for ease of removal at a later stage of the process. Ideally, a hydrocarbon with surface tension below 18 mN/m should be used to allow complete wetting of the powder (Gangal, 1994). However, since this is not practical, liquids with fairly low surface tensions are used instead. The amount of liquid in the mixture may vary from 16 wt.% to 25 wt.% (Ebnesajjad, 2000). Shear-free mixing is performed by simply rotating the container, at a temperature lower than 19°C, for the reasons discussed above. The liquid acts as a lubricating agent and as a cushion between particles so as to eliminate mechanical damage, which may occur as particles slide past one another (Mazur, 1995). The powder-lubricant mixture, which is called a paste, is allowed to age at room temperature for several hours before extrusion. This allows the paste to equilibrate at a

temperature higher than the mixing temperature, which results in the lowering of the lubricant surface tension and viscosity, and hence, better wetting of the powder particles (Ebnesajjad, 2000).

The next step of the process involves the pressing of paste to produce a preform. This serves to eliminate air voids that will render the final product mechanically weak (Mazur, 1995). A preforming pressure of 2 MPa is typically used. The preform is then extruded in a ram extruder through a die of specific shape, depending on the product requirement. In a wire coating process, a special annular (crosshead) die is used, which allows the introduction of wire into the extrudate. The extrudate is then passed through a dryer to evaporate the lubricating liquid before being sintered in an oven. Electrical spark tests may then follow. In the production of tubes and pressure hoses, a similar annular die is used. To make tapes, the preform is extruded through a simple conical entry die and calendered to a flat, continuous product before drying. In this case, however, the product is not sintered (Ebnesajjad, 2000). A schematic diagram summarizing PTFE paste extrusion is shown in Fig. 1.4 for a wire coating process (DuPont, 1994).

Each step of the paste extrusion process is critical in determining the final product properties. However, various operating variables, such as lubricant content in the paste, preforming pressure and duration, and the various die design parameters, affect the process and product in ways that have yet to be investigated. Although the process of paste extrusion has been commercialized, the fundamental mechanisms underlying the process are not fully understood. Since its inception, little work has been done on the subject. A detailed study of the experimental and theoretical aspects of PTFE paste extrusion is, therefore, necessary and will be the main focus of the present work.

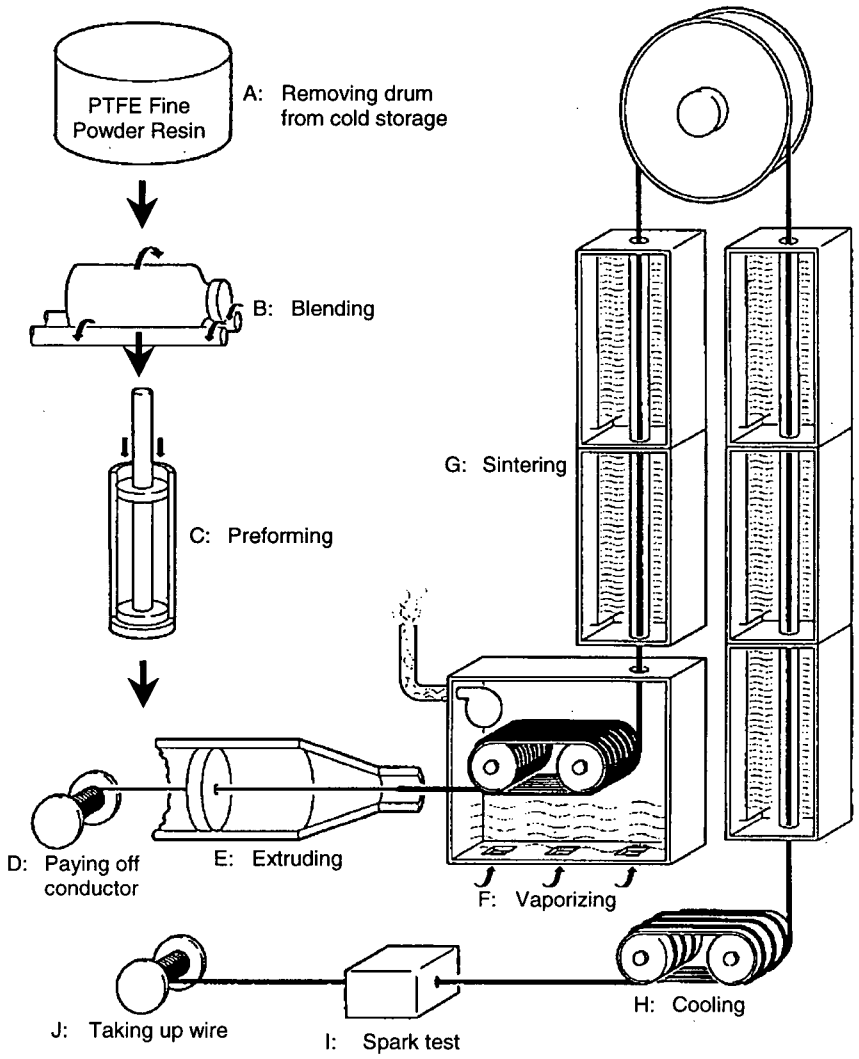

Fig. 1.4 Schematic diagram of PTFE paste extrusion for a wire coating process (DuPont, 1997).

CHAPTER 2:

PASTE EXTRUSION: GENERAL REVIEW

2.1 Introduction

Paste extrusion has been widely used as a fabrication technique for many useful objects, from everyday products such as toothpaste, pencil leads, cosmetic pencils, animal foodstuffs, and food flavorings, to less common products such as ceramic components, catalyst supports, bricks, seal tapes, PTFE wires and cables (Benbow and Bridgwater, 1993; Ebnesajjad, 2000). Surprisingly, the subject of paste extrusion does not seem to have been investigated systematically before. It has been presented previously either in entirely empirical terms or as an extension of molten polymer flow and extrusion. Furthermore, as far as PTFE paste extrusion is concerned, previous work is particularly scanty.

In this chapter, some of the previous studies on paste extrusion, particularly those related to PTFE paste extrusion, are reviewed.

2.2 Experimental Aspects of Paste Extrusion

Paste is essentially a mixture of liquid and solid particles. During paste processing, the liquid in the paste matrix serves primarily as a lubricant. In PTFE paste extrusion, the liquid has the additional function of protecting the solid resin particles from being mechanically damaged prior to extrusion (as discussed in Chapter 1, PTFE fine powder resins are highly susceptible to mechanical damage above the transition temperature of 19°C) (Mazur, 1995; Ebnesajjad, 2000). By filling the spaces between the particles with an incompressible liquid rather than air, the paste will become resistant to compressive loading, without increasing the interparticle contact area. This also reduces the adhesive forces between particles, particularly in the case of PTFE paste, since the interfacial tension for polymer-on-lubricant is much less than for polymer-on-air. This allows particles to rearrange more easily in response to mechanical forces, without being deformed (Mazur, 1995). Consequently, the particles will remain isotropic in nature after compression, a condition that is not attainable with a dry powder (Mazur, 1995).

The lubricant concentration in a paste mixture generally varies. Benbow and Bridgwater (1993) have reported typical lubricant concentrations of 35 vol.% to 50 vol.%, depending on the physical properties of the solid component, such as the particle shape and size distribution. If the solid component of the paste is considered as being made up of close-packed spherical particles of uniform size, the volume of the void spaces in the paste matrix can then be calculated to be approximately 47 % of the total paste volume. For a typical PTFE paste with a lubricant density of approximately 0.75 g/cm^3, this is equivalent to about 23 wt.%. However, PTFE paste extrusion is typically performed with a lower lubricant concentration, ranging between 16 wt.% to 25 wt.% (Ebnesajjad, 2000). Possibly, this has to do with the PTFE resins being deformable, which results in the effective void volume in the paste matrix being much smaller than calculated after compression. Perhaps a more accurate representation of the solid - lubricant arrangement in the PTFE paste matrix is the adsorption of the lubricant onto the surface of the resin particles to form a thin layer of lubricating film, rather than as a void filler.

The amount and properties of the lubricant critically affect the extrusion process. For example, based on industrial experience, Mazur (1995) has reported that increasing the amount of the lubricant above some critical value results in an extrudate that is too soft to retain its shape. On the other hand, if an inadequate amount of lubricant is used, the extrudates tend to be rough and irregular. The viscosity of the lubricant has also been found to have an effect on the quality of the paste. The use of a more viscous liquid as a lubricant has been found to result in a less uniform mixture (Benbow and Bridgwater, 1993). Kim *et al.* (1997) studied the fabrication of $Yba_2Cu_3O_{7-\delta}$-Ag composite super-conducting wires by a paste extrusion technique and found that, if the viscosity of the paste is too low, the paste may not extrude into a continuous body, or that microcracks could be developed during the drying process after extrusion.

An excellent general review on the subject of paste extrusion is contained in the book co-authored by Benbow and Bridgwater (1993). The authors have discussed various aspects of paste extrusion, including the overall logic behind the design procedure for paste fabrication, extrudate surface defects and swell, lubricant migration, and the methods of data analysis for paste extrusion. The authors also discuss the various types of extruders that can

be used for the extrusion process, namely the rotating extruder, the ram extruder, and the screw extruder, along with their practical implications. In addition, comparisons are made between paste extrusion and other techniques related to powder processing. However, most of these discussions are valid only for the extrusion of rigid pastes, i.e. where the solid particles do not deform or change morphologically during the extrusion process, such as alumina-based pastes. In PTFE paste extrusion, however, where the resin particles undergo a morphological change during processing, it is not possible to use a screw extruder as a processing device, as will be discussed later in Chapter 5. Nevertheless, several conclusions from the work are worth reviewing, since they are generally valid for most paste systems, including PTFE pastes.

For example, Benbow and Bridgwater (1993) have found that the transient extrusion pressure profile from a ram extruder typically rises steeply at the beginning of the extrusion process. After reaching a maximum, the pressure usually decreases gradually to a minimum until a zone of dried and highly compacted paste (static zone) is formed around the die entrance. Further extrusion in the presence of such a static zone was found to cause the pressure to rise again. The authors point out that, at the point when the extrusion pressure begins to initially rise, the piston is in contact with the paste in the barrel for the first time. The authors also suggest that the minimum pressure level during the extrusion process be considered as the steady-state pressure level for analysis purposes. They claim that this is the point when the friction on the barrel wall is at its minimum. A similar description of the pressure curve has also been reported by Malamataris and Rees (1993).

From the experimental results obtained in this work, it has been found that the above description of the pressure response curve is applicable to PTFE paste systems as well, although the initial pressure rise appears more like a peak in the case of PTFE paste extrusion. Also, during the steady-state extrusion of PTFE paste, the pressure response appears to be more level than that described by Benbow and Bridgwater (1993), allowing it to be more easily identified for the purpose of experimental analysis. Further discussion of this general aspect of PTFE paste extrusion is given in Chapter 5.

Benbow and Bridgwater (1993) have also suggested a more convenient experimental extrusion procedure, in which a single batch of paste is extruded at different speeds (during a

single experimental run) to obtain the steady-state pressure level corresponding to each of those speeds. The authors, however, cautioned that this should only be carried out when there is sufficient confidence that a static zone has not formed near the die entrance. This is difficult in the case of PTFE paste extrusion, as will be discussed in Chapter 5.

In paste extrusion, lubricant migration is an important phenomenon. It is caused by the movement of the mobile liquid phase in the paste matrix that eventually results in its non-uniform distribution in the mixture (Mazur, 1995). This effect is enhanced with time, especially in the presence of high extrusion pressure. Solid particle size distribution, shape and orientation during flow have been thought to influence the extent of lubricant migration during paste extrusion (Benbow and Bridgwater, 1993), although no known quantitative analysis has been performed previously. It is an indication that excessive lubricant migration has occurred during extrusion when droplets of liquid accumulate at the die exit, and when the pressure at a lower extrusion rate is found to be higher than that at a higher rate (Benbow and Bridgwater, 1993). The later and progressive rise of the extrusion pressure with time, as discussed above with reference to the pressure response from the ram extruder, also indicates that lubricant is being filtered out of the bulk paste. Several authors have suggested using finer powder, or blending fine and coarse powders in the paste mixture to reduce the extent of lubricant migration during extrusion (Benbow and Bridgwater, 1993). It should be noted, however, that particle size also affects the porosity of the extrudates. A method has been described by Benbow *et al.* (1987), which enables the prediction of extrudate pore structure from particle size distribution.

Lubricant migration also occurs during preforming. In studying the leftover ceramic paste after extrusion through a die having a sudden contraction, Burbidge *et al.* (1995) found that a conically-shaped stagnant zone was consistently formed around the die entry. For pastes that had been preformed prior to the extrusion, the size of this artifact was larger in size. This implies that preforming promotes lubricant migration, especially when too high a preforming pressure is used. However, inadequate pressure will yield a weak product, due to insufficient removal of entrapped air in the paste matrix (Mazur, 1995; Ebnesajjad, 2000). A detailed study on the effects of preforming on paste quality is discussed in Chapter 6 for several PTFE paste systems.

Another common phenomenon in paste extrusion is extrudate surface fracture. Although surface defects in polymer melt extrudates have been the subject of a large number of studies (see, for example, Tordella, 1956; Ramamurthy, 1986; Kalika and Denn, 1987; Hatzikiriakos and Dealy, 1991), very little work has been done on the origin and elimination of surface defects of extruded pastes. Furthermore, there is no basis to presume similar mechanisms for fracture in melt and paste extrusions. A general introduction on surface defects in paste extrusion has been provided by Benbow and Bridgwater (1993). The authors reported that the type and severity of surface defects are very much dependent on paste formulation, die design and operating conditions. To reduce the severity of extrudate surface defects, the authors suggested the use of extrusion dies with longer length to diameter ratios and smaller entrance angles. Increasing the lubricant concentration in the paste mixture and reducing the extrusion rate were also found to improve extrudate appearance. A more comprehensive study on the subject has been conducted by Domanti (1998) and reported in the author's doctoral dissertation.

Numerous other studies have been carried out on the extrusion of various paste systems (see, for example, Harrison *et al.*, 1986; Popovich *et al.*, 1997; Burbidge *et al.*, 1998; Wildman *et al.*, 1999). However, work on PTFE paste extrusion is particularly limited. In a recent reference source for fluoropolymers, Ebnesajjad (2000) has summarized various experimental aspects of PTFE paste extrusion. The author has discussed the general properties of PTFE, including PTFE fine powder resin and its processing behavior. Appropriate selection criteria for fine powder resins and lubricants for specific applications have also been suggested, along with their appropriate processing conditions. The process of PTFE paste extrusion has been described in detail for various applications, such as wire coating and the fabrication of tapes and tubes. The general practical implications of many processing variables, such as die design, lubricant concentration and resin properties, have also been assessed qualitatively. Most importantly, the author has provided a discussion on fibrillation as a characteristic defining phenomenon in PTFE paste extrusion. A detailed discussion on fibrillation can also be found in a work by Mazur (1995).

The first published report on the creation of fibrils during PTFE paste extrusion is probably by Lewis and Winchester (1953). The authors noticed that, during the extrusion process, the morphology of the PTFE resin changed from spherically shaped individual

particles to an extrudate consisting of particles that are connected by fibrils of submicrometer size. However, the authors provided no further detail on the subject, particularly as far as the mechanism of fibril creation, and the role of operating conditions in affecting the fibril and hence, extrudate quality are concerned. In the same work, the authors discussed the qualitative effects of extrusion pressure, temperature and die design on the extrudate flow rate using a constant pressure ram extruder. The authors also investigated the flow pattern of paste at the die entry region, by performing visualization experiments, which are repeated in this work (see Chapter 4) for the purpose of further analysis. Their results were later confirmed by Snelling and Lontz (1960) and summarized by Mazur (1995). In other earlier work, Lontz and Happoldt (1952) conducted a general study on the dispersion properties of PTFE powder. This was then followed by a study on the extrusion properties of lubricated PTFE resin, in which the method of preparing lubricated compositions for a wire coating process was investigated (Lontz *et al.*, 1952).

It can be said that, although numerous studies on paste extrusion have been carried out, the process of PTFE paste extrusion, in particular, has yet to be completely investigated. Furthermore, most of the available published works on PTFE paste extrusion are based on industrial experiences that tend to be empirical in nature. The present work is aimed at a systematic study of the process of PTFE paste extrusion.

2.3 Mathematical Modeling of Paste Flow

The behavior of any material under flow can be generally described as viscous, elastic, plastic, or any combination thereof. The subject of flow rheology has been discussed in great detail elsewhere, and it would be inappropriate to repeat all of that information here. Mathematically, numerous constitutive models have been developed for flows of viscoelastic materials, such as polymer melts (see, for example, Larson, 1998), and for flows involving solids under plastic deformation, where they are considered as ideal plastic materials (see, for example, Hoffman and Sachs, 1953), or as elastic-plastic materials that exhibit strain hardening (see, for example, Davis and Dokos, 1994), as in the case of metal forming or wire drawing. However, little work has been devoted to the flow modeling of paste as an elasto-viscoplastic material (this will be discussed in Chapter 8). Even with the available

mathematical models, significant modifications are often necessary to improve their predictions of the experimental data.

Benbow and Bridgwater (1993) have proposed empirical constitutive relationships to describe the general behavior of paste flow. These were incorporated into their derivation of an analytical equation that predicts the effects of die design and extrusion conditions on the steady-state extrusion pressure. Depending on various simplifications, the resulting equation may have four or six parameters that need to be determined experimentally. The authors have provided experimental verification of their model predictions, using various paste systems. The fits are generally acceptable, and the solution can be generated without much computational effort (see also Benbow *et al.*, 1987; Benbow *et al.*, 1989). However, the equation fails to predict the effect of die entrance angle on the steady-state extrusion pressure, as will be elaborated in Chapter 8. It has also been found that, due to its empirical nature, modifications having a theoretical basis are difficult to incorporate into the final equation.

Doraiswamy *et al.* (1991) developed a non-linear rheological model for concentrated pastes, which takes into account the elastic, viscous and yielding behavior of such materials. A key feature of the model is the incorporation of a recoverable strain term. The model consists of parameters which can be determined solely from dynamic data. The authors claimed this as being advantageous, since these data are easily accessible by performing experiments using a parallel-plate rheometer. The authors have also shown that a correlation exists between steady shear viscosity and complex dynamic viscosity for materials that exhibit yield stress, similar to the Cox-Merz rule for polymer melts. By defining a new term, called the "effective shear rate", the authors were able to show the effectiveness of the steady shear viscosity predictions from the more accessible dynamic data. However, in the present work, experiments using a parallel-plate rheometer with PTFE pastes were found to be difficult and non-reproducible. It was also found that the results obtained were not useful, due to the significant slip that occurs between the paste and the rheometer plates.

In another work, Louge (1996) has proposed a two-phase model for paste flow, taking into consideration phenomena such as liquid migration, particle segregation along the walls, shear dilatancy and induced localization. The model also includes a Darcy-like interaction

force and a non-linear viscous dissipation term. The author has shown that the model reduces algebraically to a problem involving only one velocity field, one pressure field and the particle volume fraction. Solution to the model, however, requires significant computational effort. Furthermore, the model was derived based on a rigid paste system, and hence, is not applicable to PTFE pastes.

A simple and experimentally more consistent model to describe the flow of PTFE pastes has been proposed by Snelling and Lontz (1960). The authors consider the maximum shear stress experienced by the paste during extrusion as being made up of two components: one proportional to the maximum shear rate (strain hardening component) and one proportional to the strain rate (viscous component). This is essentially a modified Kelvin constitutive relation (Hoffman and Sachs, 1953). By performing visualization experiments, the authors found that the flow of PTFE paste in the die conical zone can be described reasonably well by considering the "radial flow" hypothesis. This hypothesis assumes that all paste particles at the same radial distance from the die apex move towards the die apex at the same velocity (see Chapter 8). Based on this hypothesis, an expression for the pressure drop was derived, which was in good agreement with the experimental data. However, the equation does not take into account the frictional force on the die wall, which becomes more important when a tapered die having a small entrance angle is used. Also, the analysis provided by the authors does not account for the pressure drop across the capillary length of the die that follows the entrance region. In this work, the equation proposed by the authors is rederived, in order to include the effects that had been previously neglected.

There are several other previous studies that have attempted to mathematically describe the flow of pastes in general, such as that by Horrobin and Nedderman (1998), who used the slip line analysis to predict the upper and lower boundary to the entrance pressure drop associated with the flow of a perfectly elastic paste (see also Horrobin, 1999). Other works include those by Kudo (1960), Kobayashi and Thomsen (1965), Jiri *et al.* (1989) and Adams *et al.* (1997). However, these solutions are generally only partially valid for PTFE paste. The fact that PTFE fine powder resin does not qualify as a rigid, or perfectly elastic material, and that it is easily fibrillated, requires PTFE paste to be categorized into a unique material class of its own and analyzed differently.

CHAPTER 3:

SCOPE OF WORK

3.1 Introduction

Although PTFE paste extrusion is of a great commercial interest, little is known of its mechanisms. This limits the ability to predict the effects of various operating variables on the outcome of the extrusion process. Consequently, process optimization is often made through experimental trials, instead of the more efficient modeling approach.

Previous work on general paste extrusion on ceramics, alumina-based pastes, foodstuffs, etc. provided little understanding of the PTFE paste extrusion process. The properties of PTFE resins have made their rheology unique and PTFE paste extrusion fundamentally different from other more typical paste extrusion processes. It is tempting to describe the rheology of PTFE pastes during extrusion as similar to that of polymer melts. However, this is certainly not valid, as will be clear from this work. Mathematically, previous work on the development of constitutive equations to model the flow of polymer melts is also of only limited relevance to the PTFE paste system. This is because both solid and liquid phases are present in PTFE pastes, with the solid particles being fibrillated during extrusion. Thus, rheological consideration has to be extended to other systems as well, encompassing highly filled suspensions and even molten metals, rather than limiting it to polymer melt systems.

3.2 Thesis Objectives

This research project is fundamental in nature. From this work, it is hoped that a clearer insight into the nature of PTFE paste flow, its relation to the rheology and processing of PTFE pastes, and the properties of PTFE paste extrudates will be gained.

The objectives of this work can be summarized as follows:

1. To study the various experimental aspects of PTFE paste extrusion, such as preforming, paste preparation, and the extrusion process itself, in order to identify important

operating variables in PTFE paste extrusion and possibly, provide recommendations to improve the current commercial procedure.

2. To study the flow mechanism and morphological development of PTFE paste during extrusion by means of scanning electron microscopy (SEM), differential scanning calorimetry (DSC), and visualization experiments.

3. To understand the mechanism of fibrillation in PTFE paste extrusion and its effects on extrudate properties.

4. To determine the effects of die design, resin molecular structure, and processing conditions on the rheology of PTFE pastes and the properties of PTFE paste extrudates.

5. To develop a mathematical model that is capable of describing the rheological behavior of PTFE pastes during extrusion.

3.3 Thesis Organization

The first chapter of this thesis provides fundamental information on PTFE as well as its chemistry, commercial production and applications. The various fabrication techniques for PTFE resins are also reviewed in Chapter 1, with particular emphasis on the paste extrusion process. Following this, important literature on paste extrusion, particularly those studies that pertain to the experimental and theoretical aspects of PTFE paste extrusion, is reviewed in Chapter 2. The detailed objectives of this work are described in this chapter. This is followed, in Chapter 4, by descriptions of the experimental apparatus and procedures used in the present study. In Chapter 5, the general characteristics of PTFE paste extrusion are discussed, with reference to the general shape of the transient extrusion pressure profiles and the extrusion procedure. Experimental findings on the preforming behavior of PTFE pastes are described in Chapter 6. Chapter 7 focuses on the flow mechanism of PTFE pastes during extrusion and the theory of fibrillation, as deduced from experiments involving SEM, DSC and flow visualization. The rheology of PTFE pastes is discussed in Chapter 8. In the same chapter, a one-dimensional mathematical model to describe the flow of PTFE pastes is proposed and derived. The model predictions are illustrated in separate subsections, along with their experimental verification. In Chapter 9, the effects of various operating variables

on the properties of PTFE paste extrudates are discussed, with reference to the quality and quantity of the fibrils formed during extrusion. Finally, the thesis is concluded in Chapter 10, with a general summary of the experimental findings, the knowledge contributions resulting from this work, and some recommendations for future work. For ease of reference, various symbols used throughout this thesis are listed in a separate nomenclature section following Chapter 10.

CHAPTER 4:

EXPERIMENTAL WORK

4.1 Introduction

This chapter describes the experimental equipment and procedures used to study the paste extrusion of PTFE fine powder resins in this work. A capillary rheometer, an excellent mimic of the industrial ram extruder, is an indispensable tool in a study such as this. Detailed descriptions of the capillary rheometers used in the present work are given in this chapter, along with the various terms associated with the extrusion die design. Other equipment and procedures used to determine the properties of the extrudates are also described. This chapter also discusses the method used in the visualization experiment. Since paste preparation is a crucial step in PTFE paste extrusion, it is dealt with separately. Finally, one section of the chapter is devoted to the descriptions of the physical and molecular properties of the fine powder resins, and of the properties of the lubricants used in this work.

4.2 Experimental Equipment

4.2.1 Preforming and Extrusion Equipment

Preforming was normally done before extrusion using a capillary rheometer with a blank die in place, as will be discussed later. However, for the purpose of investigating the preforming behavior of the different PTFE pastes, a separate unit was built. The preforming unit consisted of an aluminum pipe with polished interior surface (Average Roughness, $R_a \approx$ 0.6 μm) and a steel plug, resembling a blank die. The unit was assembled under the capillary rheometer load frame, in place of the rheometer barrel, as shown in Fig 4.1. Since the inside diameter of the preforming unit (see Fig. 4.1) was larger than the rheometer piston diameter, the piston head needed to be replaced with a custom-made unit (it was required that the preforming unit diameter be sufficiently large to facilitate later analysis). The simple and light design of the preforming unit, without the bulkiness and the weight associated with the rheometer barrel, allowed the removal of the fragile preform for analysis without much effort. This reduced the chances of breaking/cracking the preform during handling. At the same time, by incorporating it into the capillary rheometer load frame, it was possible to take

advantage of the rheometer load cell and motor drive, and to monitor and adjust the preforming pressure precisely, through the available computer control board.

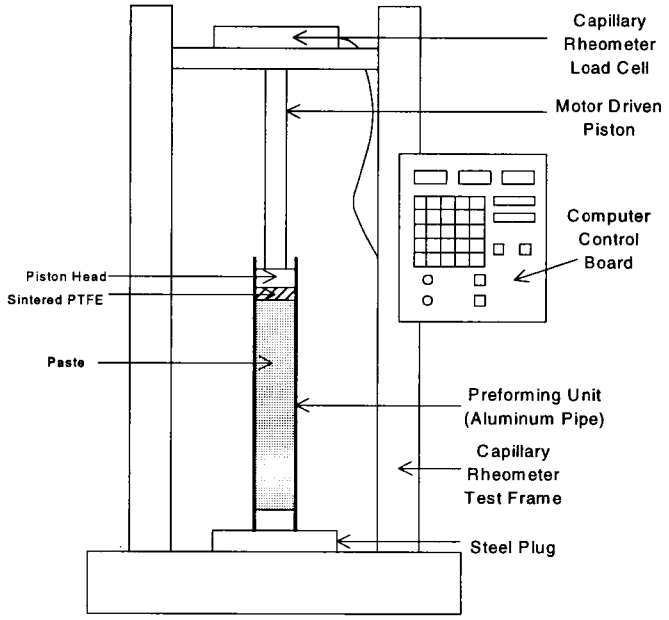

Fig. 4.1 Schematic diagram of the preforming unit used in this work. It is essentially the test frame of an Instron capillary rheometer.

Capillary rheometers were used for the extrusion experiments, with the set-up shown in Fig. 4.2. The unit is comprised of a barrel, equipped with heating bands and temperature controllers, a piston, and a load frame, complete with a load cell and motor drive, as discussed above with reference to Fig. 4.1. The piston moves at a constant speed, as specified through a computer control board. A data acquisition board allows the experimental results, *viz.* extrusion force versus distance, to be recorded automatically and stored in a computer. During data analysis, the extrusion pressure was obtained by dividing the force required to drive the piston by the cross-sectional area of the barrel.

The extrusion die was assembled into the lower end of the barrel as shown in Fig. 4.2. Stainless steel dies of various designs, each having an average surface roughness of approximately 0.02 μm, were used. For the tapered die shown in the figure, the design variables of interest were the die entrance angle (α), the die reduction (contraction) ratio (R), and the die aspect (L/D_o) ratio. The die reduction ratio was defined as the ratio of the cross-

sectional areas before and after the contraction zone (i.e. $R = (D_b/D_a)^2$). For the purpose of the visualization experiments, special dies were designed that allowed them to be disassembled into two halves, as shown in Fig. 4.3.

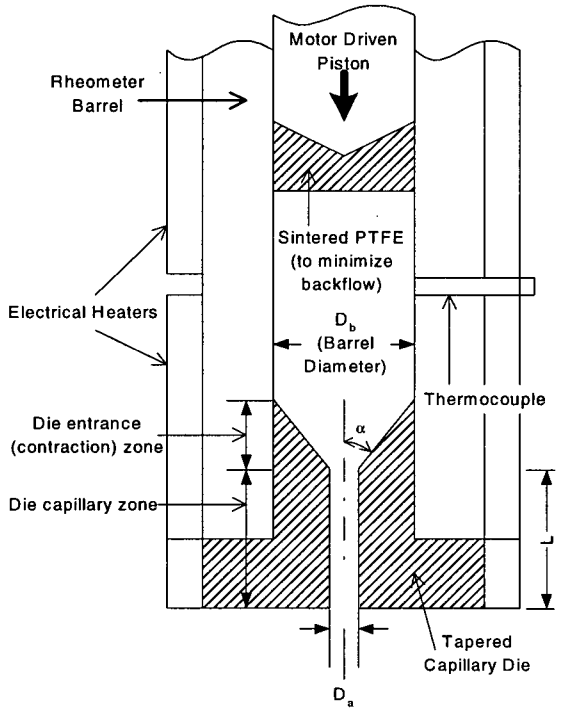

Fig. 4.2 Schematic diagram of Instron capillary rheometer. The unit was assembled under the test frame shown in Fig. 4.1 for paste extrusion. A blank die was used in place of the capillary die during preforming.

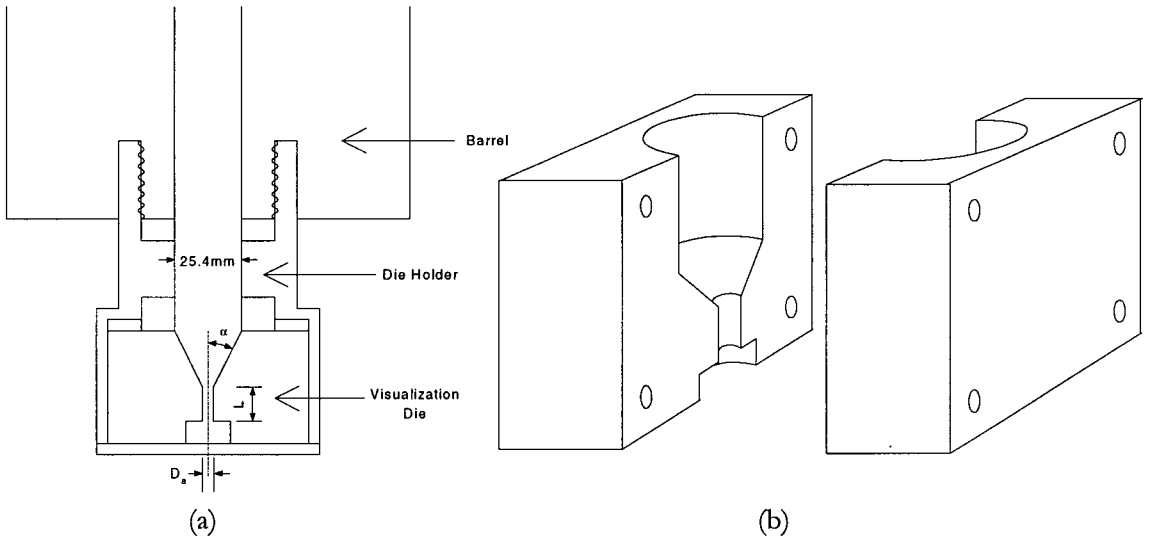

Fig. 4.3 (a) Die assembly for the 25.4 mm diameter capillary rheometer, (b) visualization die design.

Experiments were carried out at the rheology laboratory of the University of British Columbia (Rheolab), using an Instron capillary rheometer, equipped with two interchangeable barrels having diameters of 9.525 mm and 25.4 mm. The unit allowed a maximum piston speed of 4.23 mm/s and a maximum force of 22.3 kN. Dies of various designs were available, including a blank die with $\alpha = 90°$ and $D_a = 0$. The bigger diameter barrel (see Fig. 4.3) was generally used for the visualization experiments. Some experiments were also performed at DuPont Fluoroproducts, Wilmington, DE, using a similar unit that allowed a maximum piston speed of 8.3 mm/s and a maximum force of 245 kN, with a barrel diameter of 21.8 mm.

4.2.2 Other Apparatus

Other major experimental equipment used in this work included an Instron universal testing machine to determine the mechanical (tensile) properties of the paste extrudates, differential scanning calorimeter (DSC) to determine the thermal properties of the fine powder resins before and after extrusion, and a micro-Raman spectrometer to determine the degree of orientation of the fibrils created during the extrusion process. The use of Raman spectroscopy to determine the molecular orientation in drawn polymer samples has been reported previously in the literature (Voyiatzis *et al.*, 1996; Andrikopoulos *et al.*, 1998; Delmede *et al.*, 1999). It involves the projections of excited polarized Raman spectra onto a drawn polymer sample with the polarization geometry parallel and perpendicular to the drawing axis of the sample. The intensity ratios of certain Raman scattering bands between the two polarization geometries will then indicate the degree of molecular orientation in the sample (a ratio of unity indicates *isotropicity* and hence, no preferred molecular orientation). Following this procedure, Raman spectroscopy was used in this work in an attempt to quantify the degree of fibril orientation in the paste extrudates. The backscattering geometry used for the Raman spectroscopy is depicted in Fig. 4.4.

The set-up of the Raman spectrometer was as follows. The Raman spectra were excited with the linearly polarized 514.5 nm line of an air-cooled Ar^+ laser (Spectra-Physics 163-A42). A narrow-bandpass interference filter was used for the elimination of the laser plasma lines. The excitation beam was directed to the sample compartment through a properly modulated metallurgical microscope (Olympus BHSM-BH2). The microscope was

used for the delivery of the excitation laser beam onto the sample and for the collection of the backscattered light through a beamsplitter and the objective lens adapted to the aperture of the microscope. The focusing objective was a long working distance (8 mm) 50x/0.55 Olympus lens. The spectra were obtained using a ~1 mW laser beam focused on the specimen for a total integration time of 30 s. The Raman scattered radiation was focused on the slit of a single monochromator after being passed through a notch holographic filter (HFN-514-1.0, Kaiser Optical Systems) for removal of elastic Rayleigh scattering rejection. The Raman system employed was the T-64000 model of Jobin Yvon (ISA – Horiba group). Dispersion and detection of the Raman photons were done by a 600-grooves/mm grating and a 2D CCD detector (operating at 140K), respectively. The spectral slit width was approximately 10 cm^{-1}. The incident beam polarization was selected by an optical rotator (90°). A dichroic sheet polariser analyzed the scattered radiation, and a half-wave plate was used after the polariser whenever needed in order to ensure the same maximum polarization response from the grating. All spectra were corrected to take into account the beam splitter's response in the polarization of the incident and scattered radiation. The total response of the system was checked using CCl_4 as a reference (Voyiatzis, 2000).

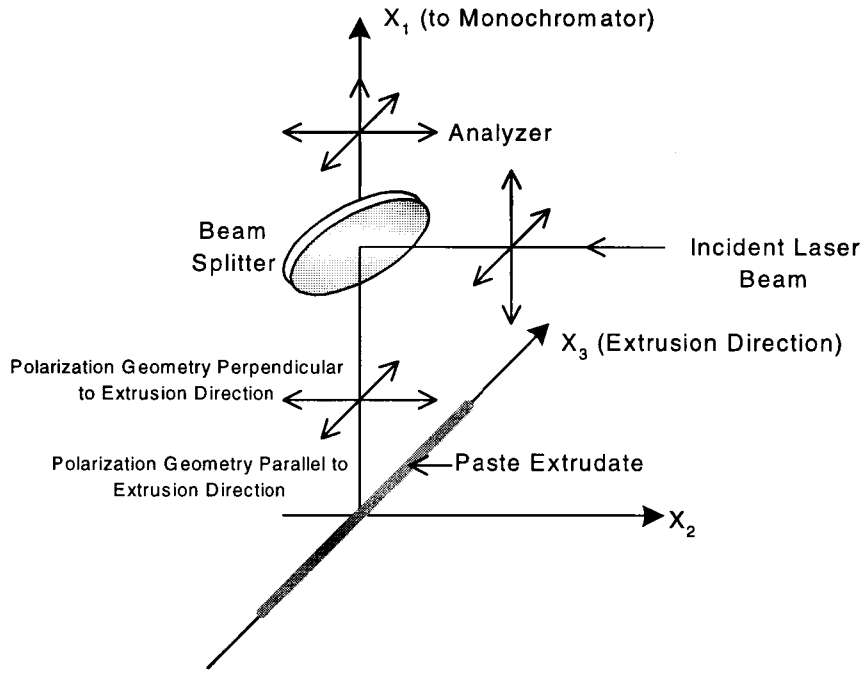

Fig. 4.4 Coordinate axes for the Raman backscattering configuration.

4.3 Materials

4.3.1 PTFE Fine Powder Resins

Five grades of PTFE fine powder resins were available for testing in this work. The resins were supplied by DuPont Fluoroproducts, and have the properties shown in Table 4.1. The resin particles are generally spherical in shape, with a uniform size distribution, as a result of the polymerization technique employed to produce these resins (Kim *et al.*, 1999a; Kim *et al.*, 1999b; Ebnesajjad, 2001). The average particle diameter reported in Table 4.1 are size based, and were obtained by performing laser light scattering measurements. Three of the resins had a homopolymer structure with different molecular weights, and two had a slight degree of branching due to the incorporation of another perfluorinated monomer. The SSG data of the resins are also included in Table 4.1 to allow a quantitative comparison of the resin molecular weight for resins in the same molecular structure group. Generally, however, the molecular weight of a PTFE resin can be inferred directly from its melt creep viscosity, regardless of the molecular structure (see Chapter 1). The SSG and melt creep viscosity of the resins were determined according to ASTM D4895-98 and US Patent 3,819,594, respectively. The resins were kept refrigerated throughout the course of this work to ensure a temperature lower than the PTFE transition temperature of 19°C.

Table 4.1 Properties of PTFE fine powder resins studied in this work. Relative magnitude of the resin molecular weight can be inferred proportionally from the melt creep viscosity data.

Resin	Relative M_n	Avg. Dia. (μm)	SSG	Melt Creep Viscosity (Pa.s)
Copolymer series:				
1	Low	0.209	2.157	1.6×10^9
2	High	0.204	2.153	2.1×10^9
Homopolymer series:				
3	Low	0.177	2.220	1.2×10^{10}
4	Medium	0.216	2.185	2.8×10^{10}
5	High	0.263	2.154	3.2×10^{10}

4.3.2 Lubricants

An isoparaffinic compound under the trade name of ISOPAR G® was used as the lubricant (supplied by ExxonMobil Chemicals). Its properties, as provided by the

manufacturer, are summarized in Table 4.2. For the visualization experiments, black dispersed pigment for PTFE extrusion supplied by Colorant-Chromatics was used in a mixture with the ISOPAR G® solvent as the lubricant.

Table 4.2 Properties of ISOPAR G® solvent (Exxon Corp., 1994).

	ISOPAR G®	Test Method
Solvency		
Kauri-Butanol Value	28	ASTM D1133
Aniline Point, °C	83	ASTM D611
Solubility Parameter	7.3	Calculated
Volatility		
Flash Point, °C	41	ASTM D56
Distillation, °C		ASTM D86
Initial Boiling Pt	160	
50%	166	
Dry Point	174	
Vapor Pressure, kPa, 38°C	1.87	ASTM D2879
General		
Specific Gravity, 15°C/15°C	0.747	ASTM D1250
Density, g/cm^3	0.744	Calculated
Color, Saybolt	+30	ASTM D156
Viscosity, Pa.s, 25°C	1.00	ASTM D445
Auto-Ignition Temp., °C	293	ASTM D2155
Bromine Index	<10	ASTM D2710
Composition, mass%		
Saturates	100	Mass Spectrometer
Aromatics	0.01	UV Absorbance
Purity, ppm		
Acids	None	Exxon Method
Chlorides	<1	Exxon Method
Nitrogen	<1	Exxon Method
Peroxides	Trace	Exxon Method
Sulfur	1	Exxon Method
Surface Properties		
Surface Tension, mN/m, 25°C	23.5	duNuoy
Interfacial Tension with water, mN/m, 25°C	51.6	ASTM D971
Demulsibility	Excellent	Exxon Method

4.4 Experimental Procedure

4.4.1 Paste Preparation

Paste was prepared by mixing PTFE fine powder resin with the lubricant in a desired mass proportion at a temperature lower than 19°C. Mixing was carried out below the PTFE transition temperature to ensure that the resin was not damaged prior to extrusion. The

transfer of the resin in and out of the containers was facilitated by pouring the resin, instead of scooping it, to further ensure the physical integrity of the resin. The mixing container was then placed in a horizontal roll mixer that rotated at 15 rpm for approximately twenty minutes. The resulting mixture (paste) was aged at room temperature for 24 hours before the start of an extrusion experiment to allow more uniform wetting of the resin particles by the lubricant. Unused paste was discarded after 10 days and replaced by a new mixture, since the lubricant concentration could have decreased with time.

4.4.2 Preforming

In order to study the preforming behavior of PTFE pastes, preforming was carried out using the unit described above with reference to Fig. 4.1. The paste inside the preforming unit was compressed with a piston driven by the Instron capillary rheometer. Since the computer controller on the rheometer allowed the load cell to move only at a constant speed, the preforming procedure required the setting of the piston speed at an initial value of 0.85 mm/s and manually decreasing it as the desired pressure approached. To maintain a constant pressure for a period of time, the speed was adjusted accordingly, sometimes to as low as 0.0021 mm/s. The speed was never set to zero since the paste would relax and pressure decrease immediately upon the stopping of the piston. To eliminate paste leakage due to back pressure, a sintered PTFE rod was placed in the preforming unit between the paste and the piston.

To determine the variation in density and lubricant concentration along the preform, sections of approximately 2.54 cm in length were sliced and immediately weighed. These were dried in an oven at approximately 90°C until the weights were constant within ± 0.5 mg. From the difference between the initial (wet) and final (dry) weights of the various slices, lubricant concentration along the preform was determined. The density of each slice was determined from its weight after drying and its corresponding volume. In the radial direction, the variation of density and lubricant concentration is not expected to have a major practical impact, since in the process of paste extrusion, the preform is extruded through a converging die, where its diameter is appreciably reduced, making any effect due to radial variation negligible.

In the rheological study, preforming was done using the Instron capillary rheometer with the barrel and a blank die in place (see Fig. 4.2). The procedure was similar to that discussed above, with the preforming pressure set to 2 MPa for approximately 30 s. Upon the completion of preforming, the blank die was replaced by a tapered die and paste extrusion then proceeded.

4.4.3 Paste Extrusion and Visualization Experiments

Paste extrusion was carried out using an Instron capillary rheometer at a constant piston speed. The temperature of the barrel was set as desired through the temperature controllers. A sintered PTFE rod was placed between the paste and the piston to eliminate paste leakage due to backpressure. The extrudates that were produced were collected for later analysis.

Visualization experiments were performed to provide insights about the flow pattern of the paste in the die conical zone. Experiments were carried out using the 25.4 mm diameter barrel, for ease of analysis, along with its own set of dies (see Fig. 4.3). The experimental procedure was similar to that discussed above. In this case, however, a second (colored) paste was prepared with the lubricant being a 1:1 mixture of ISOPAR G® and the black dispersed pigment. The rheometer barrel was filled alternately with the colored and uncolored pastes, followed by preforming and extrusion. After the extrusion had reached steady state, the piston was stopped, and the die was removed and disassembled to recover the paste within the contraction area. Subsequently, the paste was cut in half axially in order to observe the deformation pattern developed therein.

4.4.4 Extrudate Analysis

Prior to analysis, extrudates were dried in a vacuum oven at approximately 60°C until their weights remained approximately unchanged with further heating. The dried extrudates were tested for their tensile strength according to ASTM D1710-96 (PTFE rods). The thermal properties of the extrudates were determined using a DSC according to ASTM D3418-82. Raman spectroscopy was also performed on the extrudates at two polarization geometries (parallel and perpendicular to the extrusion direction) in an attempt to describe quantitatively the degree of fibril orientation in the extrudates.

CHAPTER 5:

GENERAL CHARACTERISTICS OF PTFE PASTE EXTRUSION

5.1 Introduction

Although a ram extruder can be used to study the rheological behavior of both polymer melts and PTFE pastes, the pressure responses obtained from the extruder are characteristically different for the two types of materials. Not surprisingly, the physical significance of each response is also different. This is largely due to the fact that both solid and liquid phases are present in the paste matrix, while only a liquid phase is present in the polymer melt system. The general industrial procedure for the extrusion process itself is different for the two types of materials. For example, while it is possible to conduct a continuous extrusion of polymer melts, PTFE paste extrusion has to be carried out in a batch fashion, for reasons that will be discussed below.

In this chapter, the general characteristics of PTFE paste extrusion are discussed with respect to the extrusion pressure response obtained from the ram extruder (capillary rheometer) and the general industrial procedure for the process. This will provide an insight into the macroscopic flow behavior of PTFE pastes during extrusion.

5.2 Characteristics of Extrusion Pressure Curves

A typical transient pressure response for PTFE paste extrusion is shown in Fig. 5.1. Generally, the pressure curve can be classified into three distinct regions, which are identified as regions I, II, and III in the figure. Similar pressure curves are usually obtained for other paste extrusion processes (Benbow and Bridgwater, 1993). The pressure peak in region I has been commonly attributed to the initial wetting of the extrusion die or the initial filling of the die conical zone by the paste (McAdams, 2000). In region II, the paste flow is essentially at steady state. In region III, the gradual rise in pressure has been thought to be a manifestation of non-uniform lubricant concentration, due to the liquid phase migration in the paste matrix (Benbow and Bridgwater, 1993; Burbidge *et al.*, 1995). It is noted that these variations

in the extrusion pressure may result in the non-uniformity of extrudate properties, as will be discussed in subsequent chapters.

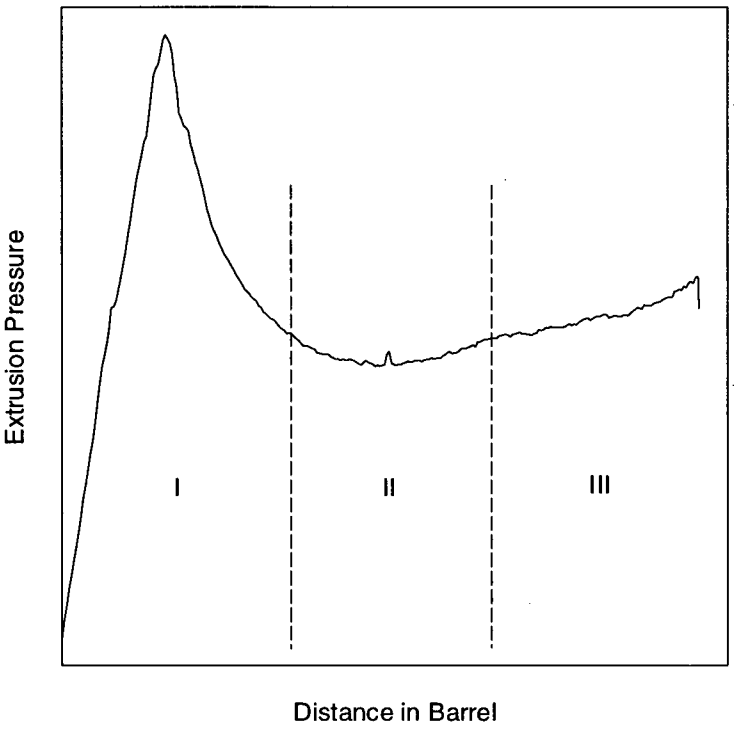

Fig. 5.1 Typical transient extrusion pressure response from a ram extruder during PTFE paste extrusion.

While it is clear that region II is the steady-state region of the extrusion profile, it is also reasonable to consider region III as the extrusion zone of a drier paste that results in the gradual increase in the extrusion pressure. However, preliminary experiments have indicated that region I is not entirely due to the wetting of the extrusion die by the paste. This is apparent from Fig. 5.2, which shows the transient experimental results of two extrusion runs using resin 2. In case (i), preforming was done using a blank die having a flat surface (α = *90°*) at a preforming pressure of 2 MPa. In case (ii), preforming was done at the same pressure, but with a tapered extrusion die in place, to ensure that the die conical zone is filled and hence, wetted by the paste prior to extrusion. It can be seen from Fig. 5.2, however, that the latter procedure does not eliminate the pressure peak. This raises doubt about whether the mechanism suggested for the pressure peak is indeed valid.

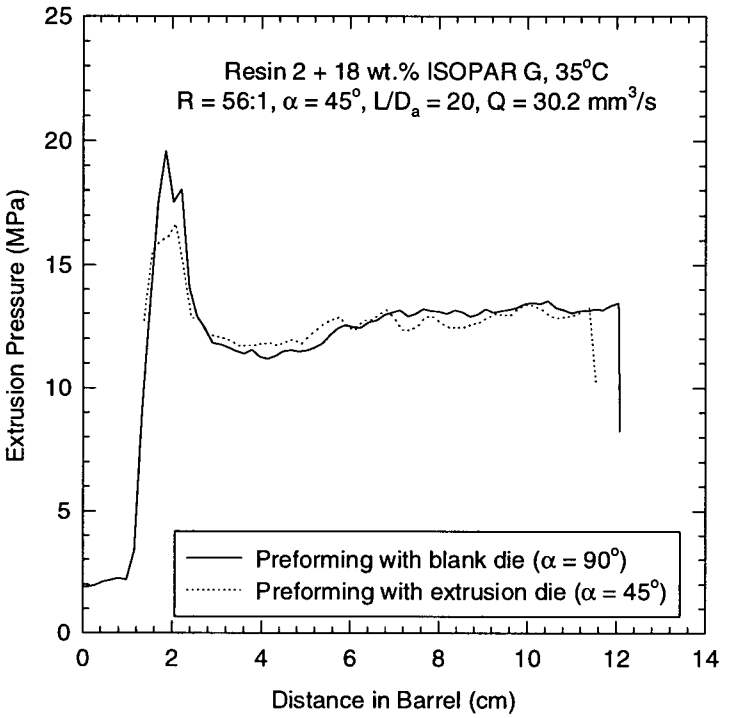

Fig. 5.2 Extrusion pressure responses with preforms obtained using different procedures. It can be seen that there is little effect on the magnitude of the pressure peak.

Fig. 5.3 shows the results obtained for an experiment in which extrusion was stopped twice after reaching steady state. During the first stop, the extrusion die was removed and reassembled immediately, before allowing the extrusion to continue until the second steady state was reached. During the second stop, the extrusion die was removed and the conical part of the partially extruded preform, which was molded to the shape of the die, was removed to obtain a flat surface. The extrusion was then allowed to proceed until completion. It can be seen that, after the first and second stops, the peaks reappeared with a similar magnitude (peaks 2 and 3). Both were considerably lower than that of the initial one (peak 1). If the pressure peak is due to the initial wetting of the die by the paste, then such a peak should not reappear after the first stop. However, it should reappear after the second stop, with a magnitude similar to that of peak 1. As can be seen from Fig. 5.3, this is clearly not the case. In a similar but separate experiment, cutting the conical part of the partially extruded preform followed by wiping the die surface free of lubricant, did not cause the reappearing pressure peak to have the same magnitude as that of the initial one.

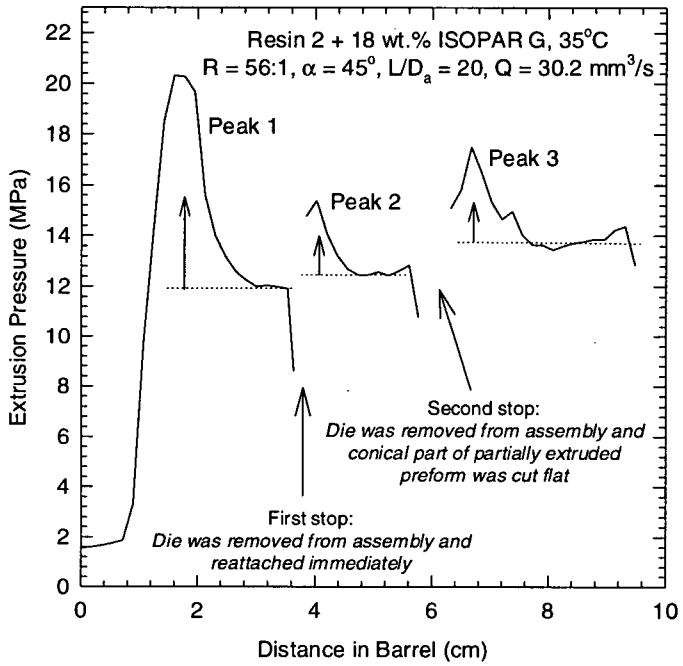

Fig. 5.3 Extrusion pressure responses obtained by stopping the extrusion process twice. During the first stop, the die was removed from its assembly and immediately reattached. During the second stop, the conical part of the partially extruded preform that conformed to the shape of the die was cut to result in a flat surface.

To determine if the pressure peak is due to the elastic nature of the paste, experiments were conducted in which the extrusion process was stopped after reaching steady state. Then the paste was allowed to relax without disassembling the die, before proceeding further. The results are shown in Fig. 5.4. It can be seen that allowing the paste to relax for a short time (less than 10 minutes) caused the peak to reappear in subsequent extrusions, although with much smaller magnitudes. However, when the paste was allowed to relax for a sufficient length of time (45 minutes), the peak did not reappear. This implies that forming the paste into the conical shape of the die for a sufficiently long time causes the paste to lose its elastic memory (fading memory effect), and the pressure peak to be eliminated in subsequent extrusions. This explains the high pressure peak normally observed in region I and the fact that its magnitude is irreproducible in subsequent extrusions. That is, a virgin paste, exhibiting full elastic memory, will extrude with a high pressure peak at the beginning of the process. However, due to the fading memory effect, it is not possible to reproduce the magnitude of the first peak in subsequent extrusions of the same paste, without disassembling the die. It is worthwhile noting that the steady-state extrusion pressure

increases with the waiting period between extrusions, as can be seen in Fig. 5.4. This is not surprising since the paste becomes drier with time.

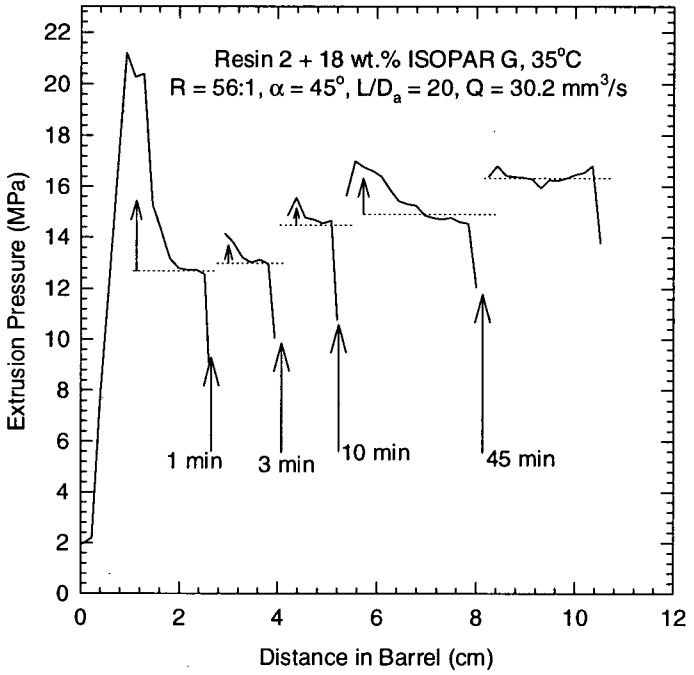

Fig. 5.4 Extrusion pressure responses obtained by stopping the extrusion process a number of times, for various waiting periods (see figure). The results show the fading memory effect of PTFE paste.

Further experiments were conducted in which the waiting periods between subsequent extrusions were longer. For these experiments, the 25.4 mm diameter barrel was used in order to facilitate the removal of the partially extruded paste from the rheometer. The partially extruded paste was kept in the refrigerator for approximately 48 hours before further extrusion. The experimental results are shown in Fig. 5.5 (since this set of experiments was conducted using the bigger diameter barrel, response (ii) is included for comparison purposes). It can be seen that the elastic memory of the paste appears to be reversible. As discussed previously, the pressure peak did not reappear in a subsequent extrusion after a waiting period of 30 minutes (response (ii)). However, after removing the partially extruded paste from the die and extrusion assembly for 48 hours, the pressure peak reappeared, with a magnitude similar to that of the original peak (response (iii)). From these experiments, it can be concluded that the pressure peak in region I of the extrusion pressure

profile is more likely to be due to the elastic nature of the paste, as opposed to the initial wetting or filling of the die conical zone by the paste.

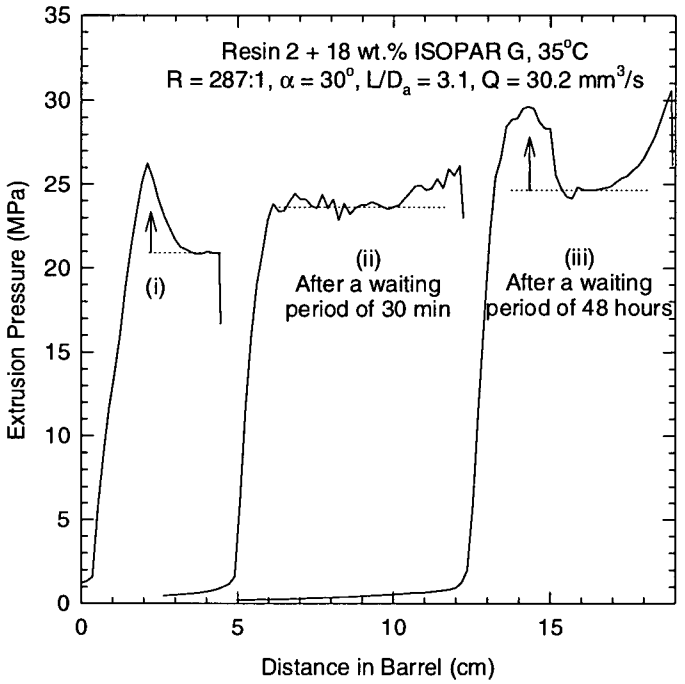

Fig. 5.5 Extrusion pressure responses obtained with longer waiting periods between re-extrusions. Experiments were conducted using the 25.4 mm diameter barrel. The results indicate that the fading memory effect is in fact reversible.

5.3 General Procedural Characteristics

That both liquid and solid phases are present in the paste matrix, and that the solid resin particles are highly susceptible to mechanical damage, affect the general procedure with which PTFE paste extrusion can be carried out. Variations in the general extrusion procedure are usually very limited, if possible at all. For example, Fig. 5.6 shows the transient pressure responses from two sets of experiments performed according to different procedures. In case (i), the extrusion flow rate was initially set to 60.3 mm^3/s (i-a). After reaching a steady state, the rate was decreased to 30.2 mm^3/s (i-b), but later, increased back to the initial rate of 60.3 mm^3/s (i-c). In case (ii), the cycle was reversed. The extrusion was initially carried out at 30.2 mm^3/s (ii-a), then increased to 60.3 mm^3/s (ii-b) and later decreased back to 30.2 mm^3/s (ii-c). It can be seen that, in case (i), slightly different steady-state extrusion levels were obtained for (i-a) and (i-c), although both were performed at the

same extrusion rate. Also, the steady-state extrusion pressure corresponding to (i-b) was similar to that for (i-a), although (i-b) was performed at a slower rate. In case (ii), the difference in the steady-state extrusion pressures between (ii-a) and (ii-c) was larger than that between (i-a) and (i-c). These results indicate that PTFE paste extrusion is an irreversible process. That is, unlike in polymer melt processing, where intermittent change in the rate during an extrusion run has no effect on the steady-state pressure, the extrusion pressure of PTFE paste is dependent on its shear history. It can be seen from Fig. 5.6 that, where an extrusion run has exhibited a higher steady-state pressure level at some particular rate, decreasing the rate will not lower pressure (comparing (i-a) to (i-b), and (ii-b) to (ii-c)), but increasing it will increase the steady-state extrusion pressure to an even higher level (comparing (i-b) to (i-c) and (ii-a) to (ii-b)). This is simply due to the fact that the consistency of the paste changes with time and the application of pressure. Longer times and higher extrusion pressures provide the necessary driving force for causing the lubricant to migrate out of the paste matrix, leaving the paste remaining in the extrusion barrel drier. Clearly, this effect is irreversible and will have a significant influence on the product properties, as will be discussed in later chapters.

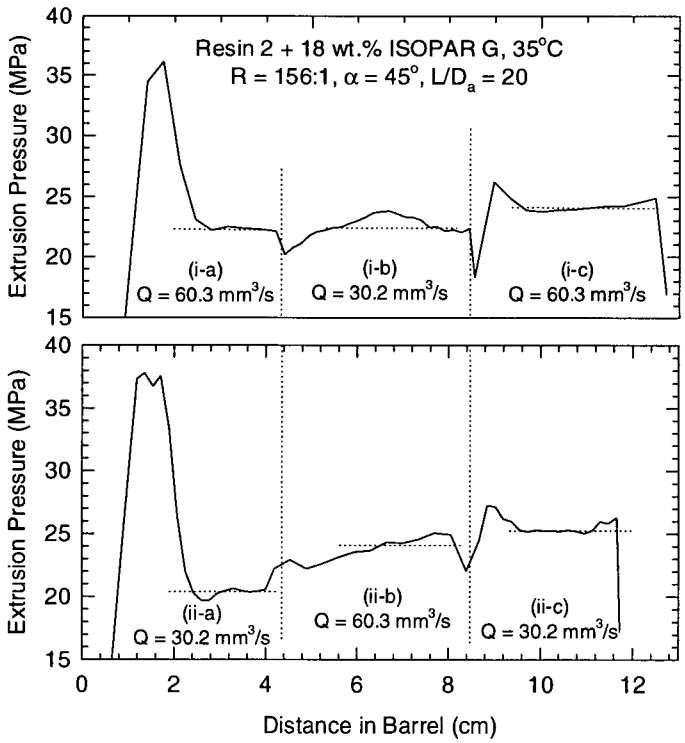

Fig. 5.6 Effects of changing extrusion rate during a single extrusion run.

In order to improve the efficiency of the PTFE paste extrusion process, modifications should be made to the current industrial procedure that involves a batch-wise processing technique, to allow the process to be carried out in a more continuous fashion. However, preliminary experiments have proven this to be difficult. Firstly, since PTFE fine powder resins are highly susceptible to mechanical damage, it is not possible for PTFE paste extrusion to be carried out using a screw extruder, with which a fully continuous process can easily be attained. The shear created by the rotating action of the screw will damage the resins by prematurely creating fibrils and at the same time, breaking them, causing the extrusion pressure to be excessively high. The damaged paste will eventually clog the barrel, making it impossible to obtain an extrudate. Therefore, it is only possible to perform PTFE paste extrusion using a ram extruder. In order to make the process more continuous, the procedure will then have to be modified to allow continuous feeding of preforms into the extrusion barrel of the ram extruder. Preliminary experiments were conducted to investigate the practical feasibility of this procedure. The results are shown in Fig. 5.7.

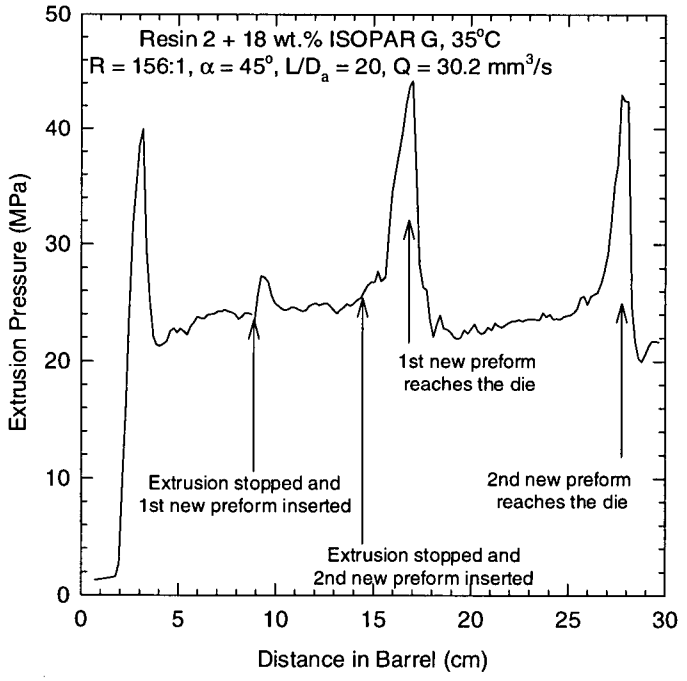

Fig. 5.7 Effects of continuous extrusion using individually prepared preforms.

It can be seen that when the beginning of each new preform was being extruded, the extrusion pressure peaked. This indicates that different preforms do not continuously weld

to each other. Since the variation in pressure will consequently affect the extrudate properties, the proposed procedure essentially provides no improvement over the current commercial process, and therefore, has to be considered as practically unattractive.

5.4 Conclusions

Due to the presence of both solid and liquid phases in the PTFE paste matrix, the extrusion pressure responses of PTFE pastes are characteristically peculiar. The transient pressure profile for PTFE paste extrusions can be distinctly classified into three regions. The first region includes a pressure peak, which was found to be due to the elastic memory of the paste, rather than due to the initial wetting or filling of the die conical zone by the paste. The second and third regions correspond to steady-state paste flow and the extrusion of a drier paste, respectively. Variations in the procedure for PTFE paste extrusion were found to be very limited, if possible at all. This is largely due to the nature of the paste mixture, and the fact that PTFE fine powder resins are highly sensitive to mechanical damage. In an attempt to improve the efficiency of the process by making it more continuous, it was found that different preforms do not continuously weld to each other during extrusion. Extrusion of continuously fed preforms into the extrusion barrel has resulted in a pressure response that periodically peaked when the beginning of each new preform was being extruded. This makes the proposed modification to the procedure commercially impractical.

CHAPTER 6:

PREFORMING BEHAVIOR OF PTFE PASTES

6.1 Introduction

As discussed in Chapter 5, the extrusion pressure typically rises steeply at the beginning of a paste extrusion process, before reaching a peak (region I) and settling to a lower steady-state level (region II). Near the end of the extrusion, the pressure tends to rise slowly but continuously (region III). These variations in extrusion pressure will correspondingly affect the quality of the extrudate. In the wire coating process, for example, it has been found that large variation in the extrusion pressure can result in the periodic failure of the dielectrical spark test (McAdams, 2000).

It was found that a variation in the extrusion pressure could also occur in region II, due to the uneven densification of paste during preforming. This necessitates a study on the preforming behavior of PTFE pastes. The similar subject of soil consolidation has been of much interest to soil engineers and, accordingly, much work has been done in this area (see, for example, Craig, 1997). The subject of liquid migration through the soil has also been of theoretical interest in soil mechanics. In this study, experiments were conducted to investigate the preforming behavior of PTFE pastes by determining the effects of pressure, resin molecular weight and preforming duration, on the preform density and lubricant distribution in the preform, using the homopolymer resins listed in Table 4.1. The experimental findings of this investigation are summarized and discussed in this chapter: firstly, in relation to the density variation in the preform and secondly, to the extent of lubricant migration during preforming. An empirical relationship that relates resin SSG and preforming pressure to the effective length of the preform (that is the length at which density begins deviating) is proposed. In addition, the effect of applying pressure on both ends of the mold during preforming is also discussed, before the chapter is concluded in Section 6.7.

6.2 Effect of Preforming on Extrusion Pressure

Figure 6.1 plots the extrusion pressure profiles obtained using the capillary rheometer under the same extrusion conditions, with the preforms produced at the same pressure but

handled differently. In case (i), the top of the preform was extruded first, that is, the preform was turned upside down in the barrel. In case (ii), the top of the preform was extruded last. In case (iii), preforming was performed on both ends of the paste. It can be seen that the paste near the end at which pressure was applied during preforming, i.e., the top portion of the preform, extrudes at a lower pressure than that of the other end. This is shown as an increase in pressure during the course of extrusion for case (i) and a decrease in pressure for case (ii). When preforming is performed on both ends, the extrusion pressure in region II appears to be more uniform.

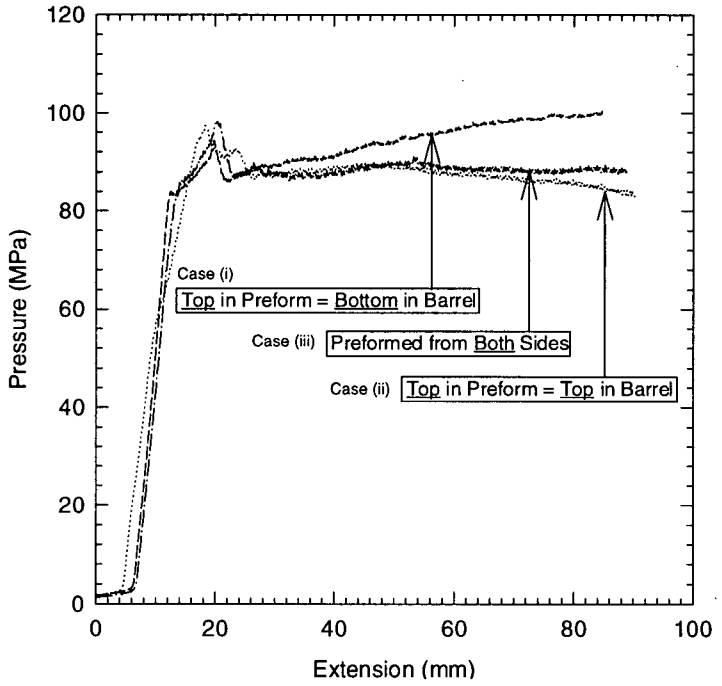

Fig. 6.1 Effect of non-uniform preform densification on the transient pressure profile during extrusion (performing pressure of 2 MPa).

Visually, there is also an apparent difference between the top and the bottom portions of the preform. This can be seen in Fig. 6.2, where photographs of the two ends of a preform are shown. The compacted (top) end (Fig. 6.2 (i)) looks smoother, while the opposite end (Fig. 6.2 (ii)) looks rougher and more granular. This is due to radial lubricant migration and densification that are more pronounced in the top part of the preform. From these observations, it may be concluded that the applied pressure is dissipated after a certain distance along the preform. Macleod and Marshall (1977) have proposed that, besides being

used to compact the paste, the applied pressure is also used to overcome frictional forces, which manifest themselves between powder particles and along the wall of the preforming unit. Hence, the paste far from the compacted surface does not experience as much pressure, unlike in a liquid system where pressure is distributed uniformly and instantly throughout. It was also found that this effect is more pronounced with paste of higher molecular weight, as will be discussed later.

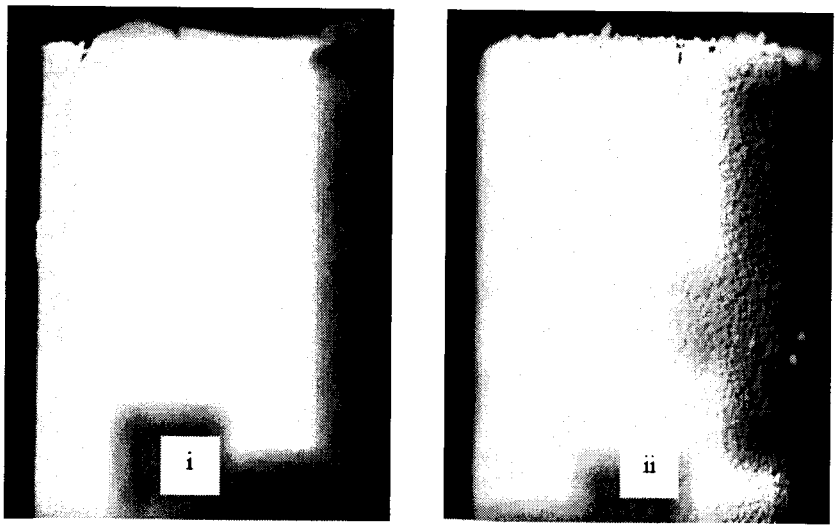

Fig. 6.2 Photographs showing parts of a typical PTFE preform: (i) top and (ii) bottom. The top portion is the end at which pressure is applied.

6.3 Density Studies

6.3.1 Effect of Preforming Pressure

Figure 6.3 shows a typical density variation along the preform for a high and a low molecular weight resin at different levels of pressure. It can be seen that the portion of the preform near the point where pressure was applied (top) generally has a higher density. Physically, this portion also looks smoother and glossier, compared to the bottom part of the preform, which looks rougher, drier and more granular (see Fig. 6.2). This indicates a non-uniform densification of the preform.

During preforming, the resin particles are highly compacted and those adjacent to the wall of the preforming unit undergo plastic deformation that results in a smooth film of deformed powder surrounding the preform. This layer keeps the rest of the resin particles

inside and protects them from premature mechanical damage. It has been shown previously that these particles remain spherical even after high pressure preforming (Mazur, 1995). This can also be seen from Fig. 6.4, where SEM micrographs of the preform surface are shown at two different magnifications. The highly compressed powder forms a film and appears as a dark region in Fig. 6.4 (ii). It can be seen that the particles surrounded by this film remain spherical. It is noted that no fibrillation occurs on the preform surface, since all particles are moving in a plug flow manner and no extensional or shear forces are present.

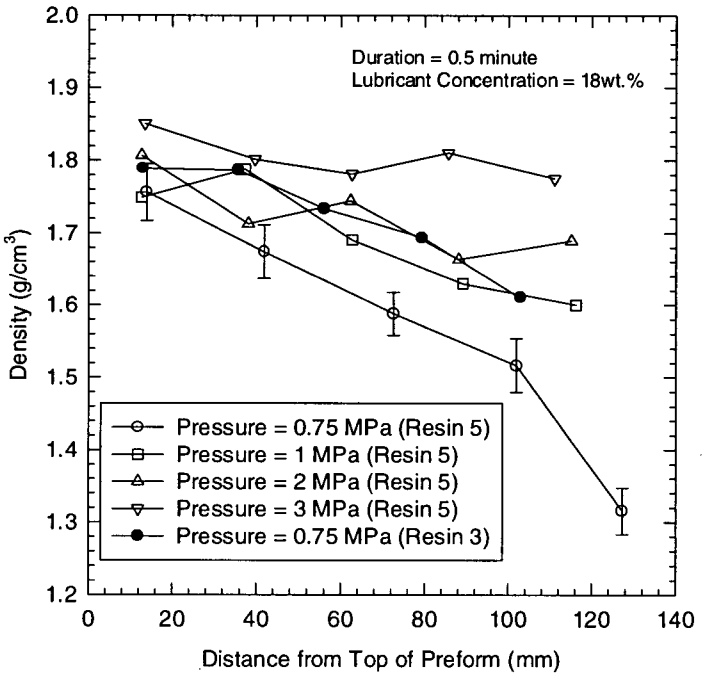

Fig. 6.3 Density variation along preforms for the high molecular weight (open symbols) and low molecular weight (closed symbols) resins. The preforming duration was kept constant at 0.5 minute. Error bars, indicating the standard deviation of duplicate runs, are shown only for one of the plots for clarity reasons. Similar levels of reproducibility apply to the other results.

The high pressure at the top of the preform results in a greater extent of powder compaction in that area. This causes the displacement of the lubricant (the mobile phase) from the spaces between particles to all directions, including the radial direction towards the wall, causing this part of the preform to look glossier. As a result, the peripheral surface of this portion of the preform will be more lubricated and will extrude at a lower pressure, as discussed above with reference to Fig. 6.1.

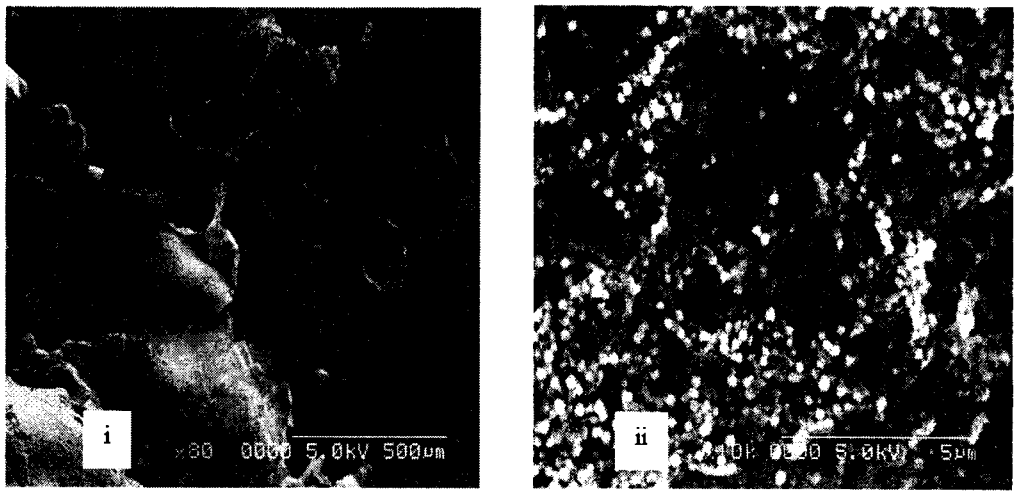

Fig. 6.4 SEM micrographs showing a typical surface of a perform with magnifications of (i) 80x and (ii) 10,000x.

In Fig. 6.3, one can see that a pressure of 0.75 MPa is insufficient to ensure relatively even densification throughout the preform. The lower part of the preform still contains significant air voids, and insufficient lubricant has been displaced radially towards the surface. This explains the higher pressure, which is generally observed with the extrusion of the lower part of the preform (see Fig. 6.1 and the text referring to Fig. 6.1). A pressure of 3 MPa seems to be the minimum pressure necessary to produce approximately 120 mm of uniformly dense preform using this particular paste (resin 5). It was found that this pressure varies depending on the molecular weight of the resin. For example, the same extent of densification can be achieved for paste of lower molecular weight (higher SSG) at a lower preforming pressure. In Fig. 6.3, the density variation along the preform made using resin 3 at 0.75 MPa is also shown for comparison. One can see that the density variation is less for resin 3 than that of resin 5 at a comparable pressure.

The relative total average preform density, normalized with the corresponding SSG value to account for the different molecular weights, is plotted versus preforming pressure in Fig. 6.5. It can be seen that the total average density is generally lower for preform made of resin with lower SSG (higher molecular weight). This is especially apparent at lower preforming pressures. At higher pressures, the total average preform density becomes approximately independent of molecular weight.

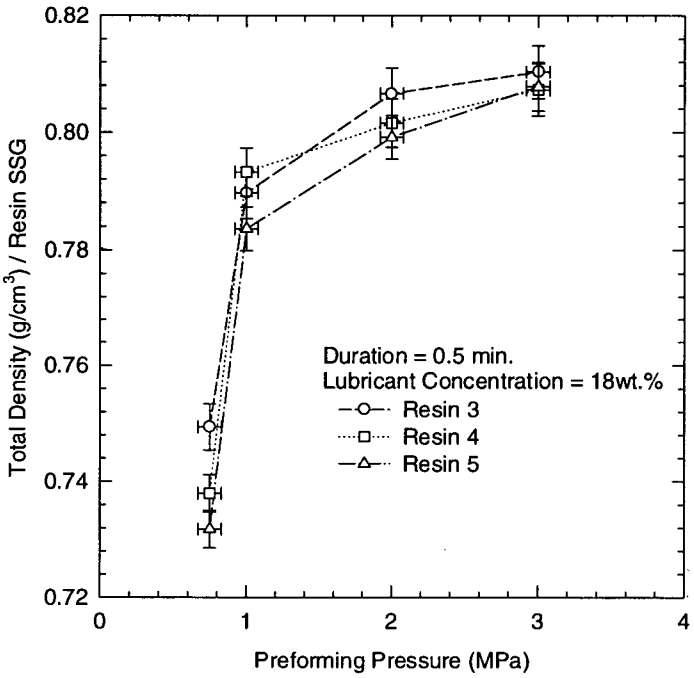

Fig. 6.5 Total average preform density for the three resins, normalized with respect to the individual resin SSGs, as functions of preforming pressure.

These results suggest that resin particles form a highly dense and resistive layer near the top surface of the preform that dissipates most of the extrusion pressure. For paste of higher molecular weight (lower SSG), possibly due to the harder (see discussion below) and larger resin particles, higher pressure is required to cause yielding. If the pressure is insufficiently high, particles are not being pushed down the preform, creating only a small portion of dense preform near the top. Hence, pressure is not transmitted axially, and this causes a large variation of density along the preform length. Since only a small portion of the preform is densely compacted, the overall average preform density will be low. As one would expect, this becomes especially significant at lower preforming pressures. For paste of lower molecular weight, the resistive layer near the top of the preform yields at a lower pressure. Hence, at the same preforming pressure, particles are now more "mobile" along the preform. Consequently, the density variation along the preform is less, and the overall preform density is higher. A good analogy to this may be that of pouring particles through a conical funnel. Blocking of the funnel opening is more likely to occur if the particles are harder and larger, and a higher pressure force is required to remove such a blockage. This

explains the relative ease of compacting a paste, which is composed of a lower molecular weight (higher SSG) resin, having softer particles, as will be discussed later.

To further study the bulk compression behavior of PTFE resins, each resin of predetermined mass was compressed in the preforming unit without lubricant at a piston speed of 0.21 mm/s. The pressure was monitored as a function of time. At a particular time, the volume of the resin in the preforming unit and hence, the resin density, can be calculated knowing the piston speed and the total length and diameter of the preforming unit. The results are plotted in Fig. 6.6 as a function of pressure. It can be seen that the bulk compressibility of each resin is approximately the same, as indicated by the same slope at each pressure. However, there is a jump in density at about 5.5 - 7.5 MPa, as shown in the insert of Fig. 6.6. The jump is more sudden in the case of resin 3, occurring at a lower pressure. In the case of resin 5, the density increases over a larger pressure interval. This sudden jump in density implies that the resin is yielding, where the bulk volume of the resin suddenly gives way to the applied pressure.

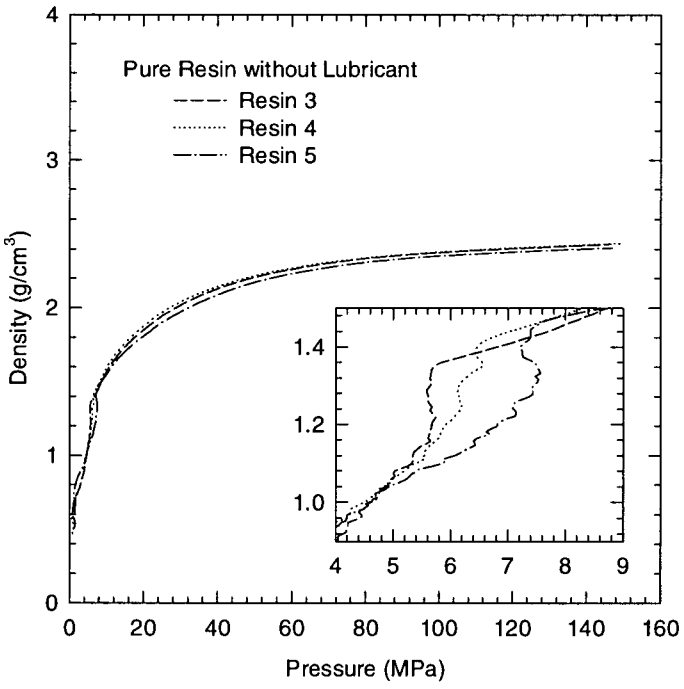

Fig. 6.6 Bulk (volume) compressibility of unlubricated resins 3, 4, and 5 at room temperature under the application of a changing pressure applied by means of a piston moving at constant speed.

6.3.2 Effect of Preforming Duration

Preforming duration is defined as the length of time the paste is pressed at a specified pressure. Figure 6.7 plots the density variation along the preform for the high molecular weight paste (resin 5) produced with a preforming pressure of 0.75 MPa for different preforming durations. One can see that longer preforming duration produces less axial density variation, which is as expected. The effect of preforming duration on the total average preform density is shown in Fig. 6.8. One can see that, at longer times, the preform becomes denser and hence, contains less voids. This is interesting since it indicates that time relaxation is involved. The resistive layer of paste near the top surface of the preform relaxes with time and dissipates its normal stresses onto the adjacent layer. This process continues eventually distributing the applied stress to the rest of the preform body as much as the time allows. As a result, the preform becomes denser and more uniform with time.

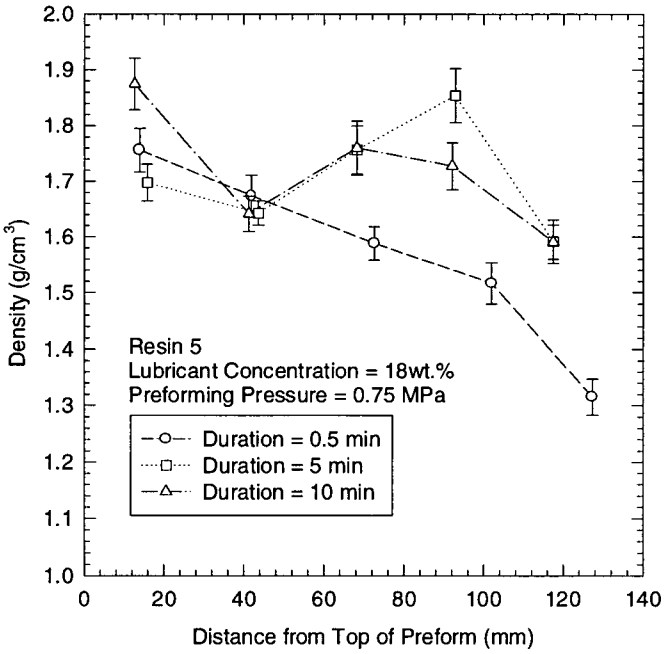

Fig. 6.7 Density variation along preforms produced at 0.75 MPa with different preforming durations for the high molecular weight resin (resin 5).

The time relaxation behavior of the three resins was investigated and the results are plotted in Fig. 6.9. The pure PTFE resins were initially compressed to a pressure of 140 MPa. The pressure for each resin was then monitored with time. It can be seen that resin 5

relaxes faster than resin 3. This implies that the higher molecular weight resin is harder (more elastic), behaving like a hard rubber, compared to the lower molecular weight resin that is softer (less elastic). This explains why it is relatively easy to preform lower molecular weight PTFE paste.

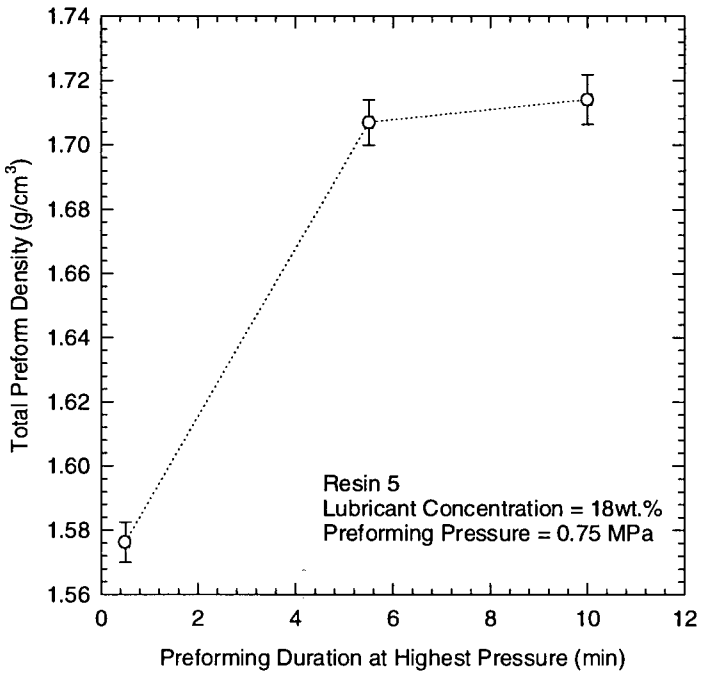

Fig. 6.8 Total average preform density for the high molecular weight PTFE resin as a function of preforming duration. Preforming pressure was kept constant at 0.75 MPa.

6.3.3 Effect of Lubricant Concentration

Figure 6.10 depicts the variation in preform density as a function of initial lubricant concentration for the high molecular weight (resin 5) paste, preformed by applying a pressure of 0.75 MPa for 0.5 minute. It can be seen that a paste having a lower lubricant concentration shows a greater density variation. Visually, its preform also looks drier and rougher. On the other hand, preforms that are made up of 20 wt.% lubricant show minimal density variation for at least 120 mm. This implies that a greater lubricant concentration allows the resin particles to slide past one another more easily, thereby making the paste more compressible. Also, being the continuous body in the paste, the lubricant is able to distribute stress more uniformly. Hence, with more lubricant in the paste, stress is more evenly distributed, resulting in a preform having lesser density variation. This can be seen

clearly in Fig. 6.10, which also contains a plot of the average preform density as a function of lubricant content.

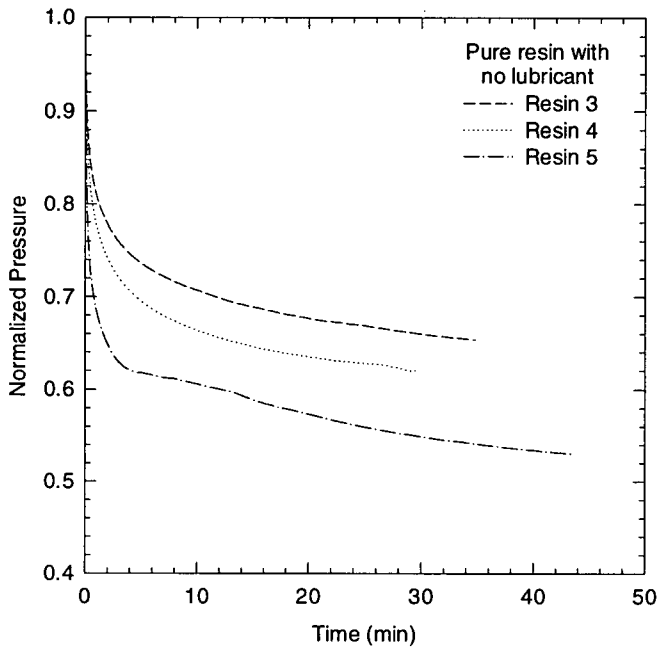

Fig. 6.9 Relaxation of pressure with time after compression of unlubricated resins.

6.4 Lubricant Migration Studies

6.4.1 Effect of Preforming Pressure

Figure 6.11 shows the lubricant concentration at various points along the preform for three pastes produced by applying different pressures for 0.5 minute. The initial lubricant concentration of the pastes was 18 wt.%. It can be seen from Fig. 6.11 that, for the range of pressures used in this work, no significant pressure effect on lubricant migration is observed during preforming. This effect may become apparent at higher preforming pressures. However, in view of practical considerations, such high pressures may be of little significance.

Comparing the profiles of the three preforms, the lubricant concentration seems to be consistently lower in the case of lower molecular weight preforms. This is not surprising, considering the fact that lower molecular weight paste is easier to preform. Better densification of preform implies that a greater amount of lubricant will be displaced towards

the peripheral region and be lost onto the surface of the preforming unit. The distribution of lubricant in the preform is also more symmetrical in the case of the low molecular weight resin (resin 3), with more lubricant being concentrated near the center region. This is consistent with the finding reported by Yu *et al.* (1999) for an alumina-starch-bentonite-water paste system. In the case of high molecular weight PTFE (resin 5), however, lubricant concentration is much lower near the top, relative to the bottom. This is due to better compaction near the top region of the preform, resulting in greater lubricant displacement towards the surface of the preforming unit and hence, lower lubricant concentration in the preform body. The bottom region is not as dense and looks drier, indicating that lubricant is not displaced to the periphery but remains trapped inside the paste.

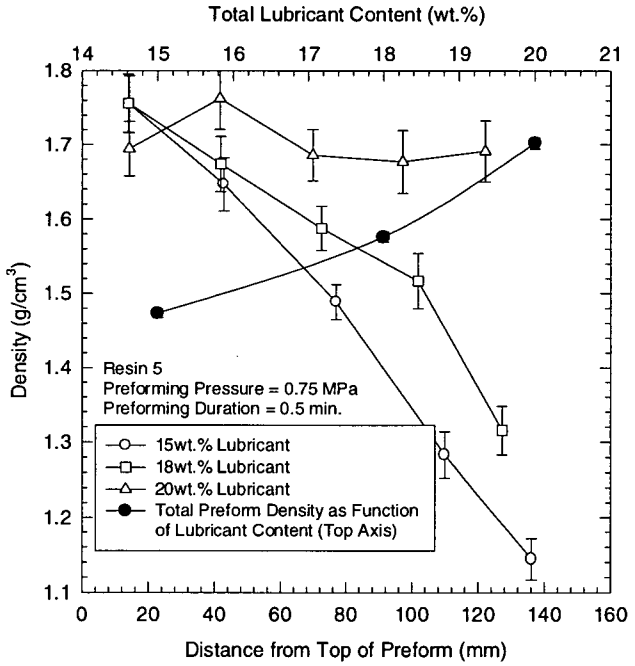

Fig. 6.10 Density variation along preforms (high molecular weight resin) and total average preform density as functions of initial lubricant concentration. Preforming was carried out at 0.75 MPa for 0.5 minute.

This observation is intriguing. Although preforming pressure significantly affects the distribution of density along the preform, it does not significantly affect the extent of lubricant migration. As far as lubricant migration is concerned, the effect of molecular weight far outweighs the effect of preforming pressure, for the range of pressure

investigated. However, an effect of preforming pressure on lubricant migration should not be ruled out as it is expected to become more significant at higher pressures.

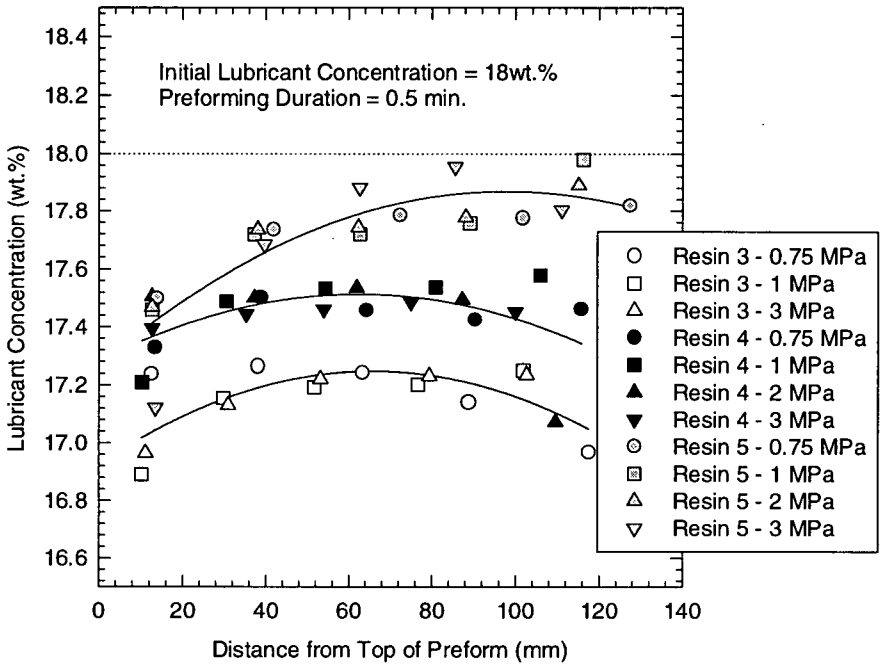

Fig. 6.11 Lubricant concentration along preforms produced by applying different levels of pressure for 0.5 minute.

6.4.2 Effect of Preforming Duration

Due to the presence of the liquid phase, the length of time for which preforming is carried out is expected to have a significant effect on the quality of the preform. Figure 6.12 shows the effect of preforming duration on lubricant distribution in the high molecular weight preform (resin 5), produced by applying a pressure of 0.75 MPa. One can see that the effect is significant. At 0.5 minute, the lubricant concentration is relatively constant along the preform. At longer times, a gradient of lubricant concentration develops. Due to the loss of some lubricant at the wall of the preforming mold, the lubricant concentration in the preform is generally lower than 18 wt.%.

During preforming, the pressure imposed at the top surface of the preform provides a driving force, in addition to the force of gravity, for the lubricant to migrate downward. Keeping the preforming pressure constant for a longer period of time will result in a more

severe lubricant migration and hence, a greater lubricant concentration gradient. Consequently, at longer times, lubricant concentration becomes higher near the bottom of the preform, as shown in Fig. 6.12. It can be seen that the bottom part of the preform may have a lubricant concentration even higher than the original 18 wt.% when the preforming duration is sufficiently long. Hence, in such cases, the top part of the preform will extrude at a higher pressure, while the bottom part of the preform may become "too wet" and extrude at a lower pressure, resulting in an extrudate of varying strength. (It has been previously reported that unnecessarily large lubricant concentration will result in a weak extrudate (DuPont, 1994; Ebnesajjad, 2000).) Therefore, while longer preforming duration may reduce the variation in preform density, it significantly increases the extent of lubricant migration. This results in a preform with a gradient of lubricant concentration, which, for practical reasons, is much less attractive.

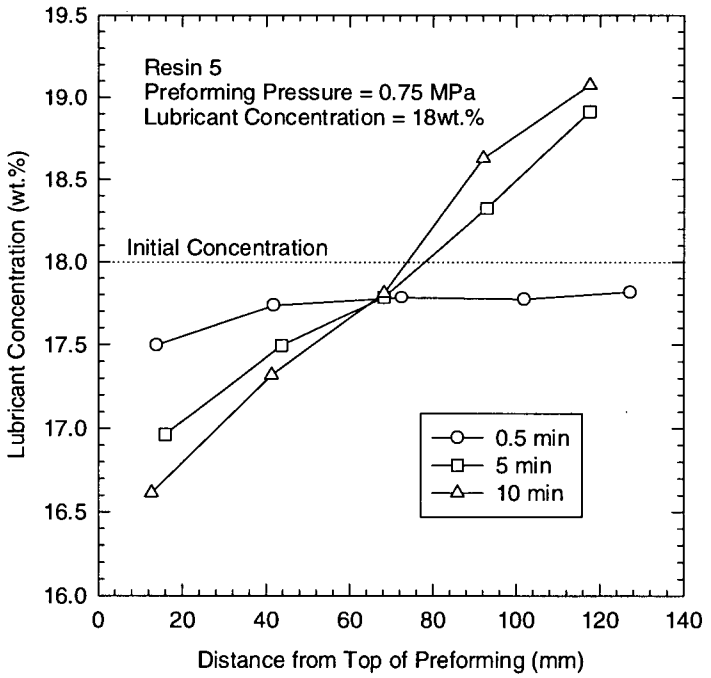

Fig. 6.12 Lubricant concentration along preforms produced at 0.75 MPa with different preforming durations (high molecular weight resin).

6.4.3 Effect of Lubricant Concentration

The effect of initial lubricant concentration on lubricant migration is shown in Fig. 6.13. It can be seen that a paste with greater initial lubricant concentration will produce a

preform having a larger lubricant concentration gradient, which is not surprising. Therefore, while increasing the lubricant concentration decreases the variation in preform density, it does so by increasing the extent of lubricant migration. It should be noted, however, that the results in Fig. 6.13 correspond to short preforming duration of 0.5 minute. The variation in lubricant concentration along the preform is expected to be more significant when longer preform times are used.

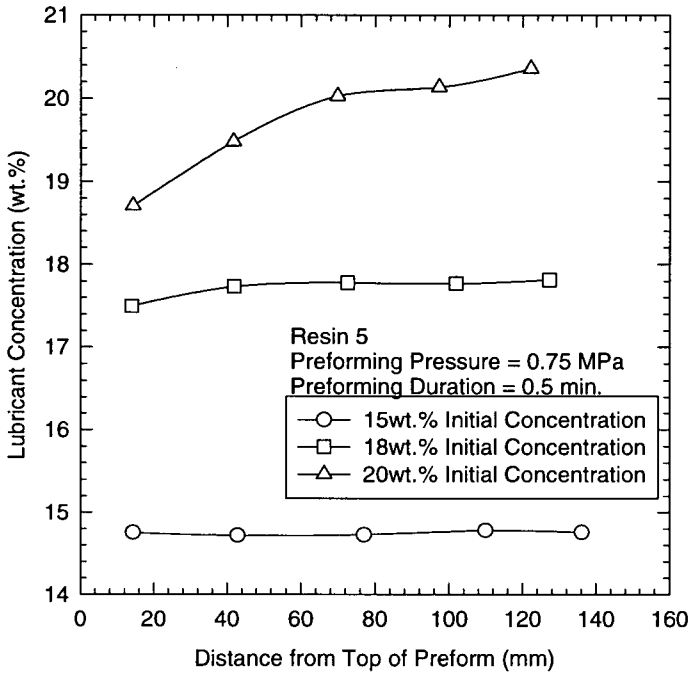

Fig. 6.13 Lubricant distribution along preforms having different initial concentrations of lubricant (high molecular weight resin). Preforming was carried out at 0.75 MPa for 0.5 minute.

6.5 Predicting the Effective Preform Length

From the above discussions, it is concluded that longer preforming times and higher lubricant contents increase the uniformity of preform density. However, these conditions are practically unattractive, since they promote lubricant migration. Preforming pressure seems to be the only adjustable variable since its effect on lubricant migration is relatively insignificant. Therefore, to minimize variation in extrusion pressure due to the uneven densification of the preform, it is necessary to prepare the preform by applying an adequate pressure. It was previously shown in Section 6.2.1 that this pressure varies depending on the molecular weight of the resin.

Figure 6.14 shows that the length of preform at which the density starts deviating is not a function of the total preform length. Two experiments performed using different amounts of paste indicated approximately the same variation of preform density. The extent of lubricant migration, however, is greater in the case of the shorter preforms, due to the fact that the same pressure is applied over a shorter distance (higher pressure gradient).

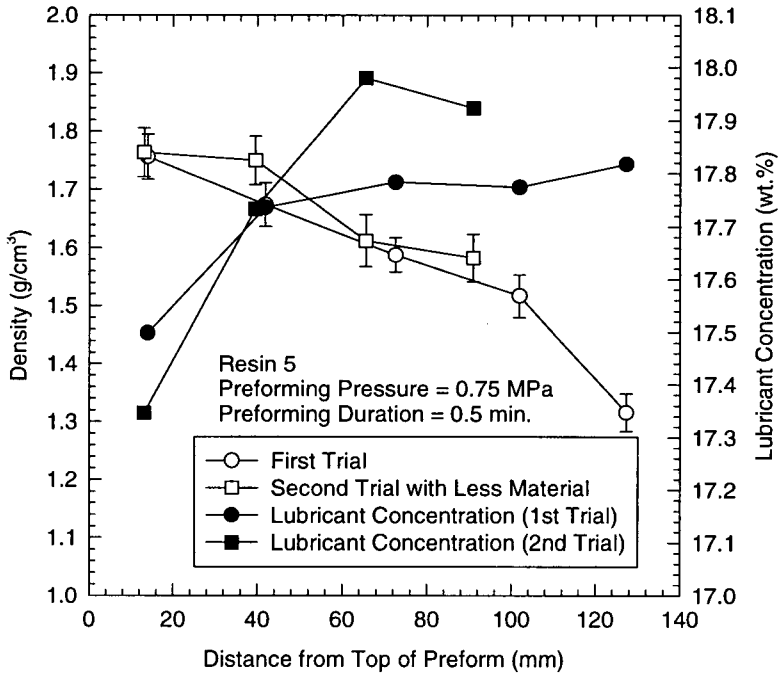

Fig. 6.14 Density variation and lubricant distribution along preforms having different lengths.

From experimental results such as those plotted in Fig. 6.3, it is possible to determine the effective lengths of preform at which the density starts deviating for the different resins at different levels of preforming pressures. Such experimental results were analyzed and found to be a function of resin SSG and preforming pressure, as shown in Fig. 6.15. For a performing pressure between 0.75 MPa and 3 MPa, and a lubricant concentration of 18 wt.%, the effective length of preform (l^*) can be written as a function of SSG and preforming pressure as:

$$l^*(mm) = a.SSG.[P(MPa)]^b + c, \qquad (6.1)$$

where l^* is taken to be the length when density starts to deviate by approximately 0.05 g/cm^3, and a, b and c are empirical constants, which are found to be *857*, *0.0229* and *-1817*,

respectively for the homopolymer PTFE pastes studied in this work. These constants are expected to vary with the initial lubricant concentration. For the high molecular weight paste at a preforming pressure of 0.75 MPa, the effective length correlates linearly with the initial lubricant concentration in a semilog plot, as shown in Fig. 6.16.

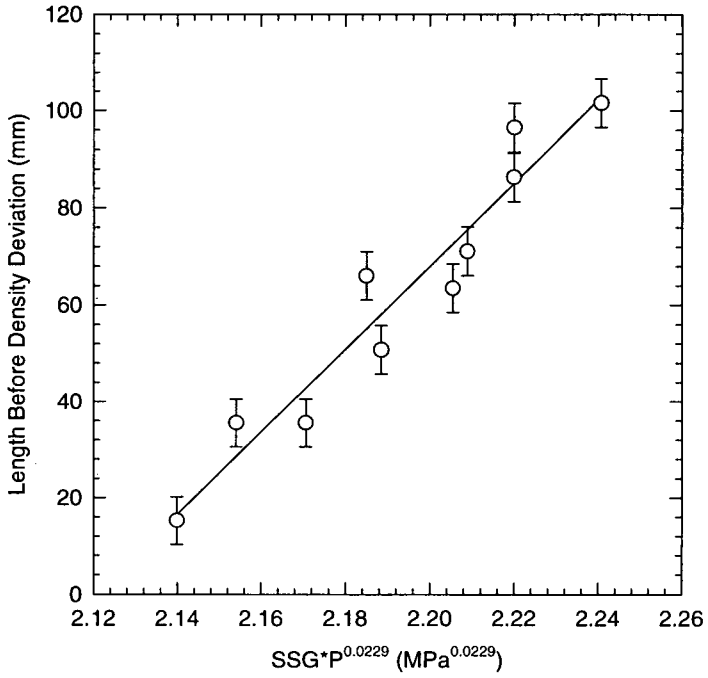

Fig. 6.15 Length of preform of uniform density as a function of resin SSG and preforming pressure.

Equation (6.1) indicates that a higher pressure is required to produce a certain length of preform of uniform density for a lower SSG or higher molecular weight resin. As discussed above, this is partially due to the hardness of the high molecular weight resin, causing it to yield at a higher pressure during compression. The larger raw particle dispersion size of the high molecular weight resin also contributes to this effect. Larger particles tend to be less mobile during compression, requiring greater pressure for densification.

Although Eq. (6.1) is empirical in nature, it is useful for determining the preforming pressure that will adequately produce a certain length of uniformly dense preform. It should be noted that preform diameter may also have a significant effect on these results (Macleod

and Marshall, 1977) but has not been considered in this discussion. This issue should be the subject of a future study.

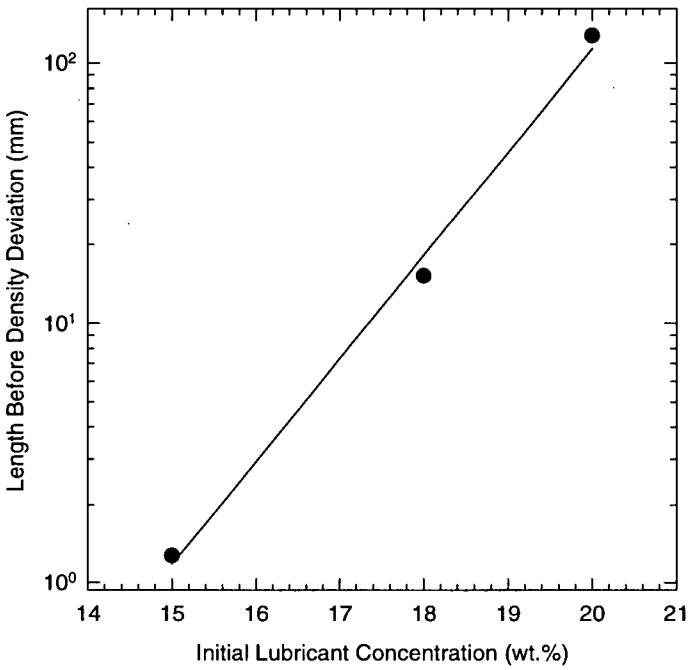

Fig. 6.16 Length of preform of uniform density as a function of initial lubricant concentration for the high molecular weight resin (resin 5).

6.6 Effect of Preforming From Both Ends

Preforming by applying pressure on both ends will decrease the variation of density as shown in Fig. 6.17. However, the total variation in lubricant concentration remains approximately the same, with the maximum concentration near the middle of the preform. This finding is encouraging. It indicates that an evenly dense preform may be produced at a lower pressure by compacting the paste at both ends without sacrificing the preform quality in terms of lubricant migration. In this case, pressure was applied first on one end and subsequently on the other. Consideration of applying pressure on both ends simultaneously would certainly lower lubricant concentration gradient further.

6.7 Conclusions

Preforming is a critical part of the paste extrusion process. It has been shown that preforming pressure and duration significantly affect the quality of preform. Lack of

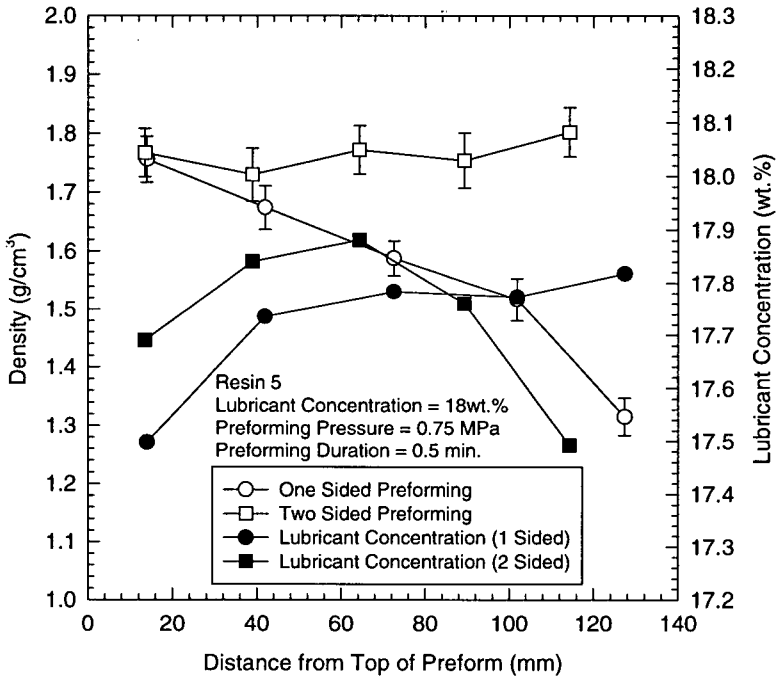

Fig. 6.17 Effect of preforming from both ends on density and lubricant distribution (high molecular weight resin).

adequate pressure will result in a preform of non-uniform density which will extrude unsteadily, resulting in an unacceptable final product. Increasing lubricant concentration and preforming time improves the uniformity of preform density, indicating that the process of preforming is time dependent. However, lubricant migration becomes important at longer times. This leaves preforming pressure as the only adjustable parameter. It was found that the pressure required to adequately produce a preform of uniform density depends on the molecular weight (standard specific gravity) of the resin. It has been shown that lower molecular weight PTFE resin (higher standard specific gravity) has softer particles, which are easier to compact. Finally, it has been shown that making a preform by compacting the paste on both ends improves the uniformity of preform density without sacrificing its quality in terms of lubricant distribution.

CHAPTER 7:

MECHANISM OF PTFE PASTE FLOW

7.1 Introduction

The flow mechanism associated with PTFE paste extrusion differs significantly from polymer melt flow. In paste extrusion, for example, the distribution of the liquid phase in the paste matrix during high pressure extrusion is an important issue, especially when longer extrusion times are involved, which may cause a non-uniformity of the liquid distribution (Mazur, 1995). Also, microscopically, solid state PTFE molecules are confined in their crystallite and spherulite configurations, while in polymer melt, molecules are randomly positioned, not conformed to a specific shape, and are significantly more mobile. In a number of ways, the process of PTFE paste extrusion is more similar to ceramic paste processing. However, since fibrillation is involved in the mechanism of PTFE paste flow (as will be discussed later), the resulting extrudate is relatively much stronger. For example, in PTFE paste extrusion, free flowing powder is processed to form a preform of some initial yield strength and later, an extrudate of significant strength (due to fibrillation) that is commercially useful, even without sintering, such as in the case of calendered PTFE tape (Ebnesajjad, 2000).

In this chapter, the mechanism of PTFE paste flow during extrusion is discussed. SEM, which was used to "track" the morphological changes that occur during the course of the process, provides an insight into the development of extrudate strength from free flowing paste and hence, the formation of fibrils. To understand the deformation pattern involved therein, visualization experiments were performed, and the results are discussed in a separate section. Finally, a "radial flow" hypothesis is proposed to describe the flow pattern of the paste in the contraction zone of the die, where fibrillation was found to occur.

7.2 Morphological Development during PTFE Paste Extrusion

To determine the morphological changes that take place during the course of PTFE paste extrusion, SEM was performed on the PTFE paste before and after preforming, as well as after extrusion. Typical SEM micrographs are shown in Fig. 7.1 for resin 2. It can be

seen that the unprocessed particles of PTFE powder are spherical in shape and have a uniform size distribution (Fig. 7.1 (a)). After high pressure preforming, the solid particles of the paste still retain their spherical shape (Fig. 7.1 (b)). This is due to the presence of the liquid phase that, besides acting as a lubricant, also provides a cushioning effect to the resin particles, preventing premature fibrillation from occurring as they slide past one another (Mazur, 1995). After extrusion through a tapered die, the resin particles remain generally spherical and do not appear deformed (Fig. 7.1 (c)). However, they are now connected to each other by fibrils of submicron size, which account for the final strength of the extrudate. This indicates that the creation of fibrils occurs in the die conical zone. Furthermore, judging from the typical thickness of a fibril and considering the fact that the resin particles remain spherical after extrusion (indicating no permanent shape deformation), it is reasonable to exclude the possibility of fibrils as being deformed particles. Instead, it is more likely that fibrils are collections of molecules that have been unwound from their crystallite configurations. In Fig. 7.1 (c), one can also see a definite preferred orientation of these fibrils in the flow direction, which may be further improved by calendering (Ebnesajjad, 2000) or using dies of longer L/D ratio (this will be discussed in Chapter 9).

7.3 Mechanism for Fibrillation

A proposed mechanism for fibrillation is shown in Fig. 7.2. During the extrusion process, compacted resin particles entering the die conical zone are highly compressed due to the reduction in the flow cross-sectional area. The amorphous regions of the PTFE crystallites (see Fig. 1.3) in neighboring particles then begin to mechanically interlock, as the particles rub against one another under the application of high pressure, while competing for an exit out of the die. This results in the interconnection of adjacent particles. At the exit of the die, these connected particles experience an accelerated flow, during which the mechanically locked crystallites are consequently unwound, creating fibrils. The particles later relax and return to their original spherical shape.

It is important to note that high pressure extensional flow such as that which occurs in the die conical zone is necessary for fibril creation. Simple shearing action of loosely compacted paste at a relatively low pressure does not result in a practically useful extent of fibrillation. This can be seen in Fig. 7.3, which shows a SEM micrograph of a PTFE paste

(resin 2) obtained after a simple shearing action between two circular plates, one of which rotates in a cyclic manner (parallel plate rheometer). When Fig. 7.3 and Fig. 7.1 (c) are compared, the difference in the extent of fibrillation is clear.

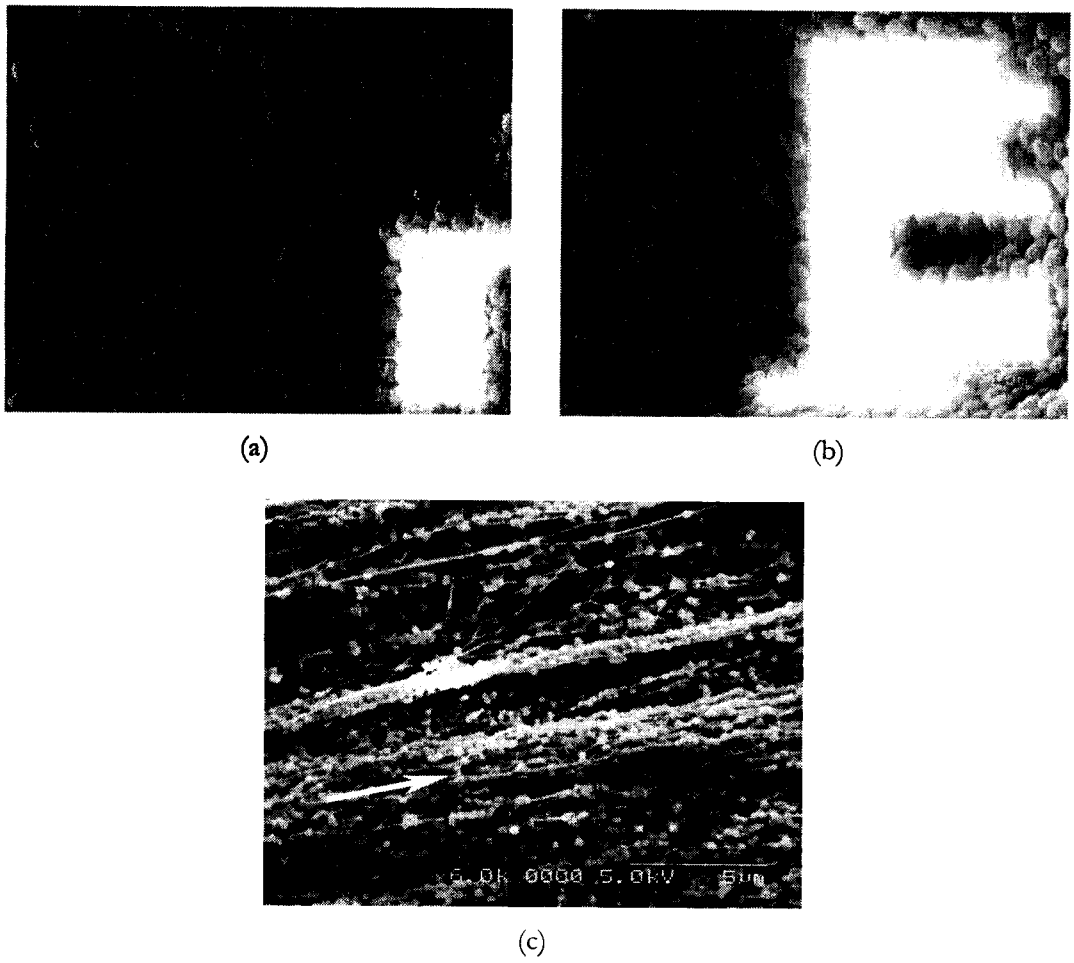

Fig. 7.1 SEM micrographs of resin 2: (a) before processing (virgin), (b) after preforming, and (c) after extrusion. Similar morphologies are observed for other pastes.

To test the validity of the proposed mechanism, DSC analyses were performed on the extruded samples. Since the value of the PTFE first heat of melting, ΔH_{m1}, is directly proportional to the degree of the resin crystallinity (Cavanaugh, 1999), unwinding of crystallites should result in a decrease in the ΔH_{m1} value. Therefore, an extruded (i.e. fibrillated) sample is expected to have a lower ΔH_{m1} value compared to that of the virgin resin. ΔH_{m1} values of extrudates obtained under various extrusion conditions for different resins are compared with the corresponding ΔH_{m1} values of the virgin resins in Fig. 7.4

(ΔH_{m1} values of virgin resins were obtained by performing differential scanning calorimetry on the corresponding dried pastes). It can be seen that fibrillation has apparently decreased the degree of resin crystallinity, as indicated by the consistently lower ΔH_{m1} values of the extruded samples. These results help validate the proposed mechanism for fibrillation discussed above. The difference in the ΔH_{m1} values before and after extrusion should, therefore, provide a quantitative indication of the extent of fibrillation that has occurred during the extrusion process. This will be discussed in more detail in Chapter 9.

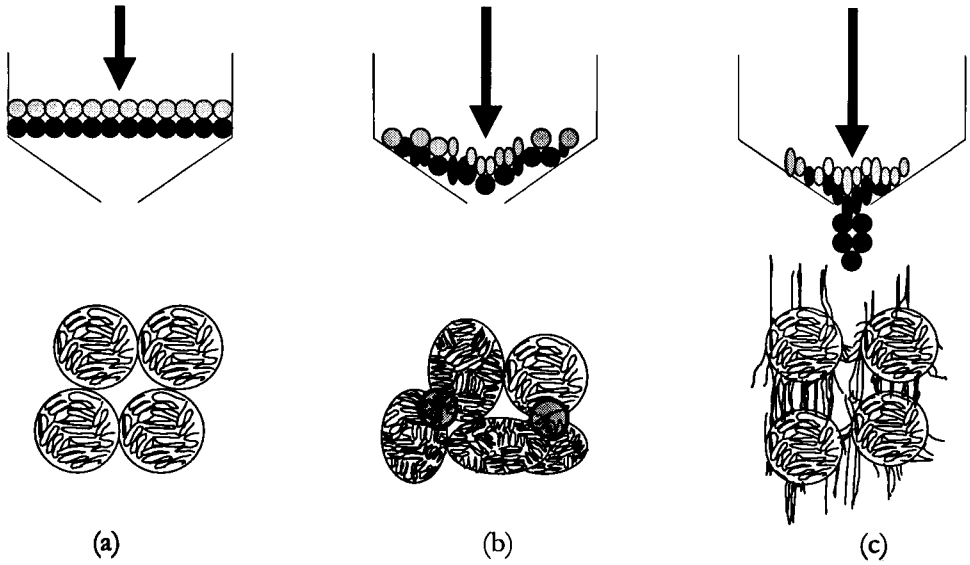

Fig. 7.2 Schematic diagram illustrating the proposed mechanism for fibrillation: (a) compacted resin particles enter the die conical zone, (b) resin particles are highly compressed and in contact with one another in the die conical zone, resulting in the mechanical locking of crystallites, (c) upon exiting the die, particles return to their original spherical shape, and entangled crystallites are unwound, creating fibrils that connect the particles.

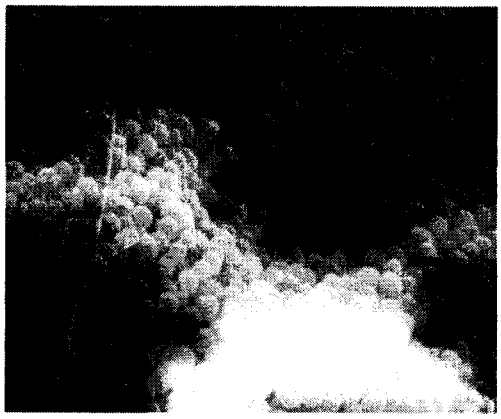

Fig. 7.3 SEM micrograph of resin 2 after shearing in a parallel plate rheometer.

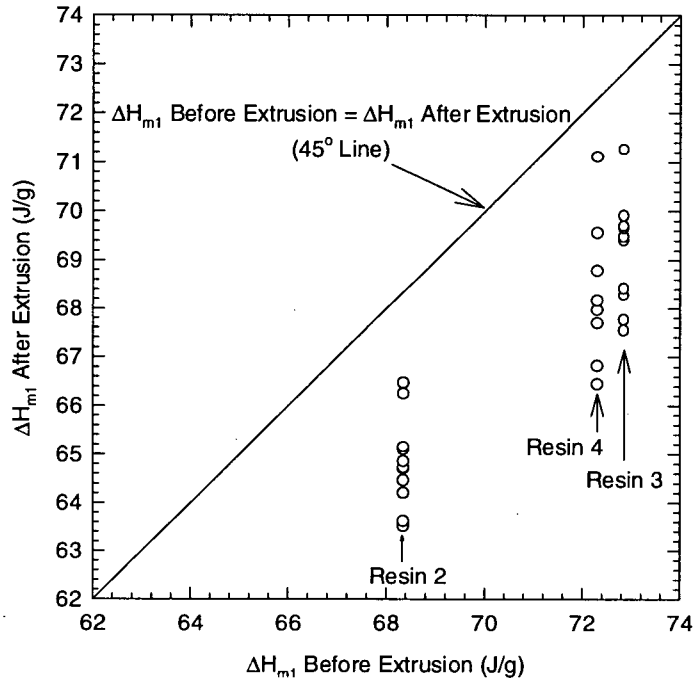

Fig. 7.4 Values of the first heat of melting obtained from DSC analysis for pastes before and after extrusion under various conditions.

7.4 Pattern of Flow Deformation

7.4.1 Visualization Experiments

By extruding alternate layers of colored and uncolored disks of paste as described in Chapter 4, the pattern of PTFE paste flow during the extrusion process can be determined. Typical results from the visualization experiments are shown in Fig. 7.5. It can be seen that in the barrel (Fig. 7.5 (a)), the paste moves in a plug flow manner with no radial velocity gradient, as indicated by the layers of paste that remain horizontally level. In the conical zone of the die, radial and axial velocity variations become more apparent. It can be seen that the center particles move towards the die apex at a velocity greater than that of the peripheral particles. This is more pronounced in a die with a greater entrance angle. In fact, when a die with an abrupt contraction ($\alpha = 90°$) is used, the paste forms a static zone at the die corner, where it becomes highly compacted and, consequently, much drier than the flowing paste. This results in the flow being streamlined at an effectively smaller entrance angle, implying

that there exists a critical entrance angle beyond which there is no further effect on the flow pattern development.

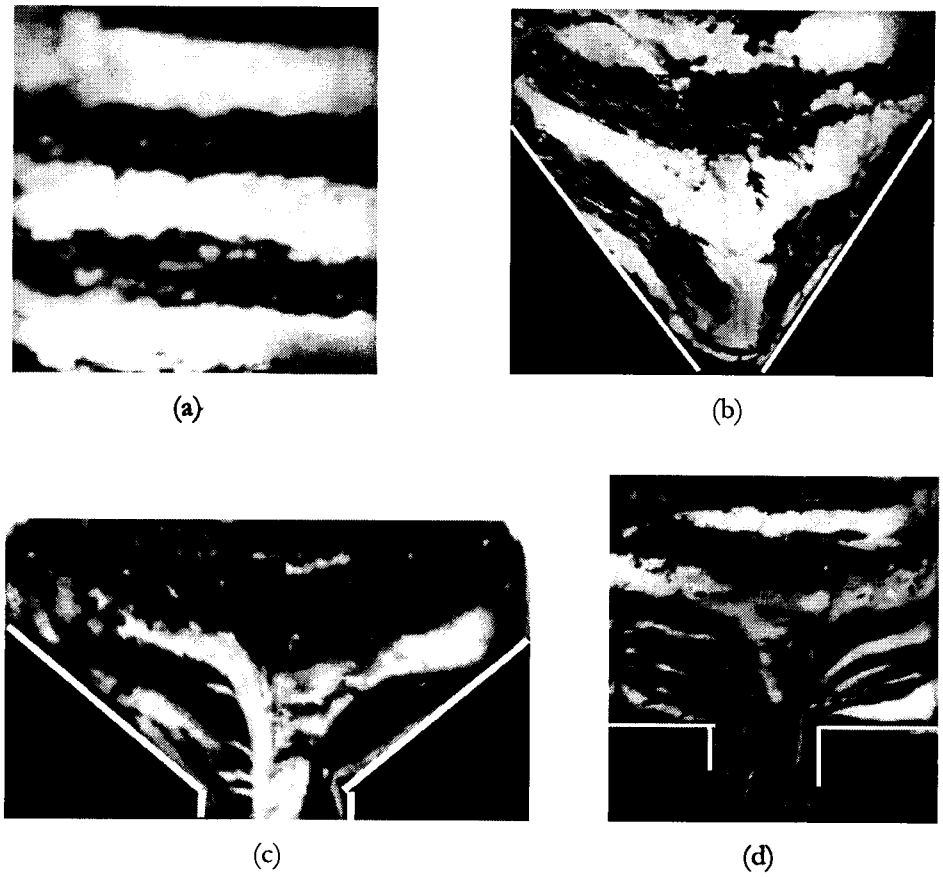

Fig. 7.5 Velocity profiles obtained from visualization experiments: (a) in the barrel, (b) in the die conical zones with $\alpha = 30^{o}$, (c) $\alpha = 45^{o}$, and (d) $\alpha = 90^{o}$.

7.4.2 Radial Flow Hypothesis

Snelling and Lontz (1960) have proposed the "Radial flow" hypothesis to describe the flow of PTFE paste in the conical zone of the die (see Chapter 2). The hypothesis assumes that paste particles at the same radial distance from the virtual apex of the die conical zone move towards the die apex at the same velocity. In other words, the hypothesis assumes the existence of a virtual spherical surface of radius r, as measured from the die apex, which spans over an angle of 2α, describing the position of the paste particles that move at the same velocity. This is illustrated in Fig. 7.6. By performing similar visualization experiments as those described above, and measuring the distances of the center and the corresponding peripheral particles from the die apex, and comparing them with the predictions obtained

from the "radial flow" hypothesis, Snelling and Lontz (1960) have shown the consistency of this hypothesis with experimental observations. In support of this claim, the positions of the paste particles in the die conical zone as they move towards the die exit have been tracked mathematically in this work for various α, using the following equation:

$$\frac{dr}{dt} = -\frac{Q}{2\pi(1-\cos\alpha)r^2}, \tag{7.1}$$

where Q is the volumetric flow rate of the paste and the term $2\pi(1-\cos\alpha)r^2$ represents the area of the virtual spherical surface, in accordance to the "radial flow" hypothesis. The results are shown in Fig. 7.7 for α = 10°, 30° and 45°. Comparing Figs. 7.5 (b) and 7.5 (c) with Figs. 7.7 (b) and 7.7 (c), respectively, one can see that there is indeed a general similarity between the experimental and predicted patterns. In Fig. 7.7 (a), one can also see that when α is sufficiently small, the flow in the die conical zone almost follows a plug flow pattern. This implies that wall slip and hence, frictional analysis, needs to be considered when modeling the flow of paste, especially when the die entrance angle is small. For α = 90°, calculation of the velocity profile provides non-informative results, since effectively, the paste flows at a smaller angle, due to the presence of the static zone discussed above. From these calculations, it can be seen that the "radial flow" hypothesis can be validly used to describe the flow pattern of PTFE paste in the conical zone of the die. Consequently, this hypothesis will be used as the basis of the paste flow model in the subsequent chapter.

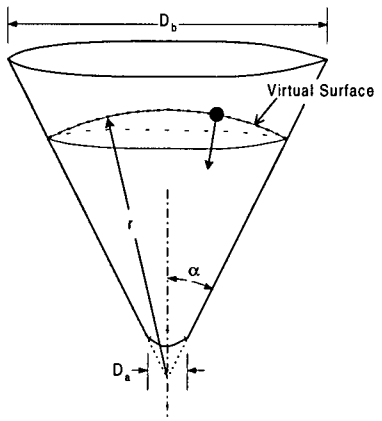

Fig. 7.6 Schematic illustration of the "Radial Flow" hypothesis. The hypothesis assumes the existence of a virtual surface of radius *r* as measured from the die apex, on which all paste particles moving towards the apex have the same velocity.

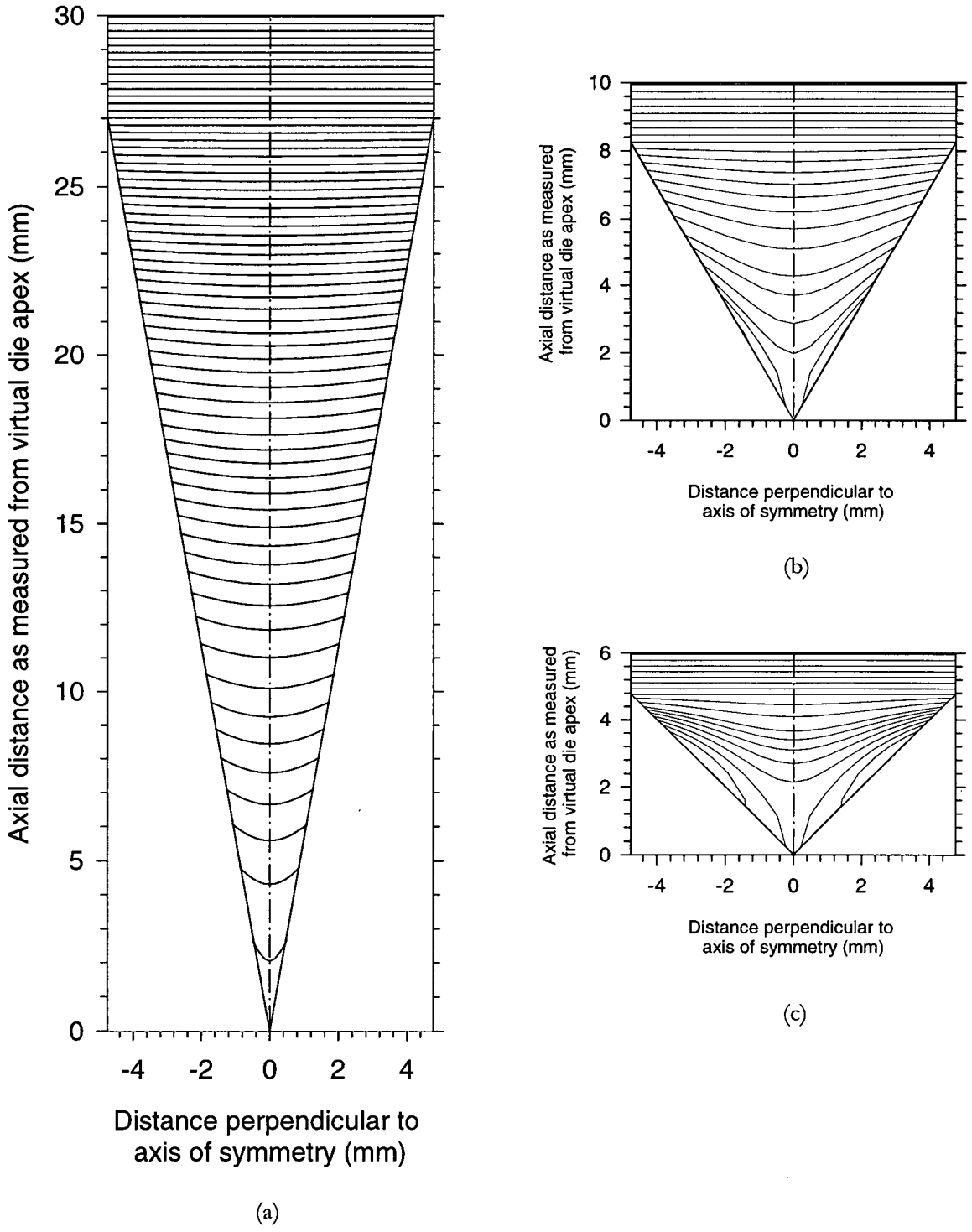

Fig. 7.7 Flow patterns in the die conical zones as calculated based on "radial flow" hypothesis with D_b = 9.525 mm, Q = 75.4 mm³/s, and (a) α = 10°, (b) α = 30°, and (c) α = 45°. Time increments were set arbitrarily.

7.5 Conclusions

The mechanism of flow involved in PTFE paste extrusion is fundamentally different from polymer melt flow. It has been shown through SEM that PTFE particles are fibrillated during the paste extrusion process. Fibrillation was found to occur at the conical zone of the die, making its design a crucial aspect of the process. A mechanism for fibrillation has been proposed and validated using DSC. The proposed mechanism considers fibrils that connect the PTFE particles in the extrudate as unwound crystallites, which are mechanically locked to one another prior to exiting the die. Through visualization experiments, the flow patterns of the PTFE paste in the barrel and in the die conical zone have also been determined. It was found that the flow in the die conical zone closely follows a plug flow pattern when the entrance angle is small. The flow pattern becomes more deformed as the entrance angle is increased. In addition, for a die with an abrupt contraction ($\alpha = 90°$), a static zone at the die corner was observed. Mathematically, it was found that the "radial flow" hypothesis is able to describe the paste flow pattern in the die conical zone consistently. The hypothesis assumes that particles at the same radial distance from the virtual die apex move towards the die apex at the same velocity.

CHAPTER 8:

RHEOLOGY OF PTFE PASTES

8.1 Introduction

This chapter discusses the rheological behavior of PTFE pastes during extrusion. A one-dimensional mathematical model, based on the "radial flow" hypothesis described in Chapter 7, is derived. The effects of extrusion conditions, in terms of extrusion temperature and rate, and the lubricant concentration in the paste, are discussed. Following this, a section is devoted to discussing the effects of die design. The model predictions are presented and discussed in the last section.

8.2 Theoretical Considerations: Development of 1-D Mathematical Model

8.2.1 Paste Flow through a Tapered Orifice Die ($L/D_a = 0$)

Figure 8.1 shows a volume element bounded by the spherical surfaces of radius r and $(r + dr)$ as measured from the virtual die apex, and by four planes at the azimuthal locations of θ, $\theta + d\theta$, ϕ and $\phi + d\phi$. The "radial flow" hypothesis implies that this element will flow towards the die apex, such that its bounding surfaces remain parallel to those at its previous position. Since the element does not rotate or deviate from its straight path, this also implies that the stresses acting on the element are purely normal stresses. In fact, these stresses are principal stresses, with the radial direction and the directions normal to the four bounding planes as the principal directions. With symmetry taken into account (i.e. $\sigma_{II} = \sigma_{III} = \sigma_\theta$), the stress tensor can, be written as:

$$\sigma = \begin{bmatrix} \sigma_I & 0 & 0 \\ 0 & \sigma_{II} & 0 \\ 0 & 0 & \sigma_{III} \end{bmatrix} = \begin{bmatrix} \sigma_r & 0 & 0 \\ 0 & \sigma_\theta & 0 \\ 0 & 0 & \sigma_\theta \end{bmatrix}. \tag{8.1}$$

The forces acting on the volume element are shown in Fig. 8.2 and the force balance in the radial direction proceeds as follows:

(a) Resultant force contribution in the radial direction from σ_r:

$$-(\sigma_r + d\sigma_r)(r + dr)^2 \sin\theta \; d\phi \; d\theta + \sigma_r r^2 \sin\theta \; d\phi \; d\theta.$$

Neglecting differentials of higher orders, this becomes

$$-r^2 \sin\theta \; d\phi \; d\theta \; d\sigma_r - 2r\sigma_r \sin\theta \; d\phi \; d\theta \; dr,$$

and integrating from $\phi = 0$ to $\phi = 2\pi$ and $\theta = 0$ to $\theta = \alpha$ yields

$$-2\pi r^2 (1 - \cos\alpha) \; d\sigma_r - 4\pi r (1 - \cos\alpha)\sigma_r \; dr.$$

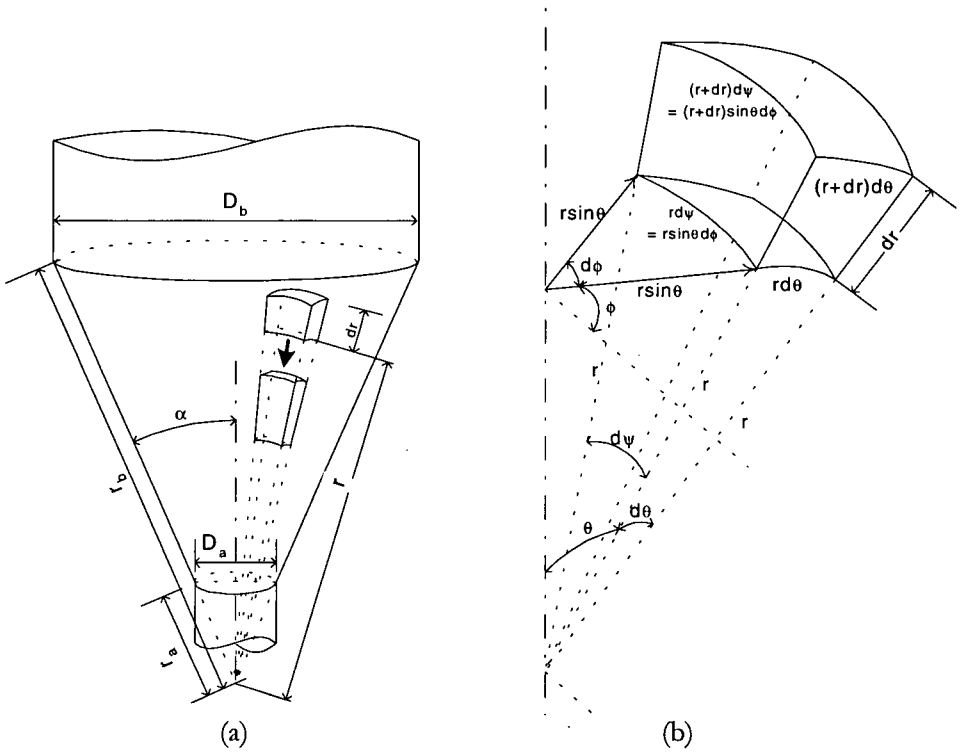

Fig. 8.1 (a) Volume element and (b) its dimensions in the conical zone of a tapered die according to "radial flow" hypothesis.

(b) Resultant force contribution in the radial direction from σ_θ:

The forces normal to the four bounding planes produce a resultant force in the radial direction of magnitude (see Fig. 8.2 (b))

$$2(\sigma_\theta r \sin\theta \; dr \; d\theta \; d\phi).$$

Integrating from $\phi = 0$ to $\phi = 2\pi$ and $\theta = 0$ to $\theta = \alpha$ yields

$$4\pi\sigma_\theta r(1 - \cos\alpha) \; dr.$$

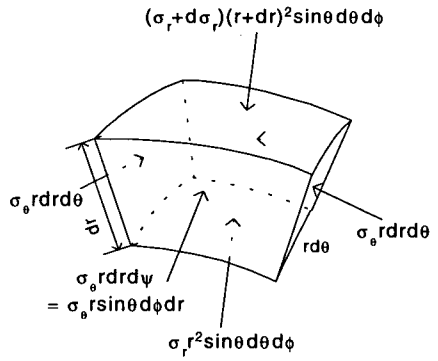

(a)

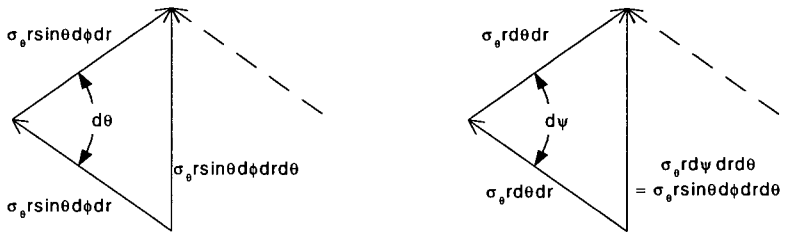

(b)

Fig. 8.2 Force balance on volume element: (a) forces acting on volume element, (b) radial contribution from the four normal forces.

(c) Frictional force contribution in the radial direction:

Coulomb's law of friction states that frictional force is proportional to the normal force acting on a surface with proportionality constant, *f*, the coefficient of friction. Hence, on the die surface, the frictional force acting in the radial direction is (see Fig. 8.3)

$$f\sigma_\theta r \sin\alpha \; d\phi \; dr.$$

Integrating from $\phi = 0$ to $\phi = 2\pi$ yields

$$2\pi f\sigma_\theta r\sin\alpha\ dr.$$

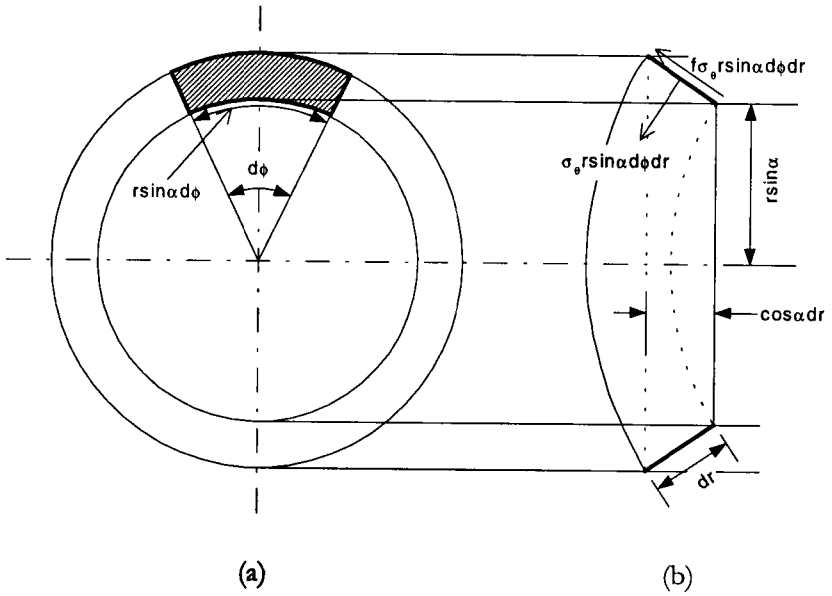

Fig. 8.3 Normal and frictional forces acting on surface element (a) top view, (b) side view.

Equilibrium condition requires that the sum of these forces vanishes, i.e.

$$-2\pi r^2(1-\cos\alpha)\ d\sigma_r - 4\pi r(1-\cos\alpha)\sigma_r\ dr + 4\pi\sigma_\theta r(1-\cos\alpha)\ dr + 2\pi f\sigma_\theta r\sin\alpha\ dr = 0. \tag{8.2}$$

By letting $B = \dfrac{f\sin\alpha}{2(1-\cos\alpha)}$ and $N_1 = \sigma_\theta - \sigma_r$, and rearranging, the following equation is obtained

$$\frac{d\sigma_r}{dr} - 2B\frac{\sigma_r}{r} = \frac{2(\sigma_\theta - \sigma_r)(1+B)}{r} = \frac{2N_1(1+B)}{r}. \tag{8.3}$$

The term N_1 is the familiar first normal stress difference in polymer melt analysis (Dealy and Wissbrun, 1990). In order to solve the above differential equation, a relationship describing the first normal stress difference for the solid-liquid (paste) system in question is, therefore, required.

For an ideally plastic material, Saint-Venant's theory of plastic flow states that, at the incipience of yielding, $N_1 = \sigma_o$, where σ_o is the initial yield stress of the material (Saint-Venant, 1870). However, for a completely plastic flow to occur within an elasto-viscoplastic material, N_1 has to sufficiently exceed σ_o so as to overcome the initial yield stress, the elastic flow zone and any viscous resistance that may develop during the flow (Hoffman and Sachs, 1953; Chakrabarty, 1998).

The generalized Newton's law for viscous flow states that $\sigma = \eta\dot{\varepsilon}$ and Hooke's law of elasticity establishes the relationship $\sigma = E\varepsilon$, where η and E are the viscosity coefficient and Young's modulus, respectively, and ε and $\dot{\varepsilon}$ are the logarithmic strain and strain rate tensors, respectively. Combining the two laws, Kelvin proposes the following stress-strain relationship for a visco-elastic material (Hoffman and Sachs, 1953):

$$\sigma = E\varepsilon + \eta\dot{\varepsilon} \quad . \tag{8.4}$$

Using the above relation, the term σ_θ - σ_r adopts the form of

$$\sigma_\theta - \sigma_r = E(\varepsilon_\theta - \varepsilon_r) + \eta(\dot{\varepsilon}_\theta - \dot{\varepsilon}_r), \tag{8.5}$$

where $\varepsilon_\theta - \varepsilon_r = \varepsilon_{II} - \varepsilon_I$ and $\dot{\varepsilon}_\theta - \dot{\varepsilon}_r = \dot{\varepsilon}_{II} - \dot{\varepsilon}_I$ are the maximum strain, γ_{max}, and the maximum strain rate, $\dot{\gamma}_{max}$, respectively. The term maximum strain was first introduced by Ludwik (1909), who realized that N_1 should be a unique function of γ_{max}. Ludwik was also credited for the modified Hooke's law expression that takes the final form of a power law equation

$$\sigma = C\varepsilon^n, \tag{8.6}$$

where C is Young's modulus when $n = 1$.

Due to the presence of both the liquid and solid phases in the PTFE paste system, it is necessary to consider PTFE paste as an elasto-viscoplastic material. To model its flow, the expression suggested by Snelling and Lontz (1960) has been adopted. It is essentially Kelvin's stress-strain relation (Eq. (8.4)), with modifications that are similarly employed in

the Ludwik power law model (Eq. (8.6)) for the elastic (strain hardening) term, and the generalized power law model for the viscous resistance term. The resulting expression for the first normal stress difference, N_1, is, then, as follows:

$$\sigma_\theta - \sigma_r = C\gamma_{\max}{}^n + \eta\dot{\gamma}_{\max}{}^m. \tag{8.7}$$

A similar stress-strain relation has also been employed by Davis and Dokos (1944) in their analysis of metal wire drawing, although without the inclusion of the viscous resistance term.

To account for the initial yield stress, an additional term may be included on the right hand side of Eq. (8.7). However, this term is expected to be negligible compared to the other terms, as indicated by the initial strength of the preform, which is much less than that of the extrudate.

Now, a volume element at a distance r_b from the virtual die apex experiences a total linear strain of

$$\hat{\varepsilon}_\theta = \frac{rd\theta - r_b d\theta}{r_b d\theta} = \frac{r}{r_b} - 1 \tag{8.8}$$

in the θ-direction as it travels to a new position r away from the die apex (see Fig. 8.1). In terms of logarithmic strain, this can be written as

$$\varepsilon_\theta = \ln(1 + \hat{\varepsilon}_\theta) = \ln\frac{r}{r_b} \tag{8.9}$$

or

$$d\varepsilon_\theta = \frac{dr}{r}. \tag{8.10}$$

Providing the volume of the element remains constant, it can be proven that

$$d\varepsilon_r + d\varepsilon_\theta + d\varepsilon_\phi = 0 \tag{8.11}$$

and since $d\varepsilon_\theta = d\varepsilon_\phi$, then

$$d\varepsilon_r = -2d\varepsilon_\theta = -2\frac{dr}{r} \tag{8.12}$$

and hence,

$$\begin{aligned}\gamma_{\max} &= \varepsilon_\theta - \varepsilon_r = 3\varepsilon_\theta \\ &= 3\int_{r_b}^{r}\frac{dr}{r} \\ &= -3\ln\frac{r_b}{r}.\end{aligned} \tag{8.13}$$

The maximum strain rate can then be expressed as

$$\dot{\gamma}_{\max} = \frac{d\gamma_{\max}}{dt} = 3\frac{dr}{r\,dt}. \tag{8.14}$$

Considering the "radial flow" hypothesis, it is noted that the local velocity of a particle on the spherical surface of radius r from the die apex is given by Eq. (7.1)

$$\frac{dr}{dt} = -\frac{Volumetric\ \ Flowrate}{Area\ \ of\ \ Surface} = -\frac{Q}{2\pi(1-\cos\alpha)r^2}. \tag{7.1}$$

Hence, the maximum strain rate is

$$\dot{\gamma}_{\max} = -\frac{3Q}{2\pi(1-\cos\alpha)r^3}. \tag{8.15}$$

Substituting into Eq. (8.3), the force balance becomes

$$\frac{d\sigma_r}{dr} - 2B\frac{\sigma_r}{r} = \frac{2N_1(1+B)}{r}, \tag{8.3}$$

where

$$-N_1 = \sigma_r - \sigma_\theta = C\left(3\ln\left(\frac{r_b}{r}\right)\right)^n + \eta\left(\frac{3Q}{2\pi(1-\cos\alpha)r^3}\right)^m. \tag{8.16}$$

Solving the above equation yields the following expression:

$$-\sigma_r = 2(1+B)r^{2B}\left\{C\int\frac{(3\ln(r_b/r))^n}{r^{2B+1}}dr + \frac{\eta}{-(3m+2B)}\left[\frac{3Q}{2\pi(1-\cos\alpha)}\right]^m\left(\frac{1}{r^{3m+2B}}\right)\right\} + r^{2B}\hat{C}, \tag{8.17}$$

where the constant of integration, $\hat{C}$, is evaluated using the boundary condition $\sigma_r = \sigma_{ra}$ when $r = r_a$, i.e.

$$\hat{C} = -\frac{\sigma_{ra}}{r_a^{2B}} - 2(1+B)\left\{C\int_{r_a}\frac{(3\ln(r_b/r))^n}{r^{2B+1}}dr + \frac{\eta}{-(3m+2B)}\left(\frac{3Q}{2\pi(1-\cos\alpha)}\right)^m\left(\frac{1}{r_a^{3m+2B}}\right)\right\}. \tag{8.18}$$

The extrusion pressure can then be calculated using Eqs. (8.3) and (8.13) with $r = r_b$, i.e.

$$P_{extrusion} = \sigma_{rb} = \sigma_{ra}R^B + 2(1+B)\left\{C\left(\frac{D_b}{2\sin\alpha}\right)^{2B}\int_{r_a=\frac{D_b}{2\sqrt{R}\sin\alpha}}^{r_b=\frac{D_b}{2\sin\alpha}}\frac{(3\ln(r_b/r))^n}{r^{2B+1}}dr + \frac{\eta}{(3m+2B)}\left(\frac{12Q\sin^3\alpha}{\pi(1-\cos\alpha)D_b^3}\right)^m\left(R^{B+3m/2}-1\right)\right\}, \tag{8.19}$$

where σ_{ra} is the stress at the die exit, R is the reduction ratio, defined as $(D_b/D_a)^2$, and C, η, n, m and f are material constants that have to be determined experimentally.

When an orifice die is used, σ_{ra} may be present at the die exit due to a pulling force during extrudate wind-up or calendering. However, σ_{ra} is typically negligible and the expression for extrusion pressure can then be simplified to

$$P_{extrusion} = 2(1+B)\left\{C\left(\frac{D_b}{2\sin\alpha}\right)^{2B}\int_{r_a=\frac{D_b}{2\sqrt{R}\sin\alpha}}^{r_b=\frac{D_b}{2\sin\alpha}}\frac{(3\ln(r_b/r))^n}{r^{2B+1}}dr + \frac{\eta}{(3m+2B)}\left(\frac{12Q\sin^3\alpha}{\pi(1-\cos\alpha)D_b^3}\right)^m\left(R^{B+3/2}-1\right)\right\}, \quad (8.20)$$

which reduces to the expression obtained by Snelling and Lontz (1960) when $B = 0$ (i.e. frictionless surface).

Numerical integration is required to solve Eq. (8.20). However, for the range of the die reduction ratio of interest, the following approximation can be used with reasonable accuracy in Eq. (8.20), allowing an analytical solution to be obtained:

$$\ln(r_b/r) \approx a(r_b/r)^b, \quad (8.21)$$

where a and b are constant fitting parameters.

8.2.2 Paste Flow through a Tapered Die ($L/D_a \neq 0$)

The forces acting on a volume element in the capillary zone are shown in Fig. 8.4. A force balance on the element yields

$$(\sigma_z + d\sigma_z)\pi\frac{D_a^2}{4} - \sigma_z\pi\frac{D_a^2}{4} = f\sigma_r\pi D_a dz \quad (8.22)$$

or

$$\frac{d\sigma_z}{dz} = \frac{4f\sigma_r}{D_a} = \frac{4f(N_1+\sigma_z)}{D_a} \quad (8.23)$$

where N_1 is the previously defined first normal stress difference, which is expected to be significant due to the elastic nature of PTFE paste. At the end of the die conical zone (hence, at the entrance of the die capillary zone), N_1 can be calculated using Eq. (8.16) with $r = r_a$. Assuming N_1 to be approximately constant throughout the capillary zone of the die, the force balance becomes

$$\frac{d\sigma_z}{dz} = \frac{4f(N_{1a} + \sigma_z)}{D_a}, \tag{8.24}$$

where

$$-N_{1a} = C\left(\frac{3}{2}\ln(R)\right)^n + \eta\left(\frac{12Q\sin^3\alpha R^{3/2}}{\pi(1-\cos\alpha)D_b^{\,3}}\right)^m. \tag{8.25}$$

Solving Eq. (8.24) and applying the boundary condition $\sigma_z = \sigma_{zL}$ at $z = L$, yields

$$\sigma_z = N_{1a}\left(e^{4f(z-L)/D_a} - 1\right) + \sigma_{zL}e^{4f(z-L)/D_a}, \tag{8.26}$$

where σ_{zL} is the stress imposed at the exit of the die, which is typically negligible or zero.

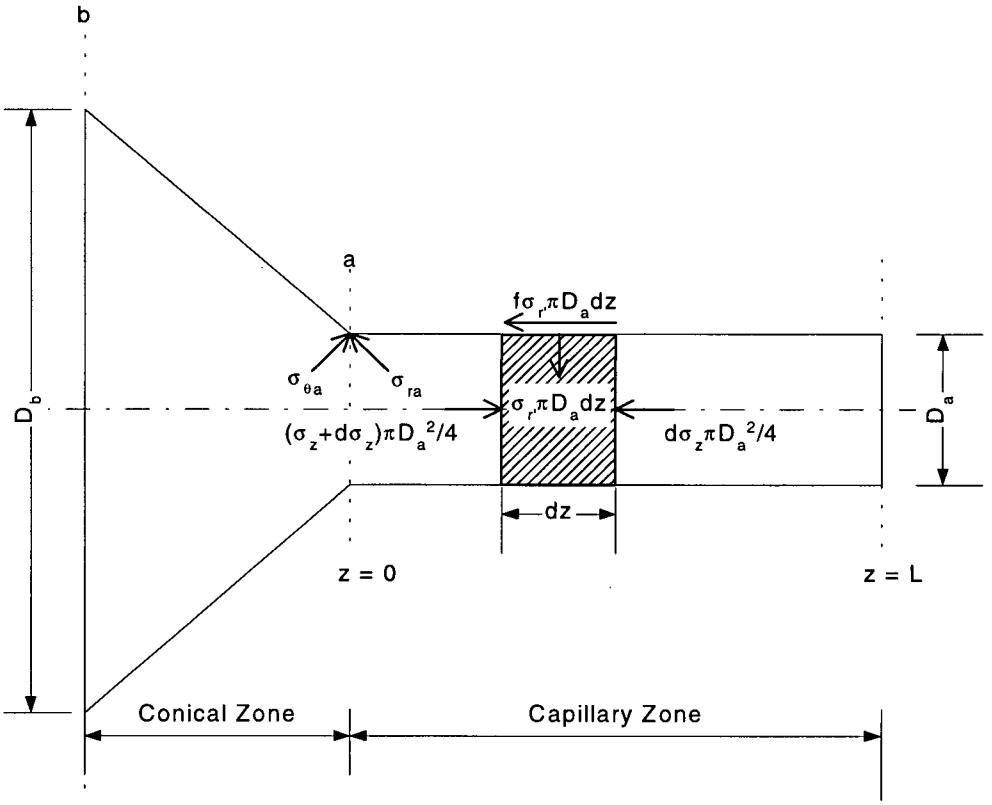

Fig. 8.4 Force balance on volume element in the die capillary zone.

The stress present at the entrance of the die capillary zone, σ_{z_o}, is obtained from Eq. (8.26) with $z = 0$. Since σ_{z_o} is essentially σ_{ru} of Eq. (8.19), the final expression for the total

extrusion pressure across a tapered die can then be obtained by substituting $\sigma_{ra} = \sigma_{z_o}$ into Eq. (8.19), i.e.

$$P_{extrusion} = \sigma_{rb} = \sigma_{ra} R^B + 2(1+B)\left\{ C\left(\frac{D_b}{2\sin\alpha}\right)^{2B} \int_{r_a=\frac{D_b}{2\sqrt{R}\sin\alpha}}^{r_b=\frac{D_b}{2\sin\alpha}} \frac{(3\ln(r_b/r))^n}{r^{2B+1}} dr + \right.$$

$$\left. \frac{\eta}{(3m+2B)}\left(\frac{12Q\sin^3\alpha}{\pi(1-\cos\alpha)D_b^3}\right)^m \left(R^{B+3m/2} - 1\right)\right\}, \tag{8.19}$$

where

$$\sigma_{ra} = \sigma_{z_o} = N_{1a}\left(e^{-4fL/D_a} - 1\right) + \sigma_{zL} e^{-4fL/D_a} \tag{8.27}$$

and

$$-N_{1a} = C\left(\frac{3}{2}\ln(R)\right)^n + \eta\left(\frac{12Q\sin^3\alpha R^{3/2}}{\pi(1-\cos\alpha)D_b^3}\right)^m. \tag{8.28}$$

8.3 Effects of Extrusion Conditions

The effect of extrusion temperature on the steady-state extrusion pressure is shown in Fig. 8.5 for resin 2. It can be seen that paste extrusion at a higher temperature requires a greater pressure, with the effect being more pronounced at a higher extrusion speed. This is due to the lower viscosity of the lubricant that causes it to be more mobile in redistributing itself non-uniformly in the paste matrix. This, coupled with the high pressure overshoot during the initial stage of the extrusion, causes most of the lubricant to be extruded early. Too high a temperature also promotes liquid evaporation. Consequently, the paste is drier and this causes the observed increase in the steady state extrusion pressure at higher temperatures.

In Fig. 8.5, one can also see that the steady-state extrusion pressure generally increases with an increase in the extrusion rate (volumetric flow rate), due to the increase in the viscous resistance of the paste. However, at low extrusion rates, an initial reduction in the extrusion pressure is observed. This can be explained by considering the residence time of the paste in the barrel and the die, which becomes sufficiently long at low extrusion rates,

providing ample time for the lubricant to re-distribute itself non-uniformly in the paste matrix. The consequence is an early extrusion of most of the lubricant, as discussed above. As a result, the required extrusion pressure is higher than expected, with the effect becoming more pronounced with further lowering of the extrusion rate. This explains the trend observed in Fig. 8.5.

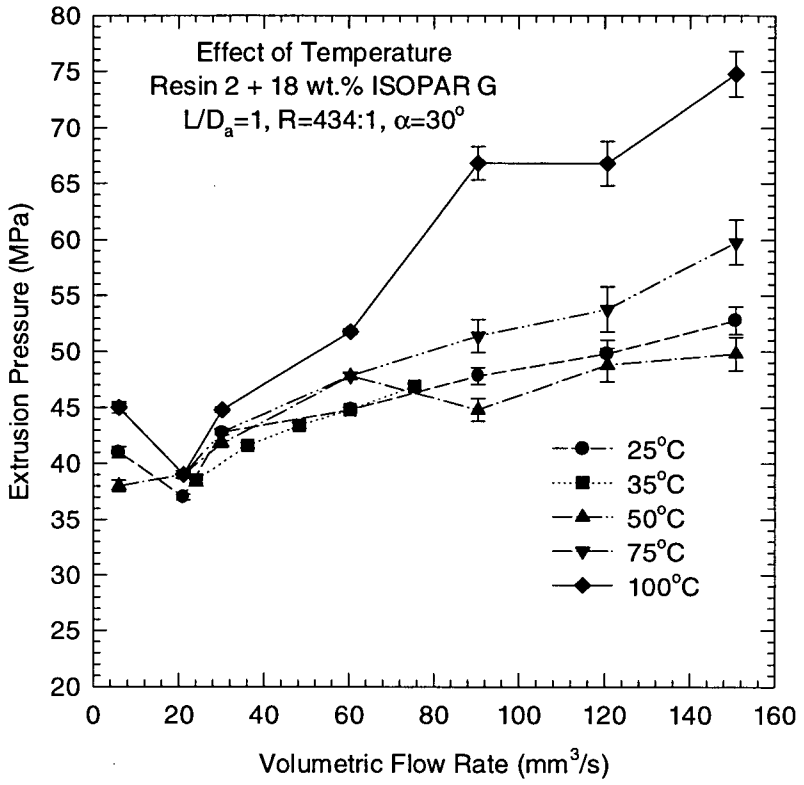

Fig. 8.5 The effects of temperature and extrusion speed on the steady-state pressure of paste extrusion.

The effect of lubricant concentration on extrusion pressure is depicted in Fig. 8.6 for resin 3 (model predictions are discussed below). As expected, increasing the lubricant concentration decreases the extrusion pressure. However, when the lubricant concentration is unnecessarily high, the extrudate becomes excessively wet and weak, sometimes not being able to hold its shape. It is the excessive local slippage between flowing particles in the die that results in a lesser quantity of fibrils being formed. On the other hand, extruding a paste with a lubricant concentration lower than the optimum value will result in a higher extrusion

pressure that may cause fibril breakage (this will be detailed in Chapter 9). This implies that the extent of fibrillation is dependent on the lubricant concentration as well.

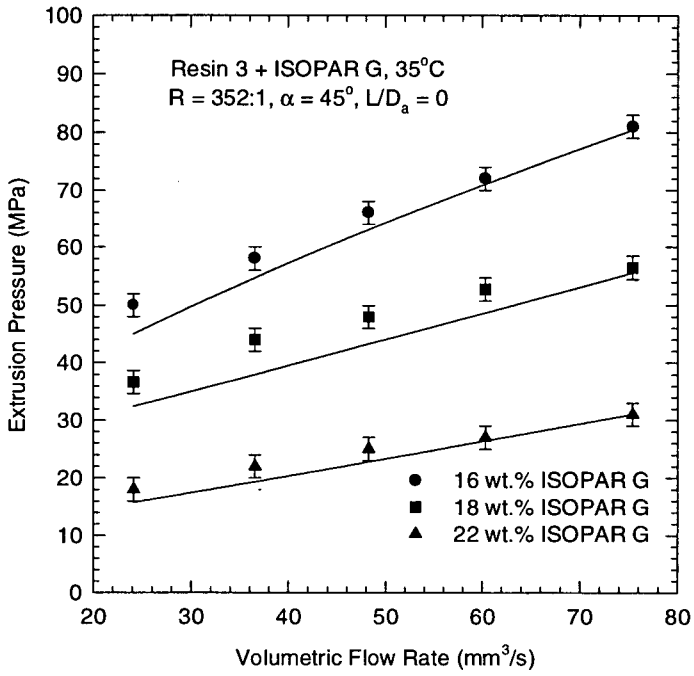

Fig. 8.6 The effect of lubricant concentration on the steady-state extrusion pressure for resin 3. Solid lines are model predictions obtained with fitted parameters listed in Table 8.2.

8.4 Effects of Die Design

The effects of the die reduction ratio, the L/D_a ratio, and the die entrance angle on the extrusion pressure are illustrated in Figs. 8.7, 8.8, and 8.9, respectively. The model predictions are also shown in the same figures, using the fitted values of the parameters listed in Table 8.1. To obtain these parameters, it was first assumed that $f = 0$. Preliminary fitting of Eq. (8.19) to the experimental data indicated that this is a reasonable assumption when α is sufficiently large ($\alpha > 10°$). Using the available data corresponding to $\alpha > 10°$, the parameters C, n, η, and m were first determined following the method described by Snelling and Lontz (1960). (Eq. (8.19) essentially reduces to the expression suggested by authors if $f =$ 0.) After obtaining the values of these parameters, f was then determined by minimizing the sum of differences between the model predictions and the experimental data.

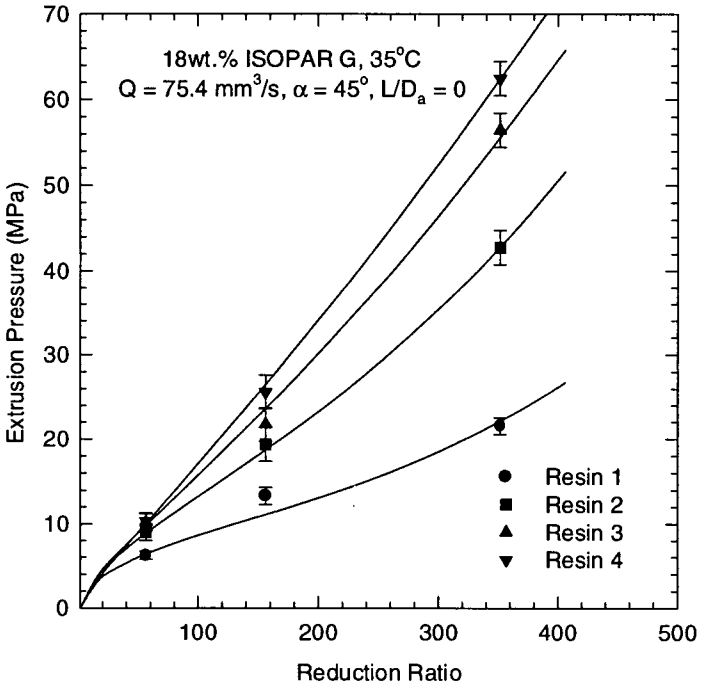

Fig. 8.7 The effect of reduction ratio on the steady-state extrusion pressure for resins 1 – 4. Solid lines are model predictions using the fitted parameters listed in Table 8.1.

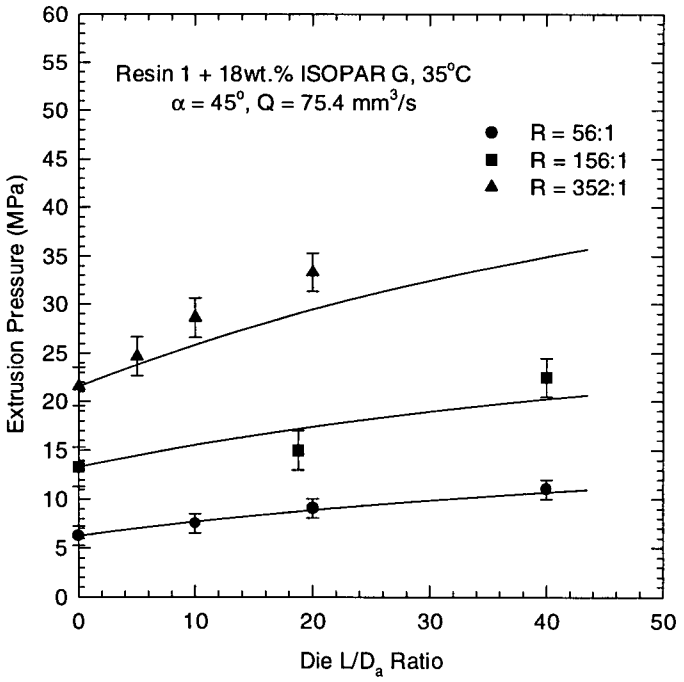

(a)

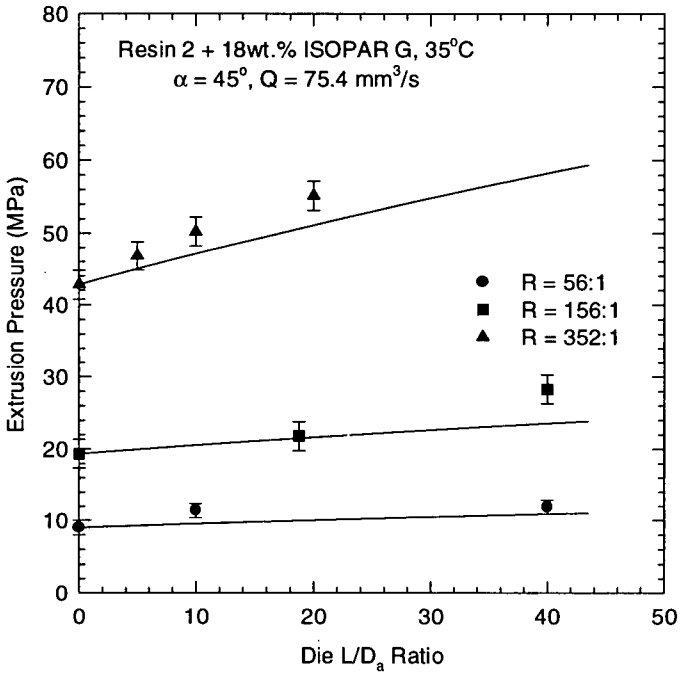
Resin 2 + 18wt.% ISOPAR G, 35°C
α = 45°, Q = 75.4 mm³/s
R = 56:1
R = 156:1
R = 352:1
Extrusion Pressure (MPa)
Die L/D$_a$ Ratio
0
10
20
30
40
50
60
70
80

(b)

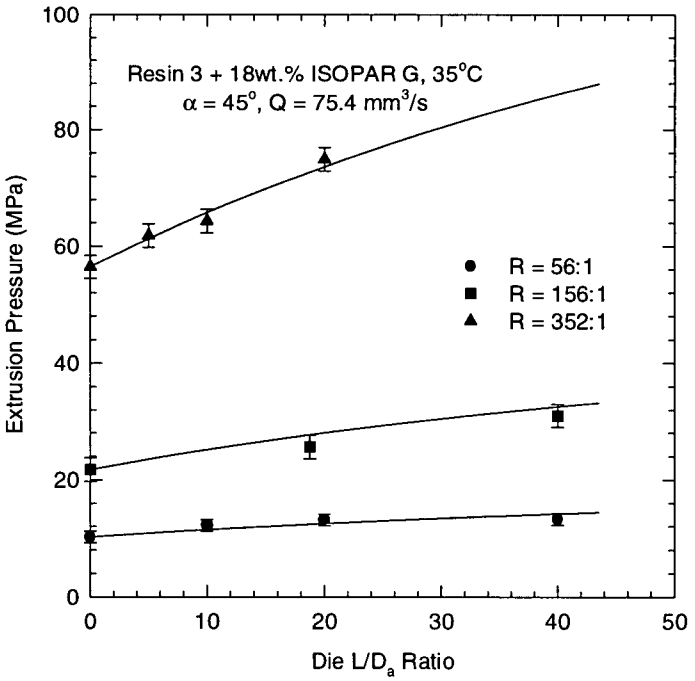
Resin 3 + 18wt.% ISOPAR G, 35°C
α = 45°, Q = 75.4 mm³/s
R = 56:1
R = 156:1
R = 352:1
Extrusion Pressure (MPa)
Die L/D$_a$ Ratio
0
20
40
60
80
100

(c)

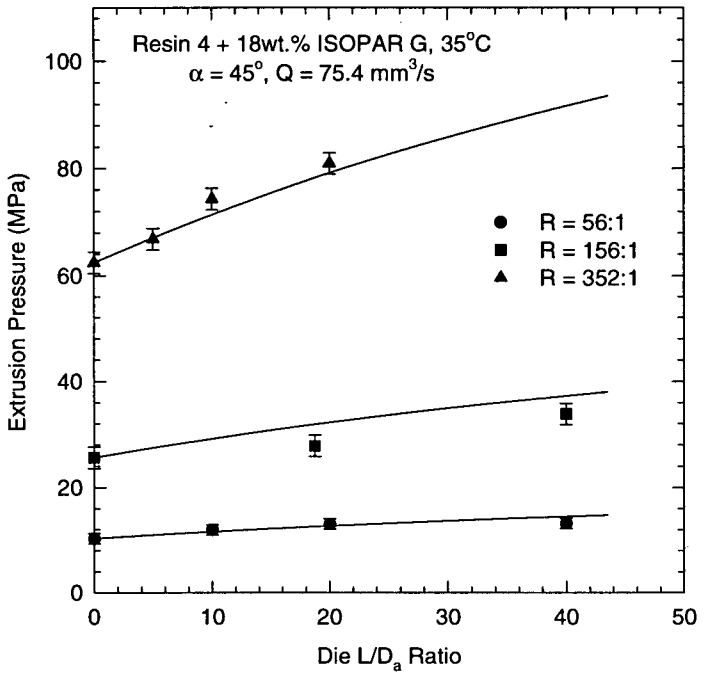

(d)

Fig. 8.8 The effect of die L/D_a ratio on the steady-state extrusion pressure at different reduction ratios for (a) resin 1, (b) resin 2, (c) resin 3, and (d) resin 4. Solid lines are model prediction using the fitted parameters listed in Table 8.1.

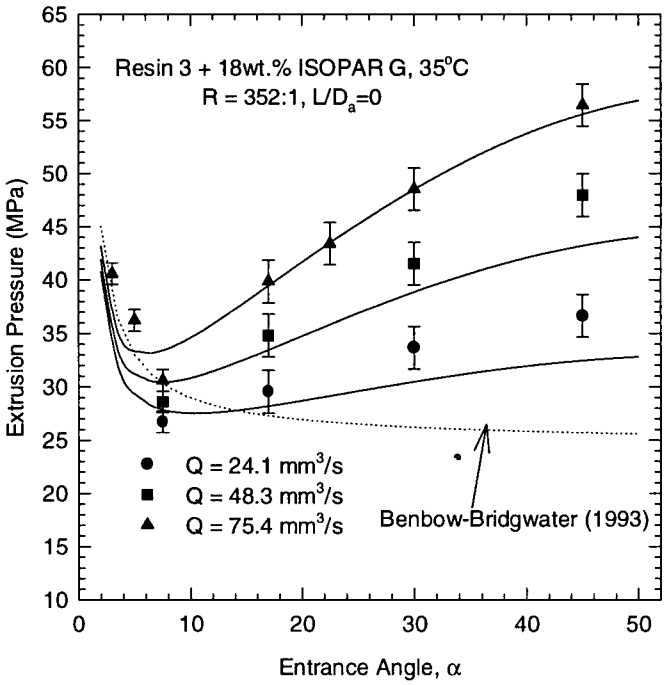

(a)

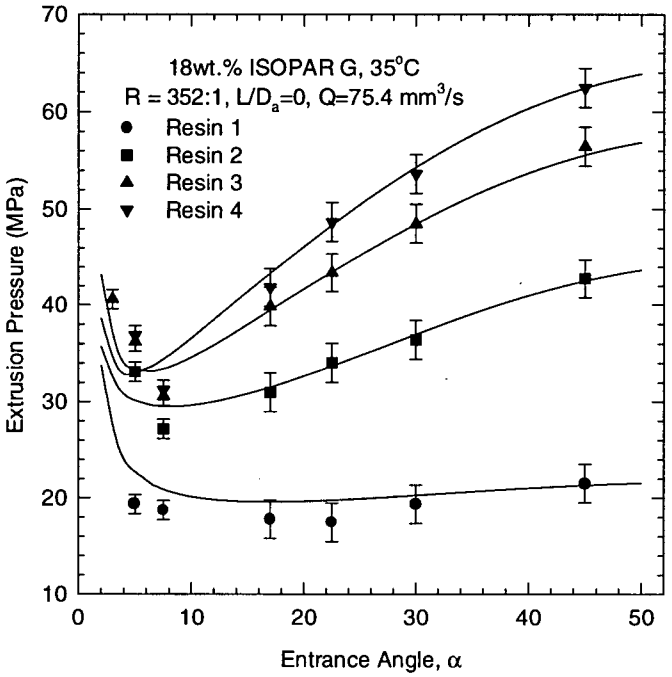

(b)

Fig. 8.9 The effect of die entrance angle on the steady-state extrusion pressure: (a) at different extrusion rates for resin 3, (b) at 75.4 mm^3/s for resins 1 – 4. Solid lines are model predictions using the fitted parameters listed in Table 8.1. Also shown in (a) is the prediction using the Benbow-Bridgwater equation (1993).

From Figs. 8.7 and 8.8, respectively, it can be seen that extrusion pressure increases with increases in the reduction and L/D_a ratios. This is due to increased levels of strain hardening and frictional losses, respectively. It can also be seen that extrusion pressure is significantly affected by the die reduction ratio, especially in the case of high molecular weight resin. Therefore, extrusion dies of precise (low tolerance) dimensions are essential in paste extrusion, especially when a small diameter barrel is used.

In Fig. 8.9, one can see that the extrusion pressure initially decreases, and then increases, with increase of the die entrance angle. The decrease in the extrusion pressure at small entrance angles is similar to the trend predicted for polymer melts using the lubrication approximation (Dealy and Wissbrun, 1990). A theoretical derivation similar to that employed in the lubrication approximation, has been used by Benbow and Bridgwater (1993) in their modeling work on paste flow. When the die entrance angle is sufficiently small, paste flow in

the die conical zone follows essentially a plug flow pattern for the most part, as has been discussed in the previous chapter with reference to Fig. 7.6 (a). The lubrication approximation approach is valid here. However, the lubrication approximation predicts a monotonic decrease in the extrusion pressure with increasing die entrance angle, which is not consistent with the experimental results plotted in Fig. 8.9. Beyond a certain entrance angle, the extrusion pressure increases with increasing α, as is commonly observed with the extrusion of elastic solids (see, for example, Horrobin and Nedderman, 1998 and the references therein). The failure of the lubrication approximation is due to the assumed plug flow pattern in the die conical zone that becomes invalid when the entrance angle is large. As discussed before, this can be remedied by considering the "radial flow" hypothesis.

Table 8.1 Values of material constants and coefficients of friction for the different pastes.

Resin	C (MPa)	n	η (MPa.s^m)	m	f
Copolymer series:					
1	0.2348	1.61	2.767×10^{-6}	1.91	4.48×10^{-3}
2	0.1974	1.94	4.242×10^{-5}	1.75	2.03×10^{-3}
Homopolymer series:					
3	0.2280	1.75	1.417×10^{-2}	1.04	4.02×10^{-3}
4	0.1420	1.94	5.286×10^{-2}	0.88	3.57×10^{-3}

8.5 Model Predictions

From Figs. 8.7, 8.8 and 8.9, one can see that the proposed one-dimensional model is able to predict the flow behavior of PTFE pastes reasonably well, considering its simple form. However, it is possible to improve the model fit further, especially at low extrusion rates, by considering the dependency of the material constants on liquid redistribution in the paste matrix, for which additional studies are required. Comparing the resin properties of the homologous series in Table 4.1 with the model parameters in Table 8.1, it can be observed that the value of n is larger for a higher molecular weight paste. This indicates that the increase in the extrusion pressure, due to the increase in the strain level, will be relatively greater for such paste. This is also somewhat apparent from the slopes of the curves plotted in Fig. 8.7. Correspondingly, in the case of a higher molecular weight paste, the extrudate strength will be more significantly affected by changes in strain, such as changes in the die

reduction (contraction) ratio. At the same strain level, however, the effect of molecular weight on strain hardening (and hence, on extrudate strength) is less apparent since the strain hardening coefficient, C, decreases with the increase in the resin molecular weight, therefore compensating the increase in n.

A paste of higher molecular weight also exhibits a greater flow resistance, as indicated by the larger value of η. In addition, since the value of m is smaller, a higher molecular weight paste behaves more like an elastic-plastic material. This implies that its flow behavior is less dependent on the extrusion rate. A lower molecular weight paste flow, on the other hand, will show a greater dependency on the extrusion rate, due to the larger value of m. This makes the assumption of an ideal plug flow in the die capillary zone less appropriate for such paste, and may possibly explain the observed discrepancies between the model predictions and the experimental data on the effect of die L/D_a ratio (Fig. 8.8), which, as one can see, is greater in the case of the lower molecular weight paste. Interestingly, as shown in Table 8.1, the coefficient of friction, f, also decreases with increasing molecular weight. Perhaps, this has to do more with the average resin particle size that affects the mechanism of liquid migration to the die wall, rather than the effect of the resin molecular weight itself.

Generally, however, it can be summarized that, at practical strain levels, a higher molecular weight paste extrudes at a higher extrusion pressure, as is found experimentally (see Fig. 8.7). For a particular paste, the relative magnitudes of the strain hardening and viscous resistance terms depend on the extrusion conditions and die design, which is apparent from Eq. (8.19). For example, this is shown in Fig. 8.10 for resin 4. The total contribution of the two terms indicates the extent of fibrillation that has occurred during an extrusion process. A higher extrusion pressure translates into the creation of more fibrils (this will be discussed in more detail in Chapter 9). However, it is worthwhile noting that too high an extrusion pressure may be detrimental to the quality of the fibrils, causing them to break. In the more severe cases, excessive extrusion pressure may even result in a non-continuous spurting of periodically broken extrudates. This was observed with the extrusion attempt with resin 5 using a die having a reduction ratio of 352:1. As a consequence, it was not possible to determine the model parameters for this resin due to the lack of experimental data.

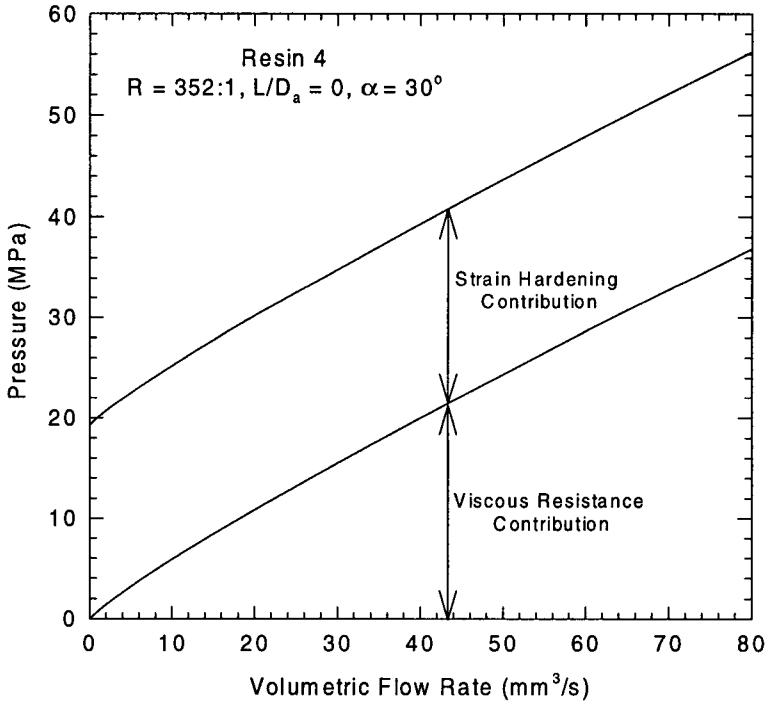
Resin 4
R = 352:1, L/D$_a$ = 0, α = 30°
Strain Hardening Contribution
Viscous Resistance Contribution
Pressure (MPa)
Volumetric Flow Rate (mm^3/s)
0
10
20
30
40
50
60
70
80

(a)

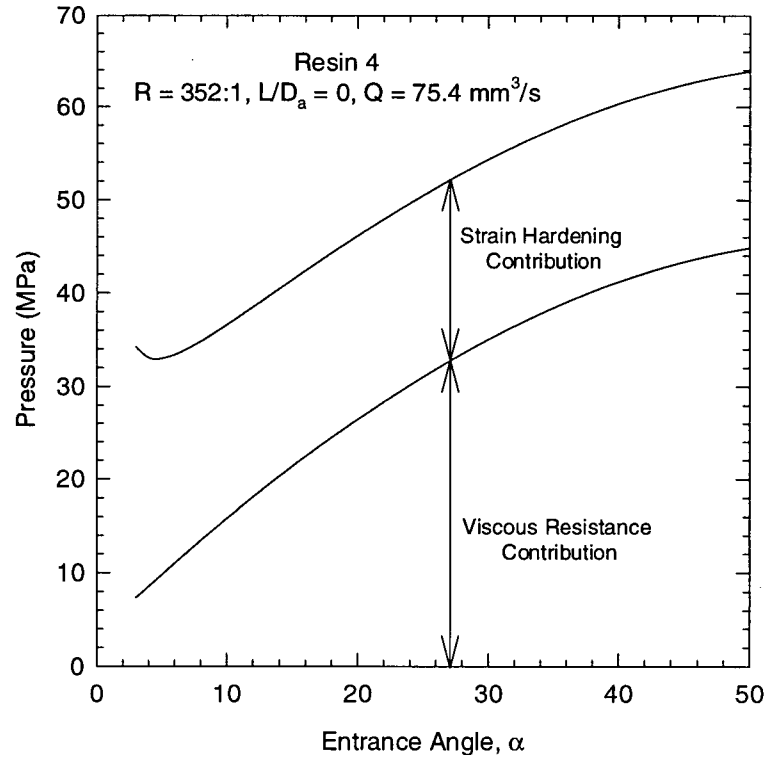
Resin 4
R = 352:1, L/D$_a$ = 0, Q = 75.4 mm^3/s
Strain Hardening Contribution
Viscous Resistance Contribution
Pressure (MPa)
Entrance Angle, α
0
10
20
30
40
50
60
70

(b)

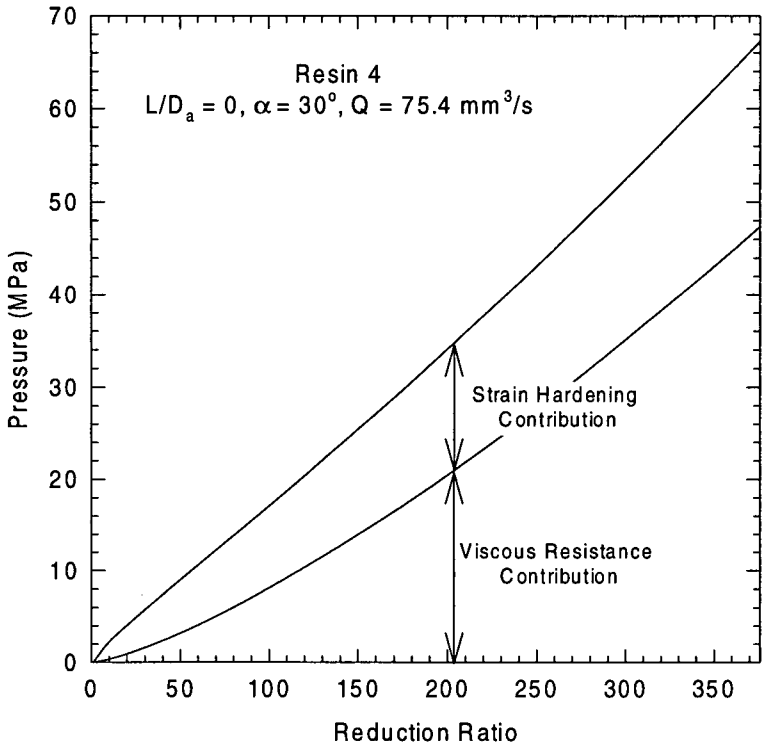

(c)

Fig. 8.10 The relative magnitudes of the strain hardening and viscous terms in Eq. (8.19) as functions of (a) volumetric flow rate, (b) die entrance angle, and (c) die reduction ratio, for resin 4 with 18 wt.% ISOPAR G® at 35°C.

The effect of lubricant concentration on the values of the material constants has also been studied using resin 3. The results are summarized in Table 8.2 and the model predictions are plotted in Fig. 8.6. It can be seen that the coefficient m, which indicates the viscous dependence of the extrusion pressure on the extrusion rate, increases with increase in lubricant concentration. This is consistent with the expectation of obtaining a more viscous response with an increase in the liquid phase concentration. The resistance to flow, as indicated by the viscosity coefficient, η, and the coefficient of friction, f, also decreases with increasing lubricant content, as expected. On the other hand, a higher lubricant concentration decreases the extrusion pressure dependence on strain, as indicated by the lower value of n. Although the strain hardening coefficient, C, increases with increasing lubricant concentration, at a practical strain level, the overall effect is a lower extent of strain hardening. Thus, a paste with a higher lubricant concentration will extrude at a lower

pressure (see Fig. 8.6), and this will translate into a lower extent of fibrillation and hence, weaker extrudates.

Table 8.2 Values of material constants for resin 3 with different lubricant concentrations.

Material Constant	16 wt.% Lubricant	18 wt.% Lubricant	22 wt.% Lubricant
C (MPa)	3.346×10^{-4}	0.2280	0.7394
n	4.97	1.75	0.53
η (MPa.s^m)	2.302×10^{-1}	1.417×10^{-2}	6.748×10^{-3}
m	0.72	1.04	1.08
f	6.55×10^{-3}	4.02×10^{-3}	1.80×10^{-3}

8.6 Conclusions

In this chapter, the rheological behavior of PTFE pastes is discussed. The effects of extrusion conditions, in terms of extrusion temperature and speed, and the lubricant concentration in the paste, on the steady-state extrusion pressure have been investigated. The effects of die design have also been assessed quantitatively, and a simple model has been proposed to describe these effects. The model considers the paste as an elasto-viscoplastic material that exhibits both strain hardening and viscous resistance effects during flow. The model was found to be consistent with the experimental data and able to predict the steady-state extrusion pressure reasonably well, given the fitted parameters of the generalized Kelvin constitutive relation used to describe the rheological behavior of the pastes.

CHAPTER 9:

PROPERTIES OF PTFE PASTE EXTRUDATES

9.1 Introduction

Discussions on fibrillation and its mechanism during PTFE paste extrusion were dealt with in detail in Chapter 7. As may be expected, the extent of fibrillation and the quality of the fibrils formed during the extrusion process are significantly affected by the resin properties, extrusion conditions and the design of the extrusion die. These variables consequently affect the final product properties, such as the mechanical strength of unsintered calendered tapes, the dielectric breakdown property of wires and the stretch void index of tubes and hoses (Ebnesajjad, 2000).

In this chapter, the effects of die design, resin molecular structure and lubricant concentration on the mechanical properties of PTFE paste extrudates, and their relations to the quantity and quality of the fibrils formed during extrusion are discussed.

9.2 Quantitative Descriptions of Fibrillation: The Issue of Fibril Quantity and Quality

In order to completely describe the state of fibrillation in an extrudate, it is necessary to consider both the extent of fibrillation in the extrudate and the quality of the fibrils that are formed. During paste extrusion, a significant portion of the extrusion pressure is dissipated to overcome the strain hardening and viscous resistance contributions of the paste flow (see Chapter 8). The frictional forces between individual solid particles, and between the bulk paste and the die wall also give rise to additional pressure drop. These factors consequently translate into the creation of fibrils, in accordance with the proposed mechanism for fibrillation discussed in Chapter 7. Therefore, the extrusion pressure can be used as a quantitative measure of the extent of fibrillation that occurs during extrusion. For example, the extrusion of paste through a die of larger reduction ratio requires a higher extrusion pressure and consequently, this will result in an extrudate that is more fibrillated, as will be discussed later. However, it is noted that since fibrillation occurs only in the die entrance (contraction) zone, the additional pressure drop across the capillary part of the die should not be taken into account when describing the extent of fibrillation during extrusion.

Since fibrillation effectively results in a decrease in resin crystallinity due to the unwinding of crystallites, it is also theoretically possible to quantify the extent of fibrillation in an extrudate using DSC. In Chapter 7, it was noted that the first heat of melting of a polymer is directly proportional to the degree of resin crystallinity. Therefore, the difference in the first heat of melting of the paste, ΔH_{m1}, before and after extrusion should be indicative of the amount of fibrils formed during extrusion, and should, therefore, correlate with the extrusion pressure. In Fig. 9.1, the relative difference in the first heat of melting of the paste before and after extrusion is plotted as a function of the steady state extrusion pressure under various processing conditions. Amid the scatter, it is still possible to extract a positive correlation between the extrusion pressure and the difference in ΔH_{m1}. The scatter can be attributed to the fact that the samples tested in the calorimeter represent only minute parts of the extrudates, making the results highly localized and hence, sensitive to any local variations in the amount of fibrils. Nevertheless, the results do conform with the proposed mechanism for fibrillation, in which fibrils are considered as unwound crystallites, and confirm the significance of extrusion pressure in fibril formation. From Fig. 9.1, one can also see that different correlations are obtained for different resins, which implies that different levels of extrusion pressure are required to fibrillate resins of different molecular structure under identical conditions.

Besides the amount of fibrils that are present in the extrudate, the quality of the fibrils is an equally important issue to consider when describing the mechanical properties of extrudates. The quality of fibrils can be described in terms of their degree of orientation and continuousness. A preliminary attempt to quantify the degree of fibril orientation in an extrudate using Raman spectroscopy showed promising results. Figure 9.2 (a) and (b) show typical Raman spectra for unprocessed and processed powder, respectively. In the case of unprocessed powder (Fig. 9.2 (a)), no difference in the scattering intensity at all Raman shifts is observed between the two polarization geometry (i.e. parallel or perpendicular to the extrusion direction), indicating no preferred orientation (isotropicity). In the case of processed powder (Fig. 9.2 (b)), however, there is a definite difference in the scattering intensity between the two polarization geometries at major Raman shifts, particularly at 734 cm^{-1} and 1383 cm^{-1}. The assignment of Raman scattering bands for PTFE is difficult and controversial, especially those at 734 cm^{-1} and 1383 cm^{-1} (Bower and Maddams, 1989;

Lehnert *et al.*, 1997). There is general agreement that these bands are due to C-F and C-C stretching (Bower and Maddams, 1989). However, the question of which band is associated with which stretching, is not yet resolved. Nevertheless, it was found that the Raman scattering intensity at 1383 cm^{-1} is consistently enhanced in the polarization geometry parallel to the extrusion direction, while that at 734 cm^{-1} is enhanced in the polarization geometry perpendicular to the extrusion direction. From SEM, it is evident that, for the fibrils to become oriented, the PTFE molecules have to be straightened with their backbones parallel to the extrusion direction (see Fig. 7.1 (c)). Therefore, it can definitely be concluded that the Raman scattering band at 1383 cm^{-1} corresponds to C-C (backbone) stretching. The ratio of the Raman scattering intensities at 1383 cm^{-1} between the two polarization geometries (parallel to perpendicular) will then provide a quantitative measure of the preferred fibril orientation. A ratio of unity indicates isotropicity or no preferred orientation, while a ratio greater than unity indicates a preferred orientation in the direction parallel to the extrusion direction.

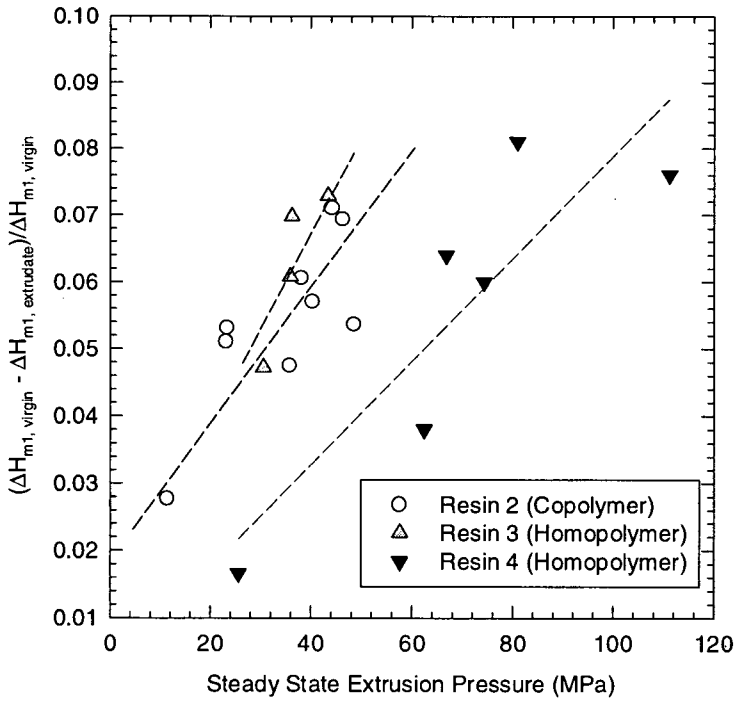

Fig. 9.1 Correlations between the relative differences in ΔH_{m1} of pastes before and after extrusion and the steady-state extrusion pressure (under various extrusion conditions). The fact that the differences in ΔH_{m1} are always positive indicates that the resin crystallinity is consistently lower after extrusion. The lines are drawn to guide the eye.

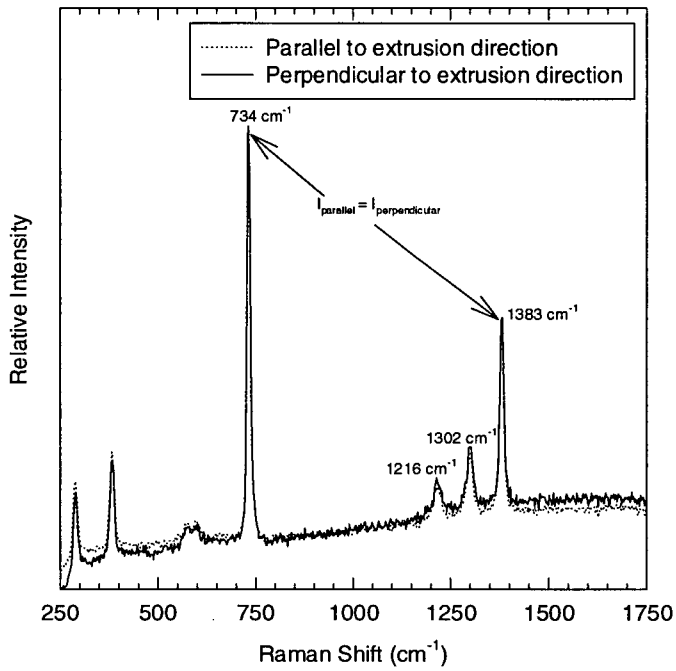

(a)

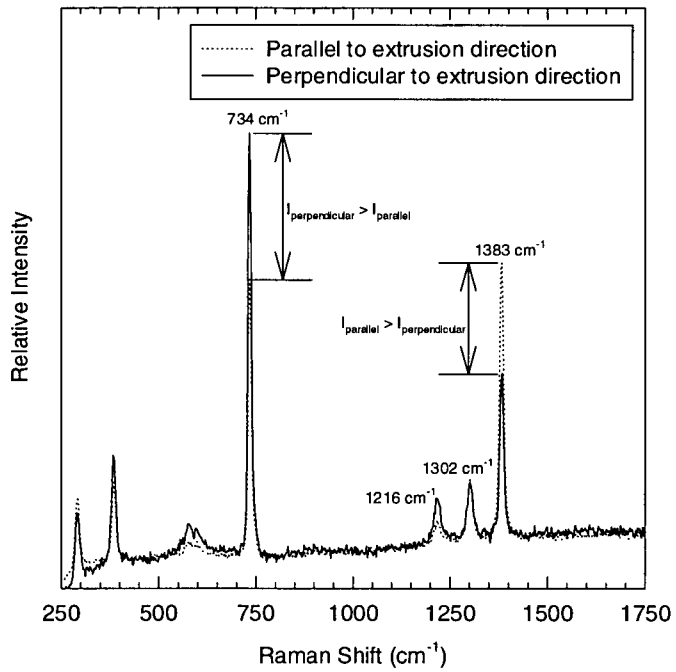

(b)

Fig. 9.2 Typical Raman spectroscopy results for (a) unprocessed powder and (b) paste extrudate.

In this work, Raman spectroscopy has also been used to track the development of fibril orientation in the extrudate during the course of an extrusion experiment. This is shown in Fig. 9.3 for resin 4. The transient extrusion pressure response is also plotted in the same figure. The degree of fibril orientation, as shown with reference to the right axis, initially rises with the extrusion pressure. However, when the extrusion pressure is at its peak, a sudden drop in the degree of fibril orientation is observed. When the process has reached steady state, the extrusion pressure and the degree of fibril orientation in the extrudate level off to their steady-state values. The low degree of fibril orientation at the peak pressure explains the commonly observed dielectric spark test failures in the wire coating process at approximately the same point during the extrusion (McAdams, 2000). When the extrusion pressure is at its peak, the extrudate is highly accelerated out of the extrusion die. This causes the extension and breakage of fibrils. Consequently, the fibrils become less continuous and are more chaotic and hence, exhibit a lower degree of preferred orientation. This results in a non-uniform sintering and the manifestation of voids in the final product, causing the commonly observed spark test failures.

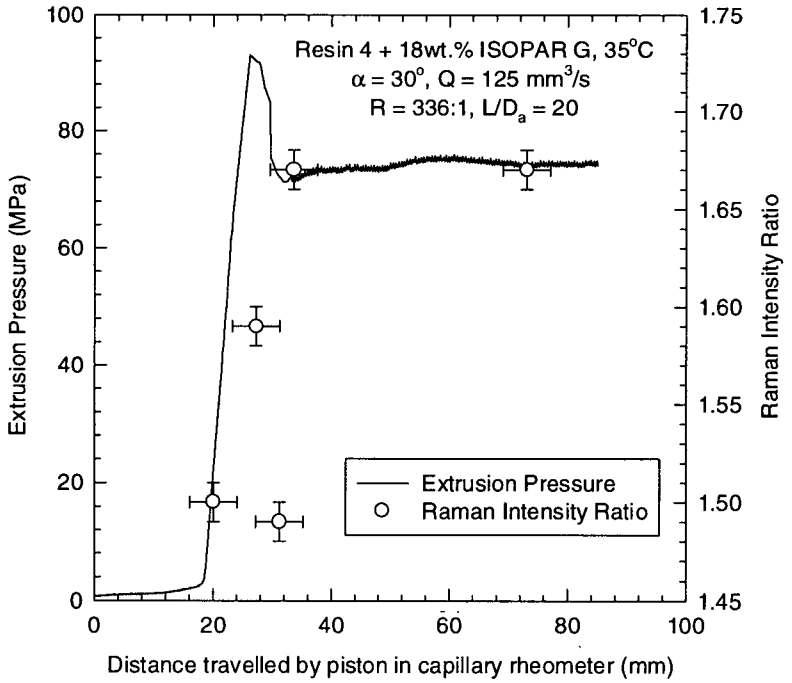

Fig. 9.3 Development of fibril orientation with extrusion pressure during transient extrusion experiment. Raman intensity ratio is defined as $I_{parallel}/I_{perpendicular}$ at 1383 cm^{-1}.

An industrially acceptable paste extrudate should, therefore, be sufficiently fibrillated, with the fibrils being mostly unbroken (continuous) and exhibit a high degree of orientation in the extrusion direction. It is also important that the extent of fibrillation and the quality of the fibrils be uniform along the extrudate. The consequence of these conditions is a mechanically strong extrudate. Considering this, the tensile strength of an extrudate may be used as a quality indicator, since it takes into account the combined effects of fibril quantity and quality. Furthermore, mechanical testing results are generally more reproducible with less variability, making extrudate tensile strength a suitable parameter for this purpose.

9.3 Effects of Die Design

9.3.1 Effect of Die Reduction Ratio

The effect of die reduction ratio on the extrudate tensile strength is shown in Fig. 9.4 for resins 2 and 4. It can be seen that increasing the die reduction ratio initially increases the tensile strength of an extrudate. At larger reduction ratios, the effect diminishes. In fact, the results for resin 2 indicate a small decrease in the extrudate tensile strength at a reduction ratio of 352:1.

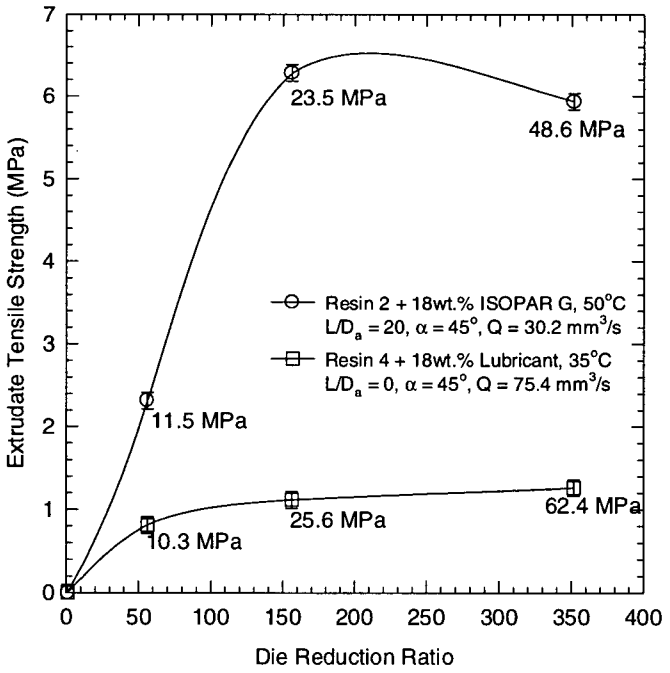

Fig. 9.4 The effect of die reduction ratio on extrudate tensile strength. Also shown are the steady-state extrusion pressures corresponding to each experimental run. Lines are drawn to guide the eye.

In a die having a larger reduction ratio, resin particles are squeezed against one another to a greater extent over a longer flow path, resulting in a higher extrusion pressure. This allows a greater extent of mechanical interlocking to occur between adjacent particles. A greater amount of fibrils is consequently created, as these interlocked crystallites are unwound while exiting the die. Provided that the quality of the fibrils is unaffected by the increase in the die reduction ratio, this translates into a mechanically stronger extrudate.

However, this is only partially observed in Fig. 9.4. Beyond a certain reduction ratio, the extrudate tensile strength is approximately unchanged or, as in the case of resin 2, decreases with further increase in the die reduction ratio. The higher extrusion pressure associated with a die of larger reduction ratio (see Fig. 9.4) causes the extrudate to be accelerated (spurted) out of the die at a greater velocity. This results in the breakage of some fibrils in the extrudate (as discussed above) and an overall reduction in the fibril quality. The consequence is a mechanical weakening of the extrudate. These competing effects between fibril quantity and quality affect the extrudate tensile strength in opposing directions and become more important at larger reduction ratios, accounting for the observed trend in Fig. 9.4.

It is noted that the maximum die reduction ratio that is suitable for a particular resin is partly dependent on the molecular properties of the resin. For example, as can be seen from Fig. 9.4, the extrudate obtained using resin 2 with a die of reduction ratio of 352:1 has a lower tensile strength than that obtained with a die of reduction ratio of 156:1. However, this is not observed with resin 4. It is also worthwhile to note again here that with resin 5, it is not possible to extrude the paste through a die of reduction ratio of 352:1. As discussed in Chapter 8, such an extrusion attempt resulted in a high velocity spurting of periodically broken extrudates, due to the excessively high extrusion pressure.

9.3.2 Effect of Die Entrance Angle

Figure 9.5 depicts the effect of die entrance angle at constant throughput on the extrudate tensile strength for resin 3. The steady-state extrusion pressure corresponding to each experimental run is also shown in the figure for comparison. The extrusion pressure generally increases with increasing die entrance angle, although at very small entrance angles

(less than $\alpha \approx 7.5°$), the frictional force becomes important and this trend reverses (see Fig. 8.9). As discussed above, this increase in the extrusion pressure translates into extrudates that are more fibrillated. However, while this is true, it appears that the overall quality of the fibrils is increasingly compromised with the increase in the die entrance angle. This is indicated by the decrease in the extrudate tensile strength shown in Fig. 9.5, contrary to an expected increase.

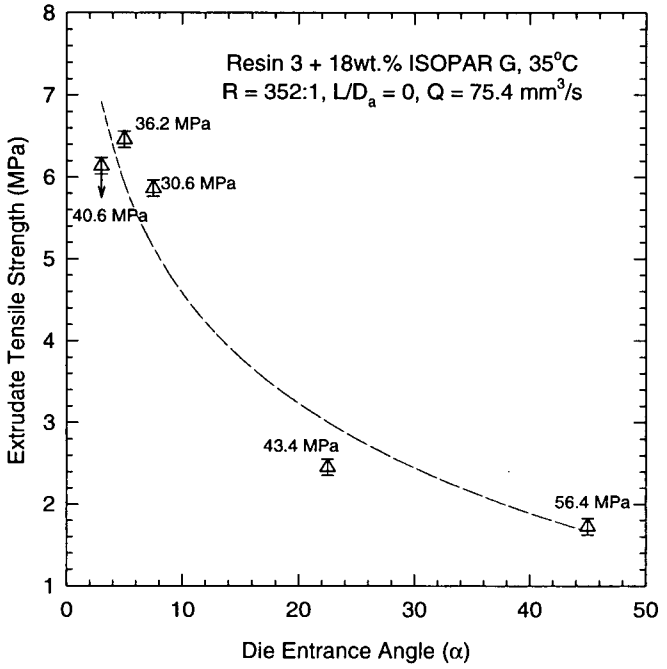

Fig. 9.5 The effect of die entrance angle on extrudate tensile strength. Also shown are the steady state extrusion pressures corresponding to each experimental run. Line is drawn to guide the eye.

The increase in the steady-state extrusion pressure with increasing die entrance angle is due to the paste flow path that becomes correspondingly less streamlined. Through visualization experiments, it has been shown previously that the paste flow pattern in the die contraction zone becomes more "deformed" as the die entrance angle is increased. As a consequence, the resulting extrudate exhibits a greater extent of fibrillation. However, the degree of fibril orientation and possibly, continuity, decreases. A greater number of fibrils exiting the die will be oriented in directions other than the flow directions, due to the lesser streamlining of the flow. This can be expected to result in a larger swelling of the extrudate. Indeed, diameter measurements of extrudates obtained using dies of various entrance angles

indicate this effect and this is shown in Fig. 9.6. It can be seen from Fig. 9.6 that extrudate obtained using a die of smaller entrance angle exhibits less swell, due to the greater streamlining of the flow. On the other hand, extrudate obtained using a die having a larger entrance angle exhibits greater swell. The overall effect is a reduction in the fibril quality as the die entrance angle is increased, and consequently a mechanically weaker extrudate is obtained (Fig. 9.5).

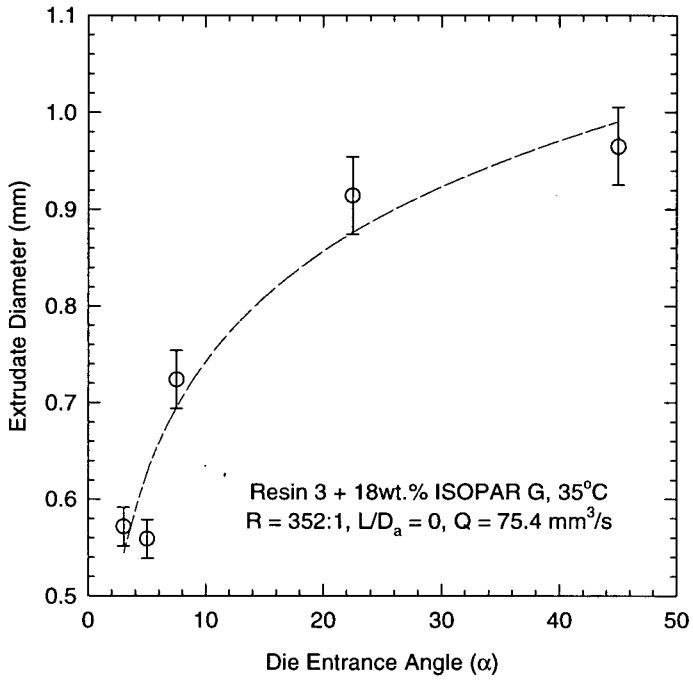

Fig. 9.6 The effect of die entrance angle on extrudate diameter (D_a = 0.508 mm). Line is drawn to guide the eye.

9.3.3 Effect of Die Aspect (L/D_a) Ratio

Fig. 9.7 shows the effects of die L/D_a ratio on the tensile strength and diameter of paste extrudates. It can be seen that increasing the die L/D_a ratio increases the mechanical strength of the extrudate. This is due to the improvement in the overall fibril quality (orientation), as opposed to the creation of more fibrils. With the increase in the die capillary length, there is sufficient time for the fibrils to relax and become more orderly in their orientation. The creation of fibrils, on the other hand, occurs only in the die entrance zone (see Fig. 7.2), where the interlocking of particles is possible. In the die capillary zone, the fibrillated paste flows in a plug flow manner, and the pressure drop across the capillary

length is due mainly to the frictional losses at the die wall. With this consideration, one is, therefore, led to believe that extrudates produced using dies of the same reduction ratio and entrance angle will exhibit the same extent of fibrillation, regardless of the length of the die capillary zone.

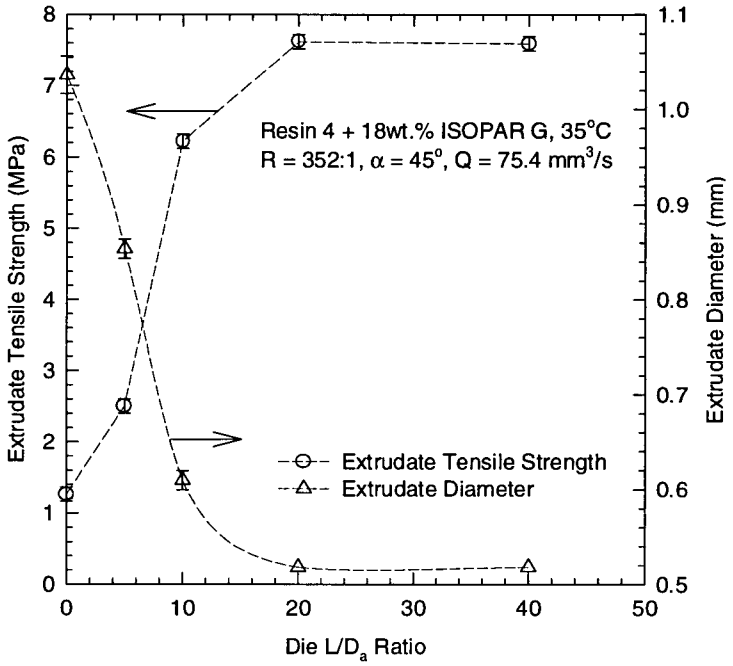

Fig. 9.7 The effect of die L/D_a ratio on extrudate tensile strength and diameter (D_a = 0.508 mm). Lines are drawn to guide the eye.

The role of the die capillary zone in improving the quality of the fibrils in the extrudate is somewhat evident from Fig. 9.7, where one can see that increasing the die L/D_a ratio suppresses the extent of extrudate swell. This implies that by increasing the capillary length, spurting of fibrils near the exit of the die entrance (contraction) zone is contained within the capillary channel. Consequently, the randomness of fibril orientation is reduced and the overall fibril quality in the extrudate is improved. Visually, this is also apparent in Fig. 9.8. Extrudates obtained using a die of $L/D_a = 0$ (Fig. 9.8 (a)) often show a fibrous appearance on the surface, which is visible even to the naked eye. This is due to the presence of broken fibrils that are chaotically oriented, as they are spurted out of the die at a high extrusion pressure. The extrudate appearance is vastly improved when a die having an $L/D_a > 0$ is used (Fig. 9.8 (b)). This explains the increase in the extrudate tensile strength as the die L/D_a

ratio is increased (Fig. 9.7). However, it is noted that since this effect occurs near the exit of the die contraction zone, beyond a certain capillary length, there will be no further improvement in the overall fibril quality, as shown by the plateau in the curves in Fig. 9.7. Apparently, using a die having $L/D_a \approx 20$ will optimize the process in terms of product quality.

(a)

(b)

Fig. 9.8 Pictures of extrudates (resin 5) obtained using dies of (a) $L/D_a = 0$ and (b) $L/D_a = 10$ under the same experimental conditions. Note the visual difference in the extrudate surfaces. The same effect was observed with other extrudates.

9.4 Effect of Resin Molecular Structure

The effect of resin melt creep viscosity (molecular weight) on the extrudate tensile strength is shown in Fig. 9.9. The results for both the homopolymer and copolymer series are plotted in the figure. It can be seen that increasing the resin molecular weight increases the mechanical strength of the extrudate for resins in the same series. However, one has to be cautious before extending this conclusion across different polymer series. Further studies involving more samples are necessary before a general conclusion can be made.

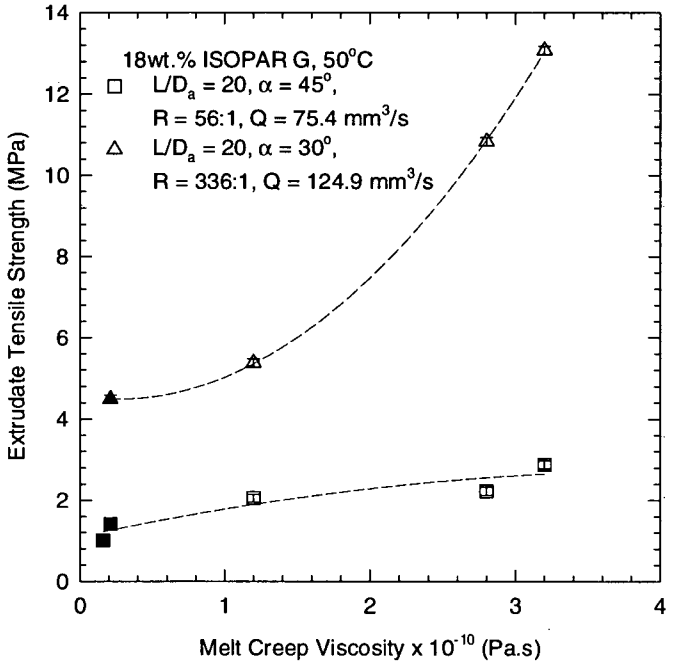

Fig. 9.9 The effect of resin melt creep viscosity (molecular weight) on extrudate tensile strength. Lines are drawn to guide the eye. Filled symbols represent copolymer series and unfilled symbols represent homopolymer series.

It is worthwhile noting that the steady-state extrusion pressure generally increases with increasing resin molecular weight. In some cases, it is not even possible to extrude a paste, due to its high molecular weight. For example, recalling the above discussion, an extrusion attempt using resin 5 at a reduction ratio of 352:1 resulted in the spurting of broken extrudate pieces out of the die in a discontinuous fashion, due to the excessively high pressure that broke the fibrils. The increase in the extrusion pressure with resin molecular weight, however, is caused by the 'hardness' of the higher molecular weight resin particles

(making them less deformable – see Chapter 6), rather than to the creation of more fibrils. In fact, the generally larger particle size of higher molecular weight resin implies that there will be a reduction in the contact area between adjacent particles and consequently, it is more reasonable to expect a smaller extent of fibrillation. The fact that these particles are also less deformable further contributes to this. Furthermore, a higher molecular weight resin particle is made up of a lesser number of molecules, although they are longer (bulkier). Hence, there will be fewer molecules to be unwound to create fibrils. Preliminary analysis using DSC has also indicated this. The difference in the first heat of melting for a higher molecular weight paste tends to be smaller than that for a lower molecular weight paste. This can be seen in Fig. 9.10, and is also apparent in Fig. 9.1. This implies that the state of crystallinity in the higher molecular weight case is only slightly disturbed (i.e. less fibrillation).

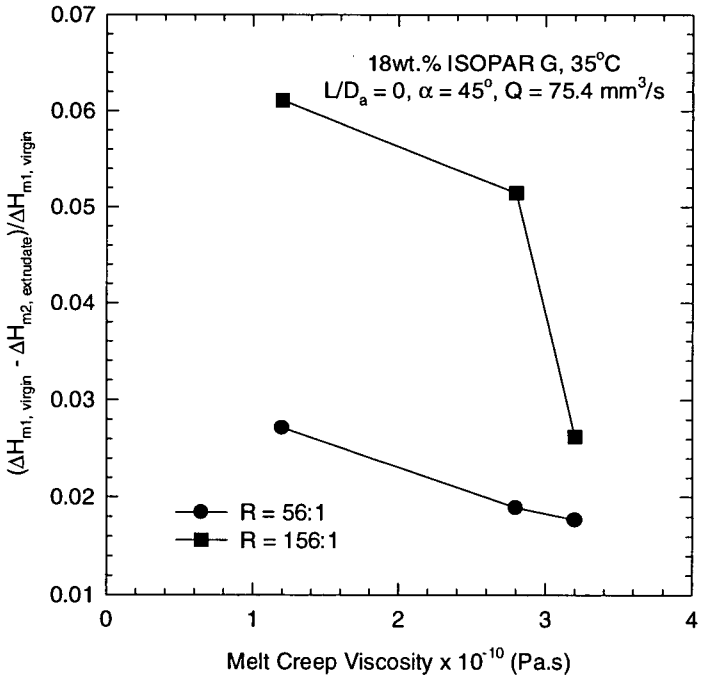

Fig. 9.10 The difference in the degree of crystallinity between unprocessed and processes pastes having different molecular weights (melt creep viscosity). Recall that a high melt creep viscosity implies a high resin molecular weight.

Extrudates obtained from a lower molecular weight resin should, therefore, exhibit a better mechanical (tensile) property, since they are more readily fibrillated, as discussed above. However, this is not observed in Fig. 9.9. It appears that, although extrudates obtained from a lower molecular weight paste are composed of more fibrils, these fibrils are

weaker compared to those obtained using a higher molecular weight paste. The difference in the strength of these fibrils may be due to the fact that, in the higher molecular weight case, molecules are longer. The fibrils created are, therefore, more continuous, as compared to the shorter fibrils associated with the lower molecular weight paste. These fibrils remain intact during the flow and this evidently results in a greater extrudate tensile strength, as can be seen in Fig. 9.9. Hence, although a lower molecular weight paste extrudate is more fibrillated, the fibrils formed are relatively easy to break.

9.5 Effect of Lubricant Concentration

The effect of lubricant concentration on the extrudate tensile strength is depicted in Fig. 9.11 for resin 3. It can be seen that there is an optimum lubricant concentration at which the extrudate tensile strength is maximized. An extrusion with a lubricant level less than the optimum results in an extrusion pressure that is too high which breaks the fibrils, although more fibrils are formed due to the increased friction between the resin particles. However, when the lubricant concentration is unnecessarily high, the extrudate becomes excessively wet and weak, sometimes not being able to hold its shape, due to the excessive local slippage between flowing particles in the die that results in a lesser number of fibrils being formed.

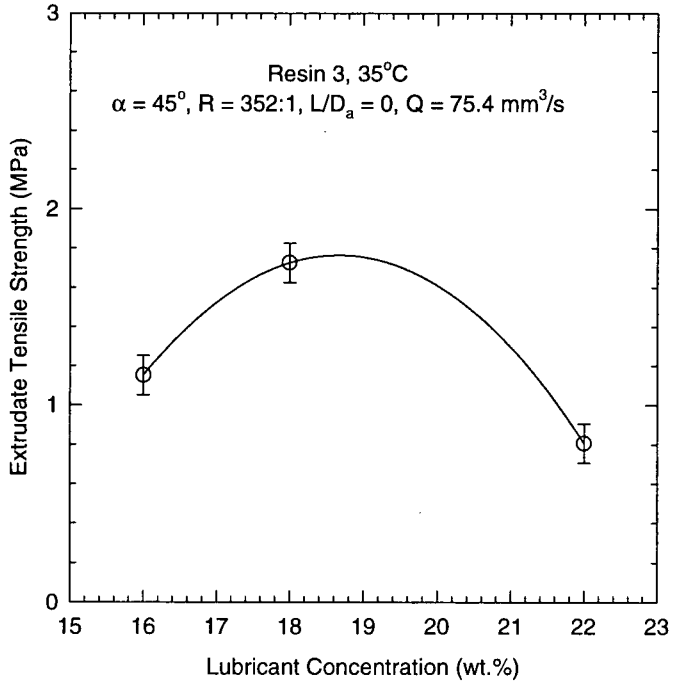

Fig. 9.11 The effect of lubricant concentration on extrudate tensile strength. Line is drawn to guide the eye.

Although the optimum lubricant concentration is expected to depend on the average particle size of the resin (molecular structure), this is not expected to be a major practical issue, since the average particle sizes of paste extrusion grade resins are typically very similar.

9.6 Conclusions

In this chapter, the effects of die design, resin molecular structure and lubricant concentration on the mechanical properties of paste extrudates, and their relationship to the quantity and quality of the fibrils formed during the extrusion process are discussed. Quantification attempts on the extent of fibrillation in an extrudate using DSC and Raman spectroscopy, in order to illustrate the issue of fibril quantity and quality, is also discussed. It was found that a balance between fibril quantity and quality is necessary to ensure industrially acceptable products. The extent of fibrillation in an extrudate can be increased by performing extrusion using a die of larger reduction ratio or entrance angle, or by decreasing the lubricant content in the paste matrix, which essentially increases the extrusion pressure level. However, too high an extrusion pressure tends to break the fibrils and is, therefore, detrimental to the quality of the extrudate. By increasing the die entrance angle, the quality of the fibrils formed is also somewhat compromised, due to less streamlining of the flow. Increasing the length of the die capillary zone (or L/D_a ratio) was found to increase the extrudate tensile strength, due to the increased degree of fibril orientation in the extrudate. The extrudate was also found to be visually more attractive (less fibrous) and exhibit less swelling. It was also noted that the pressure drop across the capillary length of the die does not contribute to the formation of more fibrils. Finally, it was found that a higher molecular weight resin produces stronger fibrils that account for the mechanical superiority of the extrudate.

CHAPTER 10:

CONCLUSIONS

10.1 PTFE Paste Extrusion: Project Wrap - Up

In this work, fundamental research has been performed on paste extrusion as a unique processing technique for PTFE resins. PTFE paste extrusion takes advantage of the near ambient transition temperatures of PTFE, which allows the resins to be fibrillated when sheared. The paste is essentially a mixture of PTFE fine powder resin and a lubricating liquid, with a typical liquid concentration of 16 wt.% to 25 wt.%. During the process, the paste is initially preformed and later, extruded through a conical entry die using a ram extruder. Due to the presence of both solid and liquid phases in the paste matrix, the mechanism of PTFE paste flow is fundamentally different from polymer melt flow.

A typical extrusion pressure response curve for PTFE paste has three characteristic regions. The first region was found to be a manifestation of the elastic nature of PTFE paste, as it wets and fills the die conical zone. This is characterized by a peak in the transient pressure curve. In the second region, the paste flow is at its steady state, and the extrusion pressure remains at an approximately steady level. In the third region, the extrusion pressure gradually increases, as the paste in the barrel becomes increasingly drier with time. This variation in the extrusion pressure has been found to result in an extrudate having inconsistent properties.

PTFE paste extrusion is carried out as a batch process. An attempt to make the process continuous was found to be practically unattractive, since preforms produced separately do not continuously mold to one another in the barrel during extrusion. It was also found that, due to the nature of the paste, analysis of experimental data obtained using a modified extrusion procedure has to be performed with caution. For example, the extrusion pressure response at a particular extrusion rate may not represent the actual response at that condition if, prior to this, the same paste has been extruded at a different piston speeds. This is due to the irreversible nature of the paste properties, as caused by the high mobility of the liquid phase (i.e. the lubricant) during the extrusion process (liquid migration).

In the preforming stage, PTFE paste is compacted to form a dense cylindrical billet. It was found that the preforming pressure has to be sufficiently high to ensure uniform compaction along the preform length. This is especially true for a paste composed of a higher molecular weight resin, which was found to be physically "harder". During the preforming of such paste, pressure was dissipated close to the end at which it was applied. Consequently, the opposite end was less compacted and an insufficient driving force was present for the lubricant to migrate outwards. This resulted in a higher extrusion pressure required for this end of the preform. Uniformity in preform density can be improved by applying higher pressure, increasing the lubricant concentration in the paste, or by compacting the paste over a longer period of time. However, the latter two procedures were found to result in the lubricant redistributing itself non-uniformly along the preform, which is clearly undesirable. This leaves preforming pressure as the only adjustable parameter. The minimum pressure required to achieve a certain length of uniformly compacted preform was found to correlate well with the resin SSG, which is inversely related to the resin molecular weight. In this study, it was also shown that better uniformity can be achieved by applying pressure at both ends of the preform.

During PTFE paste extrusion, fibrils are created. The presence of fibrils in the extrudates is clearly observable from SEM micrographs. A mechanism for fibrillation has been proposed, in which fibrils are considered as mechanically locked crystallites that are entangled in the die conical zone and unwound upon exiting the die. The consequence of fibrillation is the formation of a mechanically strong extrudate, with a degree of crystallinity lower than that of the unprocessed resin. This was confirmed using DSC. By performing visualization experiments, it was found that, in the die conical zone where fibrillation occurs, the pattern of paste flow can be described adequately by the "radial flow" hypothesis. The hypothesis assumes that all paste particles at the same radial distance from the virtual die apex are moving towards the die apex at the same velocity.

Based on the radial flow hypothesis, a one-dimensional mathematical model was developed to describe the flow of PTFE paste during extrusion. The model considers PTFE paste as an elasto-viscoplastic material that exhibits strain hardening during flow. A modified Kelvin's constitutive relation was used and a frictional analysis was incorporated into the model derivation. The model is able to predict the effects of extrusion rate and die design

(die reduction ratio, L/D_a ratio, and entrance angle) on the steady-state extrusion pressure adequately, considering its simple form. The steady-state extrusion pressure was found to increase with increasing extrusion rate, and the die reduction and L/D_a ratio. Increasing the die entrance angle initially decreases the steady-state extrusion pressure. Beyond a certain small entrance angle, however, the effect is reversed. It was also found that a higher molecular weight resin extrudes at a correspondingly higher steady-state pressure.

In order to produce commercially acceptable extrudates, adequate amounts of fibrils with reasonable quality are required. Fibril quality can be described in terms of their continuity and degree of orientation in the extrudate. Raman spectroscopy was found to be useful in an attempt to quantify fibril orientation. The quantity of the fibril formed during the extrusion process, on the other hand, can be inferred directly from the steady-state extrusion pressure. Overall, the extrudate tensile strength can be used to determine the state of fibrillation in an extrudate, since this variable takes into account the combined effects of both fibril quantity and quality. In this study, it was found that die design is critical in affecting the extrudate quality. Increasing the die reduction ratio and entrance angle was found to increase the amount of fibrils formed during the extrusion process, although the fibril quality was somewhat compromised. Increasing the length of the die capillary zone was found to improve the extrudate appearance and mechanical strength. This is due to the increased degree of fibril orientation in the extrudate, rather than to the creation of more fibrils. The extrudate was also found to exhibit less swell. Finally, it was found that a higher molecular weight resin produces stronger fibrils that account for the mechanical superiority of the extrudate.

10.2 Contributions to Knowledge

Several novel contributions to knowledge have resulted from this research work. These are identified as follows.

1. The current commercial procedure for PTFE paste extrusion has been analyzed in detail, and the physical significance of each experimental aspect of the process has been investigated. In addition, possible modifications to the process have been explored, in an attempt to improve process efficiency.

2. The preforming behavior of PTFE pastes has been studied. The results provide an understanding on how various operating variables affect the quality of PTFE preform. An empirical relationship that can be used to predict the minimum pressure required to produce a preform of uniform density has been established. An improvement in the preforming procedure, which involves the application of pressure at both ends of the preforming unit, has also been proposed and experimentally tested.

3. The mechanism of flow involved in PTFE paste extrusion has been investigated in detail using SEM. A mechanism for fibrillation has been proposed and verified using DSC. Methods for quantifying fibrils using macroscopic extrusion pressure data, tensile strength, DSC and Raman spectroscopy have been illustrated. These are novel techniques that can be used for analysis of other similar systems or processes.

4. The velocity pattern of PTFE paste during extrusion has been studied. The "radial flow" hypothesis has been used to describe the flow pattern in the die conical zone. Based on this hypothesis, a one-dimensional mathematical model has been developed and used successfully to describe the rheology of PTFE pastes. It may be possible to extend the use of the mathematical model derived here to describe the flow of other similar systems, such as highly filled polymeric systems.

5. The rheological behavior of PTFE pastes has been studied experimentally. Effects of various operating variables have been determined and discussed. The results can be used along with the developed mathematical model to improve die design and optimize the extrusion process, in accordance with the rheological behavior of an available resin.

6. The effects of various operating variables on the quality of PTFE paste extrudates have been analyzed. The results provide an understanding of the role of fibrillation in defining the final product properties. With such understanding, it is possible to optimize the extrusion operating variables, in order to produce extrudates that are commercially acceptable, with the ultimate objective of reducing the amount of process rejects. The results can also be used as a basis for resin selection, for a desired particular end use.

Most importantly, this work has contributed to the fundamental knowledge of PTFE paste extrusion, which is still at its infancy as far as research is concerned. Undoubtedly,

more in-depth studies need to be performed in the future to completely unravel the science behind the process. However, many of the findings in this work have provided significant initial steps towards a better macroscopic and microscopic understanding of the process and, therefore, allowed the commercial implementation of PTFE paste extrusion to be carried out with greater confidence. Finally, many of the analytical techniques employed here are novel, and can be used in other studies involving processes similar to PTFE paste extrusion.

10.3 Recommendations for Future Work

Several important aspects of PTFE paste extrusion are yet to be studied. These are recommended below, as possible objectives for future research work.

1. The one-dimensional mathematical model developed in this work to predict the flow of PTFE pastes is dependent on several material constants. Although the effects of resin molecular weight (melt creep viscosity) on the values of these constants have been assessed qualitatively, mathematical relationships that allow the prediction of the constant values, knowing a particular resin molecular structure, have yet to be established, primarily due to the limited number of samples available for this work. A more systematic study that involves a greater number of resin samples with tailored molecular structures is recommended to establish such relationships. The final set of mathematical relations will then allow the determination of a particular PTFE paste flow behavior, possibly without performing any experimental work.

2. As has been discussed in this work, lubricant migration is a significant phenomenon in a process such as PTFE paste extrusion. A detailed study on the subject is, therefore, warranted. The mechanism of lubricant migration during PTFE paste extrusion needs to be determined. The effects of various operating variables, such as die design, barrel diameter, resin particle size and distribution, and the lubricant concentration in the paste mixture, should also be investigated. The results can be incorporated into the mathematical model to improve the predictions of PTFE paste flow.

3. A detailed study on the effects of lubricant type, in terms of surface energy, viscosity, and volatility, on the rheology of PTFE pastes and the extent of lubricant migration during

the extrusion process, will provide a better insight into the role of lubricant in PTFE paste extrusion and is recommended for future work.

4. In order to make the rheological study of PTFE pastes more complete, the effects of other variables, such as resin particle size and its distribution (if it is indeed possible to vary in practice) and the surface roughness of the die wall, should be investigated in the future. The flow of PTFE pastes through a hyperbolic die and a crosshead die for a wire coating process are also interesting and commercially useful subjects for future investigations.

5. In the fabrication of sintered products from PTFE fine powder resins, the removal of lubricant prior to sintering is an extremely crucial step. Therefore, it is desirable to study the drying characteristics of extrudates, as functions of their diameter and the type of lubricant used in the extrusion process. It is also important to study the temperature and density distribution in the extrudate during sintering. Ultimately, a mathematical model may be developed to describe the sintering behavior of PTFE paste extrudates.

NOMENCLATURE

a, b, c	:	empirical parameters used to predict the effective length of a preform.
B	:	defined as $f . \sin \alpha/[2 . (1 - \cos \alpha)]$.
C	:	proportionality constant for the elastic term of the mathematical model developed in this work. Also refers to the proportionality constant in Ludwik's power law model.
D_b, D_a	:	die entrance and exit diameter, respectively. D_b also refers to the barrel diameter.
E	:	Young's modulus of elasticity.
f	:	Coulomb's law coefficient of friction, between PTFE paste and die wall.
L	:	length of die capillary zone.
l^*	:	effective length of a preform, defined as the length of a preform portion for which compaction density is approximately uniform.
m	:	power law index for the viscous term of the mathematical model developed in this work.
M_n	:	number average molecular weight.
n	:	power law index for the elastic term of the mathematical model developed in this work. Also refers to the generalized power law index.
N_1, N_{1a}	:	first normal stress difference. N_{1a} is the first normal stress difference calculated at the exit of the die.
Q	:	volumetric flow rate.
R	:	die reduction (contraction) ratio, defined as the ratio of the die entrance to exit cross sectional area.
R_a	:	average roughness
r, θ, ϕ	:	spherical coordinate axes used in force analysis in the die conical (entrance) zone. If used as subscripts, these indicate the directions in which a particular vector is acting.
r', θ', z	:	cylindrical coordinate axes used in force analysis in the die capillary zone. If used as subscripts, these indicate the directions in which a particular vector is acting.
r_b, r_a	:	radial distances as measured from the virtual die apex to the entrance and exit of the die conical zone, respectively.
t	:	time.
$\hat{C}$	:	constant of integration.
$\Delta H_{m1}, \Delta H_{m2}$	:	first and second heat of melting (crystallization), respectively, as obtained from DSC.

α	:	die entrance angle. $\alpha = 90^{o}$ refers to flat die.
ε_I, ε_{II}, ε_{III}	:	strains in the three principal directions
ε, $\dot{\varepsilon}$	:	strain and strain rate, respectively.
γ_{max}, $\dot{\gamma}_{max}$	:	maximum strain and strain rate, respectively. Maximum strain is defined as the difference of strains in the first two principal directions.
η	:	proportionality constant for the viscous term of the mathematical model developed in this work. Also refers to the viscosity coefficient in Newtonian's law for viscous flow.
σ	:	stress.
σ_I, σ_{II}, σ_{III}	:	stresses in the three principal directions.
σ_o	:	yield stress.

BIBLIOGRAPHY

Adams, M. J., I. Aydin, B. J. Briscoe, and S. K. Sinha, *A Finite Element Analysis of the Squeeze Flow of an Elasto-Viscoplastic Paste Material*, J. Non-Newt. Fluid Mech., 71, 41-57 (1997).

Amarasinghe, A. A. U. S., and D. I. Wilson, *Interpretation of Paste Extrusion Data*, Trans. Inst. Chem. Eng., 76A, 3-8 (1998).

Amarasinghe, A. A. U. S., and D. I. Wilson, *Statistical Analysis of Pressure Fluctuations in Paste Extrusion*, The 1997 Jubilee Research Event: A Two-Day Symposium Held at the East Midlands Conference Centre, Nottingham, 8-9 April 1997.

Andrikopoulos, K.S., D. Vlassopoulos, G.A. Voyiatzis, Y.D. Yiannapoulos and E.I. Kamitsos, *Molecular Orientation of Hairy-Rod Polyester: Effects of Side Chain Length*, Macromolecules, 31, 5465-5473 (1998).

Ariawan, A. B., S. Ebnesajjad and S.G. Hatzikiriakos, *Paste Extrusion of Polytetrafluoroethylene (PTFE) Fine Powder Resins*, Rheo. Acta, manuscript submitted for publication (2001).

Ariawan, A. B., S. Ebnesajjad and S.G. Hatzikiriakos, *Preforming Behavior of PTFE Pastes*, Powder Tech., manuscript accepted for publication (2001).

Ariawan, A. B., S. Ebnesajjad and S.G. Hatzikiriakos, *Properties of PTFE Paste Extrudates*, Polym. Eng. Sci., manuscript submitted for publication (2001).

ASTM D1710-96, *Standard Specification for Extruded and Compression Molded Polytetrafluoroethylene (PTFE) Rod and Heavy-Walled Tubing* (1996).

ASTM D4895, *Standard Specification for Polytetrafluoroethylene (PTFE) Resin Produced from Dispersion* (1997).

Baird, D. G., and D. I. Collias, *Polymer Processing*, Butterworth-Heinemann, MA, 1995.

Bates, A. J. D., and J. Bridgwater, *Modelling of Non-Uniform Paste Flow*, The 1994 IChemE Research Event: A Two-Day Symposium Held at University College London, Jan 5-6, 1994.

Bates, A. J. D., and J. Bridgwater, *The Flow of Paste in Complex Geometries*, The 1993 IChemE Research Event, Jan 6-7, 1993.

Benbow, J. J., and J. Bridgwater, *Paste Flow and Extrusion*, Oxford University Press, Oxford, 1993.

Benbow, J. J., and J. Bridgwater, *The Influence of Formulation on Extrudate Structure and Strength*, Chem. Eng. Sci., 42, 735-766 (1987).

Benbow, J. J., E. W. Oxley, and J. Bridgwater, *The Extrusion Mechanics of Pastes – The Influence of Paste Formulation on Extrusion Parameters*, Chem. Eng. Sci., 42, 2151-2162 (1987).

Benbow, J. J., N. Ouchiyama, and J. Bridgwater, *On the Prediction of Extrudate Pore Structure from Particle Size*, Chem. Eng. Comm., 62, 203-220 (1987).

Benbow, J. J., T. A. Lawson, E. W. Oxley, and J. Bridgwater, *Prediction of Paste Extrusion Pressure, Ceramic Bulletin*, 68, 1821-1824 (1989).

Bingham, E. C., *Fluidity and Plasticity*, McGraw-Hill, New York, 1922.

Blanchet, T. A., *Polytetrafluoroethylene*, in Handbook of Thermoplastics, (O. Olabisi, ed.), 1st ed., Marcel Dekker, Inc., New York, 1997, 981-1000.

Bouvard, D., *Densification Behaviour of Mixtures of Hard and Soft Powders Under Pressure*, Powder Tech., 111, 231-239 (2000).

Bower D.I., and W.F. Maddams, *The Vibrational Spectroscopy of Polymers*, Cambridge University Press, New York, 1989.

Bridgwater, J., *Paste Extrusion – an Overview, in Recent Advances in Chemical Engineering*, Tata McGraw-Hill, New Delhi, 1989.

Burbidge, A. S., J. Bridgwater, and Z. Saracevic, *Liquid Migration in Paste Extrusion*, Chem. Eng. Res. Design, 73, 810-816 (1995).

Burbidge, A. S., J. Feaey, A. Wilson, and J. Bridgwater, *Liquid Phase Migration in Extrusion Pastes*, Proceed. of The World Congress on Particle Technology, Brighton, UK, July 6-9, 1998.

Carley, J. F., and E. von Holtz, *Flow of RX-08-FK High Energy Paste in Capillary Rheometer*, J. Rheol., 41, 473-489 (1997).

Cavanaugh, R. J., Private Communication, August 1999.

Chakrabarty, J., *Theory of Plasticity*, McGraw-Hill Book Co., Singapore, 1998.

Chevalier, L., E. Hammond, and A. Poitou, *Extrusion of TiO_2 Ceramic Powder Paste*, J. Mat. Process. Tech., 71, 243-248 (1997).

Clark, E. S., MUUS, L. T. Z., *Krist*, 117-119, 1962.

Cottrell, T. L., *The strength of Chemical Bonds*, 2nd ed., Butterworths, Washington, D. C., 1958.

Craig, R.F., *Soil mechanics*, E & FN Spon, NY, 1997.

Davis, E. A., and J. Dukos, *Theory of Wire Drawing*, J. Appl. Mech., 11, 193-198 (1944).

Dealy, J. M., and K. F. Wissbrun, *Melt Rheology and its Role in Plastics Processing – Theory and Applications*, Van Nostrand Reinhold, New York, 1990.

Deimede V., K.S. Andrikopoulos, G.A. Voyiatzis, F. Konstandakopoulou and J.K. Kallitsis, *Molecular Orientation of Blue Luminescent Rigid-Flexible Polymers*, Macromolecules, 32, 8848-8856 (1999).

Doban, R. C., A. C. Knight, J. H. Peterson and C. A. Sperati, *Molecular Weight of Polytetrafluoroethylene*, DuPont Co., presented at 130th Meeting, American Chemical Society, Atlantic City, N. J., September 16-21, 1956.

Domanti, A. T. J., and J. Bridgwater, *Extrusion Induced Defects*, The 1996 IChemE Research Event: The Second Equropean Conference for Young Researchers in Chemical Engineering, April 2-3, 1996.

Domanti, A. T. J., *Surface Fracture in Paste Extrusion*, Ph.D. Dissertation, Department of Chemical Engineering, University of Cambridge, Cambridge, 1998.

Doraiswamy, D., A. N. Munumdar, I. Tsao, A. N. Beris, S. C. Danforth, and A. B. Metzner, *The Cox-Merz Rule Extended: A Rheological Model for Concentrated Suspensions and Other Materials with a Yield Stress*, J. Rheol., 35, 647-685 (1991).

DuPont Fluoroproducts, *Molecular Weight of PTFE*, Technical Bulletin, Wilmington, Delaware, 2001.

DuPont Fluoroproducts, *Teflon® Fine Powder Processing Guide*, Technical Bulletin, Wilmington, Delaware, 1991.

DuPont Fluoroproducts, *Teflon® PTFE Fluoropolymer Resin* – Processing Guide for Fine Powder Resins, Technical Bulletin, Wilmington, Delaware, 1994.

DuPont Fluoroproducts, *Teflon® PTFE Properties Handbook*, Technical Bulletin, Wilmington, Delaware, 1996.

Ebnesajjad S., Private Communication, October 2001.

Ebnesajjad, S., *Fluoroplastics, Vol. 1: Non – Melt Processible Fluoroplastics, The Definitive User's Guide and Databank*, Plastics Design Library, William Andrew, Inc., 2000.

Exxon Corp., *Isopar® Solvents*, Publication DG-1P, 1994.

Fayed, M. E., and L. Otten (eds.), *Handbook of Powder Science and Technology*, Chapman and Hall, New York, 1997.

Feiring, A. E., J. F. Imbalzano, and D. L. Kerbow, *Advances in Fluoroplastics*, Trends in Polym. Sci., 2, 26-30 (1994).

Folda, T., H. Hoffmann, H. Chanzy, and P. Smith, *Liquid Crystalline Suspensions of Poly(tetrafluoroethylene) 'Whiskers'*, Nature, 333, 55-56 (1988).

Frith, W. J., J. Mewis, and T. A. Strivens, *Rheology of Concentrated Suspensions: Experimental Investigations*, Powder Tech., 51, 27-34 (1987).

Gangal, S. V., *Polytetrafluoroethylene, Homopolymers of Tetrafluoroethylene*, in Encyclopedia of Polymer Science and Engineering, 2nd ed., John Wiley & Sons, New York, 1989, 577-600.

Gangal, S. V., *Polytetrafluoroethylene*, in Encyclopedia of Chemical Technology, 4th ed., John Wiley & Sons, New York, 1994, 621-644.

Gotz, J., D. Muller, H. Buggisch, and C. Tasche-Lara, *NMR Flow Imaging of Pastes in Steady-State Flows*, Chem. Eng. Proc., 33, 385-392 (1994).

Hatzikiriakos, S.G., and J. M. Dealy, *The effect of interface conditions on wall slip and melt fracture of high density polyethylene*, SPE ANTEC '91 Tech. Papers, 2311-2314 (1991).

Herschel, W. H., and R. Buckley, *Kolloid Z.*, 39, 192 (1926).

Hoffman, O., and G. Sachs, *Introduction to the theory of Plasticity for Engineers*, McGraw-Hill Company, 1953.

Holmes, D. A., and E. W. Fasig, Jr., Plunkett, R. J., US Patent 3,819,594, assigned to DuPont de Nemours and Company, June 1974.

Horrobin, D. J., and R. M. Nedderman, *Die Entry Pressure Drops in Paste Extrusion*, Chem. Eng. Sci., 53, 3215-3225 (1998).

Jiri, H., T. Jana, and O. Frantisck, *The Forming of Ceramic Paste*, Ceramic-Silikaty, 33, 1-10 (1989).

Kalika, D.S., and Denn, M.M., *Wall slip and extrudate distortion in linear low-density polyethylene*, J. Rheol., 31, 815-834 (1987).

Kim, C. J., K. B. Kim, I. H. Kuk, G. W. Hong, S. D. Park, S. W. Yang, and H. S. Shin, *Fabrication and Properties of $Yba_2Cu_3O_{7-\delta}$-Ag Composite Superconducting Wires by Plastic Extrusion Technique*, J. Mat. Sci., 32, 5233-5242 (1997).

Kim, C. U., J. M. Lee, and S. K. Ihm, *Emulsion Polymerization of Tetrafluoroethylene: Effects of Reaction Conditions on Particle Formation*, J. Fluorine Chemistry, 96, 11-21 (1999a).

Kim, C. U., J. M. Lee, and S. K. Ihm, *Emulsion Polymerization of Tetrafluoroethylene: Effects of Reaction Conditions on the Polymerization Rate and Polymer Molecular Weight*, J. Appl. Polym. Sci., 73, 777-793 (1999b).

Kobayashi, S., and E. G., Thomsen, *Upper and Lower Bound Solutions to Axisymmetric Compression and Extrusion Problems*, Int. J. Mech. Sci., 7, 127-143 (1965).

Kudo, H., *Some Analytical and Experimental Studies of Axi-symmetric Cold Forging and Extrusion – I*, Int. J. Mech. Sci., 2, 102-127 (1960).

Larson, R., *Constitutive Equations for Polymer Melts and Solutions*, Butterworths, Boston, 1988.

Lehnert R. J., P.J. Hendra, N. Everall and N.J. Clayden, *Comparative Quantitative Study on the Crystallinity of Poly(tetrafluoroethylene) including Raman, Infra-Red and ^{19}F Nuclear Magnetic Resonance Spectroscopy*, Polymer, 38, 1521-1535 (1997).

Lewis E.E., and C.M. Winchester, *Rheology of Lubricated Tetrafluoroethylene Compositions*, Ind. Eng. Chem., 45, 1123-1127 (1953).

Lewis, E. E., and C. M. Winchester, *Rheology of Lubricated Polytetrafluoroethylene Compositions – Equipment and Operating Variables*, Ind. Eng. Chem., 45, 1123-1127 (1953).

Li, Y. Y., and J. Bridgwater, *Prediction of Extrusion Pressure Using an Artificial Neural Network*, Powder Tech., 108, 65-73 (2000).

Lontz, J. F., and W. B. Happoldt Jr., *Teflon® Tetrafluoroethylene Resin Dispersion*, Ind. Eng. Chem., 44, 1800-1804 (1952).

Lontz, J., J.A. Jaffe, L.E. Robb and W.B. Happoldt, Jr., *Extrusion Properties of Lubricated Resin from Coagulated Dispersion*, Ind. Eng. Chem., 44, 1805-1810 (1952).

Louge, A., *A Two-Phase Model for Paste Flow Including Filtration and Segregation Effects*, Comptes Rendus de LaAcademie des Sciences, Serie II, 322, 785-791 (1996).

Ludwik, P., *Elemente der Technologischen Mechanik*, Springer-Verlag, Berlin, 1909.

Macleod H.M., and K. Marshall, *The Determination of Density Distributions in Ceramic Compacts Using Autoradiography*, Powder Tech. 16, 107-122 (1977).

Malamataris, S., and J. E. Rees, *Viscoelastic Properties of Some Pharmaceutical Powders Compared Using Creep Compliance, Extended Heckel Analysis and Tablet Strength Measurements*, Int. J. Pharm., 92, 123-153 (1993).

Mazur, S., *Paste Extrusion of Poly(tetrafluoroethylene) Fine Powders*, in Polymer Powder Technology (M. Narkis and N. Rosenzweig, eds.), John Wiley and Sons, New York, 1995, 441-481.

McAdams, J., Private Communication, April 2000.

McAdams, J., Private Communication, August 1999.

Michaeli, W., *Extrusion Dies for Plastics and Rubber*, Hanser, New York, 1992.

Oldroyd, J. G., *A Rotational Formulation of the Equation of Plastic Flow for a Bingham Solid*, Proc. Cambridge Philos. Soc., 43, 100-105 (1947).

Papanastasiou, T. C., *Flow of Materials with Yield*, J. Rheol., 31, 385-404 (1987).

Pashias, N., D. V. Boger, *A Fifty Cent Rheometer for Yield Stress Measurement*, J. Rheol., 40, 1179-1189 (1996).

Plunkett, R. J., *The History of Polytetrafluoroethylene: Discovery and Development*, in High Performance Polymers: Their Origins and Development, Proceed. of Symp. on the Hist. of High Perf. Polymers at the ACS Meeting in New York, April 1986, (R. B. Seymour and G. S. Kirshenbaum, eds.), Elsevier, New York, 1987.

Plunkett, R. J., US Patent 2,230,654, assigned to DuPont Co., February 4, 1941.

Popovich, L. L., D. L. Feke, and I. Manas-Zloczower, *Influence of Physical and Interfacial Characteristics on the Wetting and Spreading of Fluids on Powders*, Powder Tech., 104, 68-74 (1999).

Ramamurthy, A.V., *Wall slip in viscous fluids and influence of materials of construction*, J. Rheol., 30, 337-357 (1986).

Ring, T. A., *Fundamentals of Ceramic Powder Processing and Synthesis*, Academic Press, New York, 1996.

Saint – Venant, B., *Mémoire sur l'établissement des Equations Différentielles des Mouvements Intérieurs Opérés dans les Corps Solides Ductiles*, Compt. Rend. Acad. Sci. Paris 70, 473 (1870).

Schultz, M. A., and L. J. Struble, *Use of Oscillatory Shear to Study Flow Behavior of Fresh Cement Paste, Cement and Concrete Research*, 23, 273-282 (1993).

Sheppard, W. A., and C. M. Sharts, *Organic Fluorine Chemistry*, W. A., Benjamin, Inc., New York, 1969.

Shimizu, M., C. Ikeda, and M. Matsuo, *Development of High Modulus and High Strength Poly(tetrafluoroethylene) Fibers by Elongation at Liquid Crystalline State*, Macromolecules, 29, 6724-6729 (1996).

Snelling G. R., and J. F. Lontz, *Mechanism of Lubricant-Extrusion of Teflon® TFE-Tetrafluoroethylene Resins*, J. Appl. Polym. Sci. III, 257-265 (1960).

Sperati, C. A., *Physical Constants of Fluoropolymers*, in Polymer Handbook, (J. Brandrup and E.H. Immergut, eds.), John Wiley and Sons, New York, 1989.

Spitteler, P. H. J., L. F. Gladden, A. M. Donald, and J. Bridgwater, *ESEM and NMR Imaging of Water Based Ceramic Pastes*, Proceed. of World Congress on Particle Technology, Brighton, UK, July 6-9, 1998.

Suwa, T., M. Takehisa and S. Machi, *Melting and Crystallization Behavior of Poly(tetrafluoroethylene): New Method for Molecular Weight Measurement of Poly(tetrafluoroethylene) using a Differential Scanning Calorimetry*, J of Appl. Polymer Sci., 17, 3253-3257 (1973).

Tordella, J.P., *Fracture in the extrusion of amorphous polymers through capillaries*, J. Appl. Phys., 27, 454 (1956).

Tuminello, W. H., T. A. Treat, and A. D. English, *Poly(tetrafluoroethylene): Molecular Weight Distributions and Chain Stiffness*, Macromolecules, 21, 2606-2610 (1988).

Vandeneede, V., G. Moortgat, F. Cambier, *Characterization of Alumina Pastes for Plastic Moulding*, J. Euro. Ceramic Soc., 12, 225-231 (1997).

Voyiatzis, G.A., G. Petekidis, D. Vlassopoulos, E.I. Kamitsos and A. Bruggeman, *Molecular Orientation in Polyester Films Using Polarized Laser Raman and Fourier Transform Infrared Spectroscopies and X-Ray Diffraction*, Macromolecules, 29, 2244-2252 (1996).

Voyiatzis, G.A., Private Communication, May 2000.

Wildman, R. D., S. Blackburn, and D. J. Parker, *Investigation of Paste Flow Using Positron Emission Particle Tracking*, Powder Tech., 103, 220-229 (1999).

Yu, A. B., J. Bridgwater, A.S. Burbidge, and Z. Saracevic, *Liquid Maldistribution in Particulate Paste Extrusion*, Powder Tech., 103, 103-109 (1999).

Yurchenko, E. N., V. Y. Prokofev, A. P. Illyin, and Y. G. Shyrokov, *Optimum Properties of Extrudate Paste Powders on the Basis of TiO_2, Al_2O_3, and Other Substances for Production of Honeycomb Supports*, Reaction Kinetics and Catalysis Letters, 60, 269-277 (1997).

Zhang, D. Z., and R. M. Rauenzahn, *A Viscoelastic Model for Dense Granular Flows*, J. Rheol., 41, 1275-1298 (1997).

Zisman, W. A., *Surface Properties of Plastics*, Record of Chemical Progress, 26 (1965).